

---

Electronic Thesis and Dissertation Repository

---

11-19-2018 10:45 AM


# The use of current steering during subthalamic deep brain stimulation to alleviate upper limb symptoms of Parkinson's disease

Shabna Iftikar Mohideen  
*The University of Western Ontario*

Supervisor  
Jog, Mandar  
*The University of Western Ontario*

Graduate Program in Physiology and Pharmacology  
A thesis submitted in partial fulfillment of the requirements for the degree in Master of Science  
© Shabna Iftikar Mohideen 2018

Follow this and additional works at: <https://ir.lib.uwo.ca/etd>

 Part of the [Analytical, Diagnostic and Therapeutic Techniques and Equipment Commons](#), [Nervous System Commons](#), [Nervous System Diseases Commons](#), [Neuroscience and Neurobiology Commons](#), [Pharmacology Commons](#), and the [Physiology Commons](#)

---

## Recommended Citation

Iftikar Mohideen, Shabna, "The use of current steering during subthalamic deep brain stimulation to alleviate upper limb symptoms of Parkinson's disease" (2018). *Electronic Thesis and Dissertation Repository*. 5882.

<https://ir.lib.uwo.ca/etd/5882>

This Dissertation/Thesis is brought to you for free and open access by Scholarship@Western. It has been accepted for inclusion in Electronic Thesis and Dissertation Repository by an authorized administrator of Scholarship@Western. For more information, please contact [wlsadmin@uwo.ca](mailto:wlsadmin@uwo.ca).

## Abstract

Subthalamic (STN) deep brain stimulation (DBS) is an established treatment to alleviate the appendicular motor symptoms of Parkinson's Disease (PD). Current steering during DBS allows the unequal fractionation of current between two electrodes on the lead, resulting in a non-spherical electrical field. It is hypothesized that the way the electrical field is shaped will affect a patient's upper limb symptom alleviation. Seven PD patients who underwent bilateral STN-DBS were tested over four weeks post-operation. 16 current fractionation settings were tested each week at an amplitude that increased weekly. Optimal setting was defined as the setting that provided the best symptom improvement based on kinematic data detected by a motion capture system and the Unified Parkinson's Disease Rating Scale. Results assessing right and left upper limb symptoms gave 14 optimal settings in seven patients, of which eight settings employed current steering either unilaterally or bilaterally, and six settings employed bilateral monopolar stimulation. Thus, the use of current steering was patient-dependent and limb-dependent; factors contributing to this finding include differences in lead placement, symptom heterogeneity, and possible differences in STN functionality.

## Keywords

Parkinson's disease, deep brain stimulation, current steering, motor symptoms, appendicular symptoms, upper limb, electrical field, current fractionation

## List of Abbreviations

BK:	Bradykinesia
BKI:	Bradykinesia Index
CT:	Computed Tomography
DBS:	Deep Brain Stimulation
DSM:	Diagnostic and Statistical Manual of Mental Disorders
ED:	Euclidean Distance
EEG:	Electroencephalogram
EMG:	Electromyography
FEF:	Frontal Eye Field
fMRI:	Functional Magnetic Resonance Imaging
GABA:	gamma-Aminobutyric Acid
GPe:	Globus Pallidus Pars Externa
GPi:	Globus Pallidus Pars Interna
HFS:	High Frequency Stimulation
IMU:	Inertial Measurement Unit
IPG:	Implantable Pulse Generator
LFP:	Local Field Potential
M1:	Primary Motor Cortex
MER:	Microelectrode Recording
MRI:	Magnetic Resonance Imaging
OFF:	Medication-off, Stimulation-off
PD:	Parkinson's Disease
PFC:	Prefrontal Cortex
PMC:	Premotor Cortex
PPN:	Pedunculopontine Nuclei
PSA:	Posterior Subthalamic Area
PT:	Postural Tremor
RMS:	Root-mean-square
RRA:	Retrorubral Area
RT:	Rest Tremor
SEF:	Supplementary Eye Field
SMA:	Supplementary Motor Area

SNc:	Substantia Nigra Pars Compacta
SNr:	Substantia Nigra Pars Reticulata
STD:	Standard Deviation of the Signal
STN:	Subthalamic Nucleus
TSS:	Tremor Severity Score
TW:	Therapeutic Window
UPDRS:	Unified Parkinson's Disease Rating Scale
VIM:	Ventral Intermediate Nucleus of the Thalamus
VL:	Ventral Lateral Thalamus
VLp:	Ventral Posterolateral Nucleus of the Thalamus

# Co-Authorship Statement

## **Chapter 2**

Methods of feature extraction (section 2.3.1) were computed by Mehdi Delrobaei and Sara Memar and adapted by Sima Soltani.

## Acknowledgments

First off, I would like to thank my supervisor, Dr. Mandar Jog, for making this study possible; his dedication, optimism and perseverance helped me get through the pitfalls and minor mishaps along the way. Furthermore, his passion for research and commitment to advancing treatment has inspired some of my personal goals and strengthened my work ethic.

I would like to thank the members of my advisory committee, Dr. Stan Leung, Dr. Vania Prado and Dr. Arthur Brown, for their continued support and mentorship. They showed up to every meeting with an open mind and constructive criticism to help guide my work and make me a better scientist. A special thanks to Dr. Stan Leung for making time for me on numerous occasions to provide feedback and a sense of direction.

I would like to thank the members of my lab, who went from awkward coworkers to friends who gave me laughs and the downtime I sometimes desperately needed. A special thanks to Sima Soltani, Daphne Hui, Greydon Gilmore and my volunteers for their time and effort in helping with data collection and analysis.

Lastly, I could not have made it this far without the unwavering support of my parents. Being there for me in every way with their (sometimes unsolicited) advice, words of encouragement and utmost love and care, I am truly grateful and feel indebted to them nearly as much as I feel indebted as a graduate student.

# Table of Contents

Abstract .....	i
List of Abbreviations .....	ii
Co-Authorship Statement.....	iv
Acknowledgments.....	v
Table of Contents .....	vi
List of Tables .....	ix
List of Figures .....	x
List of Appendices .....	xii
Chapter 1 .....	1
1 Introduction .....	1
1.1 Parkinson’s disease: overview and etiology .....	1
1.1.1 The classical model of basal ganglia function in PD .....	2
1.2 Deep brain stimulation for PD .....	5
1.2.1 Stimulation technology .....	6
1.2.2 Functional organization of the STN.....	6
1.2.3 Fundamentals of neuronal stimulation.....	8
1.2.4 Monopolar and multipolar stimulation .....	11
1.2.5 Current-based programming and current steering .....	11
1.3 STN-DBS procedure.....	16
1.3.1 Reasons for lead misplacement.....	16
1.4 Pathophysiology of bradykinesia .....	17
1.5 Pathophysiology of rigidity.....	19
1.6 Pathophysiology of PD tremor.....	20
1.7 Rationale and hypothesis .....	22

1.7.1	Summary of objectives .....	24
Chapter 2	.....	26
2	Methods.....	26
2.1	Study participants.....	26
2.2	Assessment tools.....	27
2.2.1	Motion capture system.....	27
2.3	Clinical tasks and study timeline .....	28
2.3.1	Feature extraction.....	32
2.4	Data analysis .....	34
2.4.1	Electrode localization.....	36
Chapter 3	.....	37
3	Results .....	37
3.1	Study participants: clinical outcomes .....	37
3.2	Objective #1 results.....	39
3.3	Objective #2 results.....	55
Chapter 4	.....	67
4	Discussion .....	67
4.1	Discussion of objective #1 .....	67
4.1.1	Involvement of the ipsilateral STN.....	69
4.1.2	Lateralization of motor control .....	70
4.2	Discussion of objective #2 .....	71
4.2.1	Optimal tremor control .....	72
4.2.2	Optimal control of rigidity and bradykinesia.....	73
4.3	Implications and clinical relevance.....	74
4.4	Limitations .....	75
4.5	Future directions .....	75



4.6 Conclusion .....	76
Bibliography .....	77
Appendices.....	82
Curriculum Vitae .....	112

## List of Tables

Table 1: Participant pool demographics .....	27
Table 2: Current fractionation settings .....	32
Table 3: List of joint angles for tremor assessment .....	34
Table 4: Lower and upper amplitude limits of the therapeutic window .....	38
Table 5: Optimal setting at study conclusion according to whole-body UPDRS score .....	39
Table 6: Optimal settings for upper limb rest tremor, postural tremor and bradykinesia determined by kinematic data .....	54
Table 7: Week 1 optimal settings determined by UPDRS-III subscores .....	62
Table 8: Week 2 optimal settings determined by UPDRS-III subscores .....	63
Table 9: Week 3 optimal settings determined by UPDRS-III subscores .....	63
Table 10: Week 4 optimal settings determined by UPDRS-III subscores .....	64
Table 11: Chi-square assessment of instances involving settings that optimally alleviate hyperkinetic and hypokinetic symptoms in the same limb .....	65
Table 12: Chi-square assessment of instances involving settings that optimally alleviate only hyperkinetic symptoms in a limb .....	66
Table 13: Chi-square assessment of instances involving settings that optimally alleviate only hypokinetic symptoms in a limb .....	66

# List of Figures

Figure 1: Schematic representation of the classical model of basal ganglia function in the (a) normal and (b) parkinsonian states .....	3
Figure 2: Subthalamic Nucleus (STN) subdivision into three functional units; the sensorimotor, associative, and limbic regions .....	7
Figure 3: Altered electrical field shape using current steering .....	13
Figure 4: Dimmer-switch model of PD resting tremor.....	22
Figure 5: Position of IMU sensors on the upper limbs .....	28
Figure 6: Study timeline.....	29
Figure 7: Optimal stimulation sites.....	37
Figure 8: 3D graphs of kinematic data for BSC 01 .....	40
Figure 9: 3D graphs of kinematic data for BSC 02 .....	42
Figure 10: 3D graphs of kinematic data for BSC 03 .....	44
Figure 11: 3D graphs of kinematic data for BSC 05 .....	46
Figure 12: 3D graphs of kinematic data for BSC 06 .....	48
Figure 13: 3D graphs of kinematic data for BSC 07 .....	50
Figure 14: 3D graphs of kinematic data for BSC 08 .....	52
Figure 15: Euclidean distances (EDs) of optimal settings for alleviation of rest tremor, postural tremor and bradykinesia in the left and right upper limbs of patients with Parkinson's disease.....	54
Figure 16: Radar charts of UPDRS-III subscores for BSC 01.....	55
Figure 17: Radar charts of UPDRS-III subscores for BSC 02.....	56

Figure 18: Radar charts of UPDRS-III subscores for BSC 03.....	57
Figure 19: Radar charts of UPDRS-III subscores for BSC 05.....	58
Figure 20: Radar charts of UPDRS-III subscores for BSC 06.....	59
Figure 21: Radar charts of UPDRS-III subscores for BSC 07.....	60
Figure 22: Radar charts of UPDRS-III subscores for BSC 08.....	61

## List of Appendices

Appendix 1: Letter of Information and Consent.....	82
Appendix 2: Ethics Approval Notice.....	94
Appendix 3: Unified Parkinson's Disease Rating Scale Part 3.....	95
Appendix 4: Electrode Localization .....	99
Appendix 5: Copyright .....	104

# Chapter 1

## 1 Introduction

The current thesis investigates the effects of current steering during deep brain stimulation of the subthalamic nucleus on the appendicular motor symptoms of Parkinson's disease. This chapter lays down the foundation of Parkinson's disease, exploring its etiology and the available treatment. An in-depth review on deep brain stimulation will be presented, focusing on different targets in the brain and the technology used for stimulation. Next, the pathophysiology of the three main appendicular motor symptoms—bradykinesia, tremor, and rigidity—will be detailed, followed by the study rationale and objectives.

### 1.1 Parkinson's disease: overview and etiology

Parkinson's disease (PD) was first medically described by James Parkinson in 1817 in his short monograph "An Essay on the Shaking Palsy" (Parkinson 1817). It is a progressive neurodegenerative disease characterized by motor and non-motor symptoms (DeMaagd & Philip, 2015). The cardinal motor features include resting tremor, muscular rigidity, and bradykinesia, which are often reported as the first clinical findings of the disease (DeMaagd & Philip, 2015). Although the cardinal features mainly affect the appendages of the body, PD also includes axial symptoms such as dysarthria, gait dysfunction, and postural instability (Bejjani et al., 2000). Nonmotor presentations of the disease have been stated to occur before the onset of motor symptoms and include sleep disorders, depression, and cognitive changes (DeMaagd & Philip, 2015).

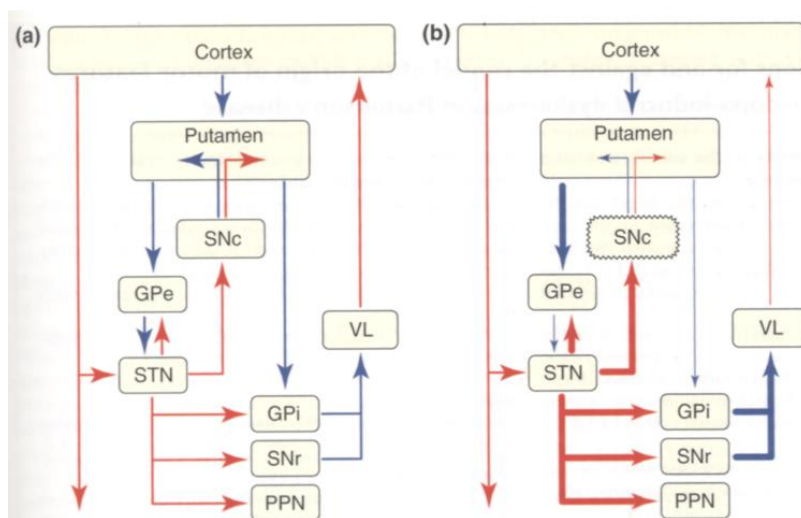
PD is one of the most common neurodegenerative diseases, with an incidence in the U.S. of approximately 60,000 cases per year and a prevalence of approximately 1% in people 60 years of age and older (DeMaagd & Philip, 2015). With the mean age of onset close to 60 years, PD is primarily a disease of the elderly although individuals have developed the disease as early as their 30s. There are gender differences in the incidence of PD, emphasized by the 3:2 ratio of males to females, with a delayed onset in females potentially due to the neuroprotective effects of estrogen (DeMaagd & Philip, 2015).

The pathophysiological hallmark of PD can be characterized by two processes: (a) the loss of dopaminergic neurons in the pars compacta of the substantia nigra (SNc); (b) the presence of Lewy bodies, composed of  $\alpha$ -synuclein, which become misfolded and accumulate in surviving neurons of the SNc and other brain regions (Connolly & Lang, 2014). There is 30-70% cell loss in the SNc when motor symptoms of PD become evident (Rizek, Kumar, & Jog, 2016). Dopamine deficiency is said to be the predominant neurochemical abnormality, with the involvement of nondopaminergic brain regions as the disease progresses (Connolly & Lang, 2014). Cognitive dysfunction, mood disorders and impulse control disorders observed in PD patients are related to a dopamine deficiency outside the basal ganglia or in serotonergic and noradrenergic systems (Rizek et al., 2016).

### 1.1.1 The classical model of basal ganglia function in PD

The basal ganglia include the striatum,—which comprises the caudate nucleus, putamen, and nucleus accumbens— the globus pallidus which contains an internal segment (GPi) and external segment (GPe), the substantia nigra which can be divided into the SNc and substantia nigra pars reticulata (SNr), and finally the subthalamic nucleus (STN) (Obeso et al., 2000). Together with cerebral regions and the thalamus, the basal ganglia form a complex network of circuits (*Figure 1a*); the motor circuit is most directly related to the pathophysiology of movement disorders including PD (Obeso et al., 2000). Cortical motor areas project in a somatotopic fashion to the putamen where they form excitatory, glutamatergic connections with medium spiny neurons containing  $\gamma$ -aminobutyric acid (GABA); these neurons give rise to the direct and indirect pathways that connect the striatum to the output nuclei of the basal ganglia, namely the GPi and SNr (Obeso et al., 2000). Neurons in the direct pathway project directly from the putamen to the GPi/SNr, they contain dopamine D1 receptors, and provide a direct inhibitory effect on GPi/SNr neurons (Obeso et al., 2000). Neurons in the indirect pathway connect the putamen with the GPi/SNr via synaptic connections in the GPe and STN and they contain dopamine D2 receptors (Obeso et al., 2000). Activation of neurons in the direct pathway leads to reduced neuronal firing in the GPi/SNr while activation of neurons in the indirect pathway leads to inhibition of the GPe, disinhibition of the STN, and excitation of the

GPi/SNr (Obeso et al., 2000). Thus, the direct and indirect pathways have opposing effects on basal ganglia output with the activation of neurons in the direct pathway facilitating motor activity, and activation of the indirect pathway suppressing motor activity (Obeso et al., 2000). In a normal brain, the model proposes that dopamine from the SNc exerts a dual effect on striatal neurons by exciting D1-receptor-expressing neurons in the direct pathway and inhibiting D2-receptor-expressing neurons in the indirect pathway (Obeso et al., 2000). In PD, dopamine deficiency causes increased activity in the indirect circuit and reduced activity in the direct circuit. Although an oversimplification, the imbalance between the direct and indirect striatal pathways partly provides an explanation for the cardinal symptoms of PD. A schematic representation of the classical model of basal ganglia function in the normal and parkinsonian state is shown below (*Figure 1*; Obeso et al., 2000).



© Elsevier. Adapted with permission.

**Figure 1: Schematic representation of the classical model of basal ganglia function in the (a) normal and (b) parkinsonian states**

Blue arrows depict inhibitory projections and red arrows depict excitatory projections; thickness of arrow signifies the degree of activation. Direct pathway connects the putamen with the output nuclei (globus pallidus pars interna (GPi) and substantia nigra pars reticulata (SNr)) directly and the indirect pathway contains synaptic connections in the globus pallidus pars externa (GPe) and subthalamic nucleus (STN). (a) In the normal state, dopamine inhibits neuronal activity in the indirect pathway and excites neurons in the direct pathway. (b) In PD, dopamine depletion leads to disinhibition of striatal neurons in the indirect pathway, leading to increased inhibition of the GPe and disinhibition of the STN; overactivity of the STN leads to excess excitation of GPi/SNr



neurons and overinhibition of thalamo-cortical motor centers. SNc: substantia nigra pars compacta; PPN: pedunculopontine nuclei; VL: ventral lateral thalamus.

The goal of therapy aims to replace dopamine with dopaminergic medications to modulate the dysfunctional circuit in the basal ganglia. Although there is no established cure or disease-modifying therapies (Connolly & Lang, 2014), there are treatments to improve the quality of life for PD patients. There is strong evidence to support the use of levodopa and dopamine agonists at all stages of PD to treat motor symptoms, levodopa being the most effective medication (Connolly & Lang, 2014). Levodopa is transported from the peripheral circulation across the blood-brain barrier and is converted to dopamine in the striatum where it exerts its dopaminergic effects. Although levodopa is prescribed to treat almost all motor symptoms, its adverse effects can hinder the symptomatic benefit gained by patients. The adverse effects of levodopa include nausea, orthostatic hypotension, hallucinations and motor complications such as motor fluctuations and dyskinesia (Connolly & Lang, 2014). Motor fluctuations are alterations between “on” and “off” periods; on periods are when patients experience a good response to medication and off periods are when the benefit from medication wears off and symptoms re-emerge (Connolly & Lang, 2014). Dyskinesia is defined as involuntary movements correlated to fluctuations in dopamine levels and can lead to impaired motor function and injury. Motor fluctuations are unexpected variations in the motor response to dopaminergic therapy whereas dyskinesias are unwanted and intrusive movements caused by levodopa (Rizek et al., 2016). In 40%-50% of patients, motor fluctuations and dyskinesias will develop within five years of chronic levodopa treatment and after 10 years of levodopa treatment in 70%-80% of patients (Rizek et al., 2016). Catechol O-methyltransferase (COMT) inhibitors, monoamine oxidase B inhibitors and dopamine agonists may be prescribed to reduce off periods. Reduction of dopaminergic medication can reduce the severity of dyskinesia; however, this will cause re-emergence of PD symptoms. For this reason, medications such as Amantadine, an antiviral with antiglutamatergic effects, and Clozapine are prescribed to improve dyskinesia (Connolly & Lang, 2014). Some patients require a combination of different types of medication for symptom management and thus require a highly regimented schedule for medication intake. Levodopa’s short half-life results in fluctuations in levodopa plasma

concentration, causing the efficacy of levodopa to decline due to the emergence of dyskinesia and motor fluctuations (Rizek et al., 2016). As a result, many PD patients look to neurosurgical interventions for managing their symptoms. The classical model of basal ganglia function and its prediction of increased STN and GPi activity in PD can be used to justify the efficacy of targeting these two nuclei with deep brain stimulation (DBS), which represents the gold standard of treatment for motor fluctuations and dyskinesia in advanced PD (Magrinelli et al., 2016).

## 1.2 Deep brain stimulation for PD

DBS is widely accepted as a treatment option for PD, dystonia, tremor, and is less known as a treatment for many other movement disorders (Fasano & Lozano, 2015). For PD, a consistent and sustained improvement in motor function and quality of life can be achieved through DBS (Fasano & Lozano, 2015). DBS works by sending an electrical current through a set of electrodes attached to a lead; the lead is placed within a target region—which differs according to the diagnosis—inside the brain. The lead is attached to the pulse generator, implanted in the chest region, through a wire that runs subcutaneously. Candidates for DBS to treat PD require a disease duration of at least 5 years and clear and significant response to levodopa is considered as a favorable predictor for surgery (Broggi, Franzini, Marras, Romito, & Albanese, 2003). Other inclusion criteria include: (1) idiopathic PD, (2) stage II or IV on the Hoehn-Yahr scale (rates the severity of PD in five levels, with I being the mildest), (3) severe motor fluctuations, (4) no dementia or psychiatric abnormalities (Broggi et al., 2003).

In PD, DBS usually involves bilateral stimulation in either the STN or the GPi. The motor benefits are similar with each target, but the number of publications and size of clinical experience is greater for STN DBS (Fasano & Lozano, 2015). There is evidence pointing to differences between STN and GPi as the target with regards to specific symptoms and features of PD. The STN is favored for greater benefit in the severity of off symptoms and also contains a cost advantage; reduction in PD medication is only seen after STN DBS and given the smaller size of the STN, the charge density required for stimulation is lower and therefore leads to less battery usage than for GPi stimulation (Fasano & Lozano, 2015). Appendicular symptoms respond better to STN stimulation

and axial motor symptoms respond better to GPi stimulation (Fasano & Lozano, 2015). Specifically, studies have pointed towards favoring STN stimulation for rigidity and bradykinesia, although no difference between targets was seen for tremor (Fasano & Lozano, 2015). Dyskinesia suppression and long-term effects on stability and cognition favor GPi (Fasano & Lozano, 2015). Because the long-term outcome is better known for STN DBS, it is viewed by many as the ultimate therapy targeting advanced stages of PD (Romanelli, Bronte-Stewart, Heit, Schaal, & Esposito, 2004).

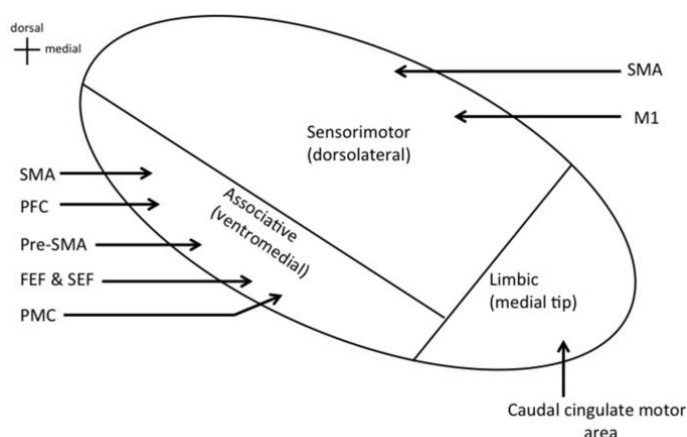
### 1.2.1 Stimulation technology

The first commercially available DBS system was manufactured by Medtronic in 1976 (Kopell, Machado, & Butson, 2009). Since then, DBS therapy has come a long way with constant modifications to the implantable pulse generator (IPG) and lead that make up the neurostimulation system. IPGs can be programmed for adjustments in current amplitude, pulse width, and frequency, as well as for the activation of individual contacts on the lead as cathodes or anodes. IPGs were initially limited in frequency output to 185 Hz and pulse widths longer than 500  $\mu$ s are rarely used (Kopell et al., 2009). The stimulation amplitude ranges from 0 to 25 mA in different devices (Kopell et al., 2009). In PD, most clinical DBS studies have found frequencies in the range of 143 to 173 Hz, pulse widths in the range of 67 to 138  $\mu$ s, and amplitudes in the range of 2.4 to 4.4 V effective in controlling motor symptoms (Wagle Shukla, Zeilman, Fernandez, Bajwa, & Mehanna, 2017). Before discussing the difference between voltage-controlled systems and current-controlled systems, as well as monopolar and multipolar stimulation, a better understanding of the mechanisms underlying the therapeutic effects of DBS can be achieved by investigating the functional organization of the STN.

### 1.2.2 Functional organization of the STN

Recent research has pointed at the STN as an input structure into the basal ganglia – a control center for motor and cognitive behavior (Tewari, Jog, & Jog, 2016). The basal ganglia are subdivided into three functional units; the motor, associative, and limbic cortical regions innervate, respectively, motor, associative, and limbic regions of the striatum, pallidum, and substantia nigra pars reticulata (SNr) (Hamani, Saint-Cyr, Fraser,

Kaplitt, & Lozano, 2004). A similar functional subdivision has been applied to the STN based on cortical projections (Tewari et al., 2016). The dorsolateral STN contains the sensorimotor region; direct projections from the primary motor cortex and supplementary motor area (SMA) are received here. The ventromedial STN contains the associative region with projections from the premotor cortex, prefrontal cortex, pre-SMA, SMA, frontal eye field, and supplementary eye field (Tewari et al., 2016). The limbic region is located in the medial tip of the STN, receiving projections from the caudal cingulate motor area (*Figure 2*; Tewari et al., 2016).



© Frontiers Media. Adapted with permission.

**Figure 2: Subthalamic Nucleus (STN) subdivision into three functional units; the sensorimotor, associative, and limbic regions**

Cortical inputs into each region depicted by individual arrows. SMA: supplementary motor area; M1: primary motor cortex; PFC: prefrontal cortex; FEF: frontal eye field; SEF: supplementary eye field; PMC: premotor cortex.

The purpose of investigating the functional organization of the STN is to determine if there is an optimal stimulation site for DBS. There is evidence to show that the dorsolateral STN border is included in the optimal stimulation site – which is valid since the dorsolateral portion is the sensorimotor region with inputs from motor cortical areas. Included in the evidence pointing towards this conclusion is a study by Herzog and his colleagues who evaluated the optimal stimulate site in 14 patients treated by bilateral STN-DBS (Herzog et al., 2004). The position of the most effective contact on a quadripolar electrode lead was evaluated using preoperative magnetic resonance imaging (MRI) scans, electrophysiological recording, and postoperative stereotactic x-ray images

(Herzog et al., 2004). The best clinical results with the least energy consumption were found in contacts located in the dorsolateral border zone, whereas contacts within the STN white matter were significantly less effective (Herzog et al., 2004). Although the study does not provide a mechanism for DBS, it reinforces the relevance of the neighboring structures at the dorsolateral STN boundary in alleviating parkinsonian symptoms (Herzog et al., 2004).

### 1.2.3 Fundamentals of neuronal stimulation

Defining the response of the neural elements, near the site of the electrode, to the applied electric field can contribute to the understanding of the effects of DBS. The DBS electric field is a three-dimensionally complex phenomenon that is generated by the redistribution of charged ions in the extracellular space of neurons (McIntyre & Anderson, 2016). Since the 1960s, an upheld view was that the primary effect of electrical stimulation in the brain was the generation of action potentials. The action potential is a change in the electrical potential across the neuronal membrane caused by the flow of electrical charges (Montgomery Jr., 2017). DBS works by depolarizing the neural membrane to reach the activation threshold for action potential generation. The axon of a neuron has the lowest threshold for activation; therefore DBS exerts its effects in the axon at the action-potential-initiating-segment, which is typically (but not necessarily) the axon hillock (Montgomery Jr., 2017). An action potential can propagate in both directions; the action potential moving toward the synapse is traveling orthodromically, which is typical in biological systems, whereas the action potential moving in the opposite direction toward the cell body or soma is travelling antidromically. Antidromic activation has important physiological implications and may mediate the therapeutic effects of DBS. Research has shown that stimulation of the GPi activates axons from the ventral thalamus pars oralis, causing antidromic activation of thalamic neurons (Montgomery Jr., 2017). This goes to show how the effects of stimulation can propagate widely beyond the local site of the DBS active contact. In addition to the composition of neural elements that make up the stimulation target, other factors also determine the effects of stimulation including the afferent and efferent pathways associated with the target and the amplitude, pulse width and frequency of the applied current (Laxton, Dostrovsky, & Lozano, 2009). Given that

electrical stimulation can spread to affect neural elements outside of the immediate nucleus being stimulated, one might argue that STN or GPi stimulation is a way of labeling where the electrodes are placed to deliver electrical pulses as opposed to using it as a convention for the stimulation of a specific nucleus. Although there is evidence to show the neuronal responses to DBS, insight into the therapeutic mechanisms and specifically, why targets such as the STN and GPi provide clinical benefit remains unclear. A growing number of studies have been conducted to investigate whether the therapeutic action of DBS is an excitatory or inhibitory nervous system response.

#### 1.2.3.1 Does DBS elicit an inhibitory or excitatory response?

Although evidence points to DBS pulses causing the generation of action potentials in axons near the electrode, other theories argue in favour of reduced neuronal firing. Due to the observation of similar clinical effects, it is possible that DBS and surgical lesions share a similar mechanism of action through the inhibition of neuronal activity (Laxton et al., 2009). One potential way of carrying out neuronal inhibition is through the alteration of cellular and membrane properties by the application of high frequency stimulation (HFS) (Laxton et al., 2009). An *in vitro* study found that HFS decreases the excitability of neurons in the rat STN through inactivation of voltage-gated sodium and calcium currents (Beurrier, Bioulac, Audin, & Hammond, 2001). Therefore, HFS shows the ability to block depolarization by transiently depressing calcium channels (Beurrier et al., 2001). Another study showed that HFS causes increased extracellular potassium levels in rat hippocampal slices (Bikson et al., 2001). These elevated potassium levels depolarize the neuron to produce a depolarization block. Persistent membrane depolarization induces this depolarization block, which results in the inactivation of voltage-gated sodium channels and by extension, prevents action potentials (Bikson et al., 2001). The application of *in vitro* findings to the understanding of DBS effects is somewhat trivial due to the fact that current densities in animal studies are much higher than those used in human DBS and the slice preparations lack many of the connections and pathological activity patterns that exist in human PD patients (Laxton et al., 2009).

A study using human PD patients found that stimulation at high frequencies (100-300 Hz) can decrease the firing rate in STN neurons that are 600 microns away from the

stimulation site (Filali, Hutchison, Palter, Lozano, & Dostrovsky, 2004). Furthermore, another study showed that low frequency microstimulation (5 Hz) within the GPi caused inhibition of GPi neurons lasting a duration of 10-25 ms (Dostrovsky et al., 2000). Although studies of HFS suggest that stimulation inhibits neuronal activity, other studies have shown that the effect of stimulation is variable and can be excitatory (Laxton et al., 2009). Electromyographic responses to HFS of the STN that were analyzed in 14 patients with parkinsonism did not reveal evidence for stimulation blocking neuronal activity; rather, the ability of HFS to reduce tremor in the contralateral limbs of five patients resulted from the activation of large-diameter axonal fibers (Laxton et al., 2009). One way to reconcile these differences in study conclusions is to keep in mind that DBS may be a chemical therapy; depending on the specific pathway being stimulated, the downstream effect could be inhibitory via modulated GABA release or excitatory via modulated glutamate release (McIntyre & Anderson, 2016). Therefore, when HFS is excitatory, the effect can be on GABAergic axons which eventually reduces the neuronal firing rates in the STN or GPi to have an inhibitory influence (Laxton et al., 2009). For example, direct stimulation of the GPe axonal afferents can theoretically generate GABA release in the STN through antidromic activation, thus having a possible inhibitory effect on STN efferents.

Local field potentials (LFPs) recorded from the basal ganglia can provide insight regarding the mechanisms of DBS. LFPs indicate the oscillatory activity of a neuronal population surrounding the recording electrode and can be categorized according to specific frequency bands (Wagle Shukla et al., 2017). Beta band oscillations contain a frequency range between 11 Hz and 30 Hz and excessive synchronization of basal ganglia neuronal activity in the beta frequency band has been implicated in some forms of PD (Eusebio & Brown, 2009). Bronte-Stewart and colleagues recorded LFPs intraoperatively from the STN and showed excessive synchronization at beta frequencies at rest in 16 PD patients undergoing DBS (Bronte-Stewart et al., 2009). The study also showed suppression of beta activity with attenuation lasting for 10 seconds after 30 seconds of DBS and for up to 50 seconds after five minutes of DBS; this finding suggests there may be long-acting functional changes to basal ganglia networks in PD after chronic DBS (Bronte-Stewart et al., 2009). However, several studies have led to the

general consensus that beta synchrony is not causally linked to parkinsonian tremor but could be a good biomarker of the akinetic-rigid state in both patients and animal models of parkinsonism (Eusebio & Brown, 2009).

#### 1.2.4 Monopolar and multipolar stimulation

Four electrical contacts on the typical DBS lead allow for a large combination of active contacts and by extension, different fields of electrical current coming in contact with neural elements (Montgomery Jr., 2017). Within the DBS target, the combinations of active contacts can be divided into monopolar or multipolar (Montgomery Jr., 2017). Monopolar refers to the active contact within the stimulated structure being negative (cathode) whereas the positive contact (anode) is the IPG itself. Multipolar configurations have more than one active contact within the stimulated structure which can include both negative and positive contacts (Montgomery Jr., 2017). A bipolar (type of multipolar) configuration has a single negative and single positive contact in the DBS target (Montgomery Jr., 2017).

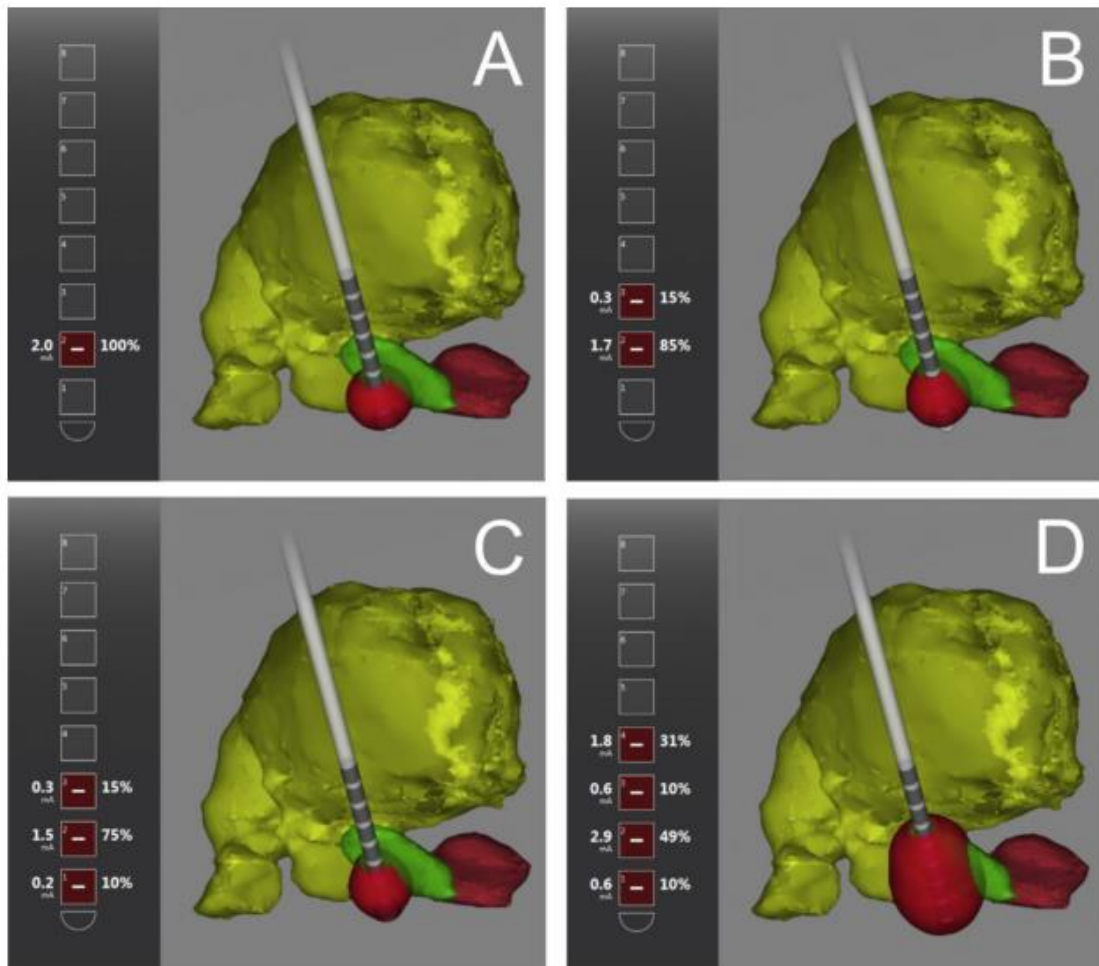
#### 1.2.5 Current-based programming and current steering

IPG output can be a voltage-controlled or, more recently, current-controlled system. Current-controlled systems adjust the voltage for a given impedance in order to deliver a constant current output (Kopell et al., 2009). Voltage-controlled systems automatically adjust the current to compensate for impedances (Kopell et al., 2009). Although for several years DBS therapy involved voltage-controlled systems, the fluctuations in impedance values at the electrode-tissue interface cause an instability in the electrical charge delivered to the target. Low impedance values could cause high current densities at the electrode-tissue interface and result in possible tissue damage (Kopell et al., 2009). High impedance values result in a large voltage drop at the electrode-tissue interface and decrease the effectiveness of stimulation (Kopell et al., 2009). The clinical results from current-controlled systems are less subject to changes in impedances over time because the voltage gets automatically adjusted (Kopell et al., 2009). As a result, DBS programming is more effective and reliable with current-controlled systems.



Conventional DBS technology relied on a single current source to produce an electrical field that is spherical; this causes limited capability to minimize unintended current spread to anatomical structures that can cause side effects. Both the clinical effects and side effects caused by stimulation depend on the direction and amount of current spread to neighboring anatomical structures (Wagle Shukla et al., 2017). As discussed, the optimal location for STN stimulation is the dorsolateral region for control of motor symptoms. Medial spread of current from the dorsolateral region can stimulate the limbic region of the STN, cranial nerve III and the red nucleus, causing side effects such as diplopia, eye deviation, dizziness, sweating, nausea, paresthesia, warm sensation, depression and impulsivity (Wagle Shukla et al., 2017). Lateral spread of current can stimulate the corticospinal tract and frontal eye field fibers of the internal capsule, causing facial pulling, limb contraction and contralateral deviation of gaze (Wagle Shukla et al., 2017). Posterior spread of current can stimulate the medial lemniscus and cause paresthesia (tingling, electrical sensation, numbness) and ventral/inferior spread of current can stimulate the SNr and internal capsule fibers, causing mood changes, depression and muscle contractions (Wagle Shukla et al., 2017). As a result, clinical benefit with minimal side effects can only be achieved by steering current away from these structures. Newer systems with multiple independent current sources makes it possible to fractionate current amplitude between two or more active contacts on a lead – a phenomenon known as current steering (Timmermann et al., 2015). DBS devices that allow the fractionation of current using a type of multipolar configuration enables the application of a shaped electrical field (Timmermann et al., 2015). This means that combinations of different percentages allow for differences in electrical field shape (*Figure 3*; Barbe, Maarouf, Alesch, & Timmermann, 2014). This shaped electrical field can possibly enhance the motor response of patients while minimizing stimulation-related side effects. The Vercise DBS system by Boston Scientific is a current-controlled system that allows for current steering. The Vercise lead consists of eight contact rings, 1.5 mm in length, placed one above the other with 0.5 mm spacing between contacts (Timmermann et al., 2015). Given the numerous combinations available for current amplitude fractionation which lead to many different electrical field shapes, current steering is part of the advancement to a more individualized form of DBS therapy. An

overview of present literature investigating the effects of current steering is discussed below.



© Elsevier. Used with permission.

### Figure 3: Altered electrical field shape using current steering

Electrode location shown in anatomical relation to the thalamus (yellow), STN (green), and red nucleus (maroon). A: 100% of the current amplitude delivered from contact #2 is a monopolar stimulation creating a spherical electrical field (red). B: Current amplitude fractionation over two contacts shifts current field (red) more dorsally. C: Current amplitude fractionation over the bottom three contacts (10% on contact #1, 75% on contact #2, 15% on contact #3) produces a non-spherical electrical field (red). D: Current amplitude fractionation over four contacts further elongates the electrical field (red) to stimulate more dorsal structures such as the zona incerta.

#### 1.2.5.1 Studies investigating current steering during STN-DBS

The available literature on clinical trials that investigate the effectiveness of current steering is limited due to the relatively recent introduction of current steering DBS

devices into the market. Most studies have either focused on the safety and efficacy of the new DBS system or have used computational modeling to predict the volume of tissue activated with current steering, but few have directly tested current steering settings on PD patients undergoing STN-DBS. One of the most cited studies in this area is the VANTAGE study; a multicenter, non-randomized clinical trial evaluating the multiple-source, constant-current Vercise DBS system by Boston Scientific. 40 PD patients who underwent bilateral STN-DBS were assessed 12, 26, and 52 weeks after implantation; the primary endpoint was the mean change in Unified Parkinson's Disease Rating Scale (UPDRS) motor scores from baseline to 26 weeks after implantation in the stimulation-on, medication-off state (Timmermann et al., 2015). The treating clinician identified the contact that provided the best clinical effect and in the case of side effects or absence of efficacy, current was fractionalized over the ideal contact and the next best contact (Timmermann et al., 2015). PD patients significantly improved by 62.6% (+/- 19.8) when comparing baseline UPDRS motor scores with six month postoperative scores. At 26 and 52 weeks post implantation, approximately 70% of stimulation programs had current fractionalized over two or more contacts. The remaining programs used a monopolar configuration. This study shows that in the case of suboptimal DBS therapy, the use of current steering across two or more contacts can be used to suppress motor symptoms more effectively than monopolar configurations.

A case study published in 2014 was the first report showing the effects of multiple source current steering in humans. The case focused on a single patient, a 60-year-old male diagnosed with PD for 13 years, who was treated with bilateral STN-DBS with the Vercise DBS system. Before surgery, he had a levodopa response of almost 80% based on UPDRS motor scores, however medications resulted in severe dyskinesia resulting in social life exclusion (Barbe et al., 2014). One week after implantation, the left lead was programmed with a monopolar stimulation setting, whereas the right lead needed more fine tuning with current steering. A standard monopolar review is a post-operative programming strategy that individually tests each stimulation contact on a lead by increasing current amplitude in small increments to test for symptom improvement or any adverse effects. After going through a series of possible settings, the patient was set on an overall current amplitude of 5.9 mA on the right STN lead, fractionalized over the bottom

four contacts. Contact #2 (from ventral to dorsal) received 50% current stimulation because the monopolar review identified this contact as producing the best therapeutic effect, however further increasing amplitude on contact #2 induced dyskinesia (Barbe et al., 2014). Contact #3 received 10% current stimulation to reshape the field and maintain the clinical effect of contact #2 (Barbe et al., 2014). Contact #4 received 30% current stimulation because the authors assumed further improvement in tremor and dyskinesia was due to the stimulation of the zona incerta (for tremor alleviation) and pallidofugal fiber tracts (for dyskinesia alleviation) located dorsal to the STN (Barbe et al., 2014). Contact #1 received 10% current stimulation because the patient continued to experience some apathy and the authors hypothesized that improvement of apathy with contact #1 stimulation was due to targeting of the limbic STN (Barbe et al., 2014). With this current steering setting, the patient's UPDRS motor score improved from 45 points before therapy to 15 points with DBS and their levodopa dose decreased by 70% three months after surgery (Barbe et al., 2014). Over two years after the surgery, the patient was still reporting excellent results including clear speech, good gait, excellent postural reflex, no rest tremor and only tiny action tremor (Barbe et al., 2014). Overall, this case report showed that current steering minimized side effects and led to a good reduction of all PD motor symptoms.

A pilot study using a novel directional DBS device was published in 2016 to evaluate the effects of current steering in horizontal directions. Seven PD patients implanted with the novel directional lead underwent bilateral STN-DBS; the novel lead has four electrode levels with the two middle levels split into three segments spanning approximately 120 degrees (Steigerwald, Müller, Johannes, Matthies, & Volkmann, 2016). Each segment is capable of independent stimulation such that 100% of current amplitude is capable of being delivered from approximately one third of the contact ring. An extended monopolar review during the first postoperative week determined a therapeutic window for 111 directional settings and 24 ring-mode settings across the seven patients. Although there was high variability between leads and directional settings, there was a general trend of an expansion of the therapeutic window with the directional settings (Steigerwald et al., 2016). Overall, this study shows the effects of directional current steering in the expansion of the therapeutic window during monopolar review, as compared to ring-

mode stimulation. The benefits of directional stimulation were best appreciated in cases of suboptimal electrode positions resulting in a narrow therapeutic window. Suboptimal lead positioning can occur at any stage during the DBS procedure.

### 1.3 STN-DBS procedure

The DBS procedure might vary between neurosurgical teams with regards to equipment, however the surgical techniques are similar. The planning of the procedure starts off by using pre-operative MRI scans, which are used to construct the stereotactic target using graphic tools and various atlases that are available on navigation software (Benabid, Chabardes, Mitrofanis, & Pollak, 2009). The planning stage allows surgeons to choose an entry point that will avoid puncturing vessels, including those located at the cortical surface, ventricle, or caudate nucleus. With the patient in a stereotactic head frame, the anterior and posterior commissures are identified; STN coordinates are based on a stereotactic brain atlas at 12 mm lateral, 2 mm posterior and 5 mm caudal to the midcommissural point (Yoon & Munz, 1999). An incision in the scalp is then made according to the desired trajectory of the lead and a burr hole is drilled. The planned track is used for electrophysiological exploration using multiple microelectrodes; participants of the current thesis usually had five microelectrodes initially inserted for exploration. Typical firing patterns obtained from the microelectrode recording (MER) is used for STN localization; asymmetrical spikes at high frequency with bursting patterns are characteristic features of the STN, whereas symmetrical spikes of large amplitude and regular activity are characteristic of the SNr (Benabid et al., 2009). Firing patterns along with patient feedback from stimulation of the microelectrodes (patient is awake with local anesthesia) is used to determine optimal placement of the chronic/permanent DBS lead. The IPG is inserted under general anesthesia into a subcutaneous pouch in the subclavicular area (Benabid et al., 2009).

#### 1.3.1 Reasons for lead misplacement

Appropriate lead placement is a vital component in the success of DBS. However, even some of the most experienced centers using the most up-to-date technology will have occurrences of misplaced leads (Ellis et al., 2008). Current pre-operative targeting is

performed using T2-weighted MRI images whose quality can be compromised enough to affect visualization of the STN. 7 Tesla (T) MRI, which uses a stronger magnet than the more common 1.5 T or 3 T MRI, offers higher contrast-to-noise T2-weighted images, but its current clinical applicability is limited (Fasano & Lozano, 2015). T2-weighted images in general contain substantial blooming artifacts that cause distortion and prevent the precise localization of the STN (Fasano & Lozano, 2015). Even if pre-operative planning is adequate to continue, complications and minor mishaps during the actual surgical procedure can contribute to lead misplacement. If the frame is misaligned or shifts during surgery, the lead may deviate to an unintended target (Ellis et al., 2008). As discussed above, intraoperative MER is used for verification of lead localization; however, errors due to poor technique or interpretation of MER data can jeopardize accuracy. Brain shifts may also occur at any time in the surgical process, including preoperative imaging, microelectrode recording, lead placement, or when a cerebrospinal fluid leak is detected (Ellis et al., 2008). Additionally, lead deflection is possible due to changes in tissue density, the angle of approach, or collision with the burr hole or the capping device (which fastens the permanent lead into place) (Ellis et al., 2008). Given the numerous reasons for lead misplacement, current steering—to an extent—allows stimulation to be directed toward the target region. As discussed next, the target region for each symptom may differ due to differences in pathology.

#### 1.4 Pathophysiology of bradykinesia

The term bradykinesia covers a range of problems in the control of movement; in all cases, the principal deficit is that movements are slow (Berardelli, 2001). Bradykinesia is often used synonymously with the terms akinesia and hypokinesia. Specifically, bradykinesia refers to the slowness of a performed movement whereas akinesia refers to poverty in spontaneous movement such as in facial expression, or associated movement such as arm swing during walking (Berardelli, 2001). Hypokinesia refers to movements that are smaller than desired, especially with regards to repetitive movements. In addition to whole-body slowness, bradykinesia also includes impairments in fine motor control, which is demonstrated in PD patients during rapid alternating movements of fingers, hands, or feet as a progressive reduction of speed and motion amplitude (Magrinelli et al.,

2016). Although secondary factors such as muscle weakness, tremor and rigidity may contribute to bradykinesia, primary bradykinesia is potentially due to slowness in formulating the instructions to move (i.e. programming) or to slowness in executing these instructions (Berardelli, 2001). Based on studies that reflect motor execution as well as programming, bradykinesia seems to result primarily from the underscaling of movement commands in internally generated movements (i.e. in the absence of external cues); this leads to insufficient recruitment of muscle force during the initiation of movement (Berardelli, 2001). This has led to the suggestion that bradykinesia is a problem of scaling motor output appropriately to the task, rather than to any intrinsic limitation in motor execution (Berardelli, 2001). Deficits in movement preparation in PD patients have been supported by slower reaction times and slower increase in premovement cortical excitability, which suggest abnormal retrieval of stored motor commands (Magrinelli et al., 2016).

The pathophysiology of bradykinesia is not completely understood; however, among the cardinal motor symptoms of PD, it fits better with the classical model of basal ganglia function which points at the prevalence of the indirect pathway over the direct one. The details of this model are outlined in section 1.1.1 and visually presented in *Figure 1*. The prevalence of the indirect pathway in this model is used to explain the pathophysiological hallmark of PD hypokinetic symptoms as resulting from increased neuronal firing in the GPi and SNr, leading to excessive inhibition of thalamocortical and brainstem motor systems and causing interference with the speed of movement onset and execution (Magrinelli et al., 2016). Furthermore, according to this model bradykinesia may result from the failure of basal ganglia output to reinforce cortical mechanisms responsible for the preparation or execution of movement (Magrinelli et al., 2016). The idea that beta synchrony in LFP recordings is implicated in bradykinesia was alluded to in section 1.2.3, which also discussed the finding that DBS was able to suppress the excessive synchronization. To add to this, premovement electroencephalogram (EEG) beta desynchronization is reduced in PD patients and this abnormality is partially normalized by dopaminergic stimulation (Magrinelli et al., 2016). In addition to suppression by DBS, there is also evidence for beta band synchrony suppression by levodopa, that was

similarly demonstrated to correlate with improvement in bradykinesia and rigidity, but not tremor (Magrinelli et al., 2016).

### 1.5 Pathophysiology of rigidity

Rigidity is characterized by increased muscle tone at rest, increased tension during passive movement and increased resistance to stretching (Rodriguez-Oroz et al., 2009). Although both flexor and extensor muscle groups are involved, flexor muscles of the limbs are more affected in the early stages of the disease (Rodriguez-Oroz et al., 2009). Rigidity may be enhanced by voluntary movement of other body parts, and increased resistance is more noticeable when the examined joint is stretched slowly (Magrinelli et al., 2016).

The pathogenesis of PD rigidity has been hypothesized to include changes in the passive mechanical properties of joints, tendons and muscles, the enhancement of stretch-evoked reflexes, and abnormalities in peripheral sensory inputs that can influence the response to muscle stretch (Magrinelli et al., 2016). The way these changes are associated with dopamine deficiency, or basal ganglia output as depicted by the classical model, remains unclear (Magrinelli et al., 2016). The classical model predicts that increased neuronal activity in the GPi/STN and the resulting inhibition of thalamocortical projections should result in decreased muscle activation and reduced response to stretching; however, the opposite is observed with rigidity (Baradaran et al., 2013). Despite the ambiguity, surgical interventions focusing on the basal ganglia and motor thalamus has a proven anti-rigidity effect, indicating a role of the motor circuit in the pathogenesis of rigidity (Rodriguez-Oroz et al., 2009).

Although the pathogenesis of rigidity remains more elusive than other PD cardinal symptoms, evidence points to a stronger link to bradykinesia than to hyperkinetic symptoms. As discussed above, excessive beta synchronization in LFP recordings relates only to the bradykinetic-rigid state that is reversed by dopaminergic therapy (Eusebio & Brown, 2009). In addition, a longitudinal study looking at the progression of parkinsonian signs found that bradykinesia and rigidity worsened at similar rates in a cohort of 237 PD patients, whereas tremor did not (Louis, Tang, & Cote, 1999).



Suppression of bradykinesia and rigidity also requires lower dosages of levodopa than tremor (Nonnekes, Timmer, Vries, & Rascol, 2016). There is also evidence to show that when stimulating the STN during DBS, dorsal/superior spread of current reaching the internal capsule, thalamus and zona incerta causes improvement in hyperkinetic symptoms including tremor and dyskinesia, but not hypokinetic symptoms (Wagle Shukla et al., 2017). Taken together, these conclusions point toward a relationship between rigidity and bradykinesia management that is separate from tremor.

## 1.6 Pathophysiology of PD tremor

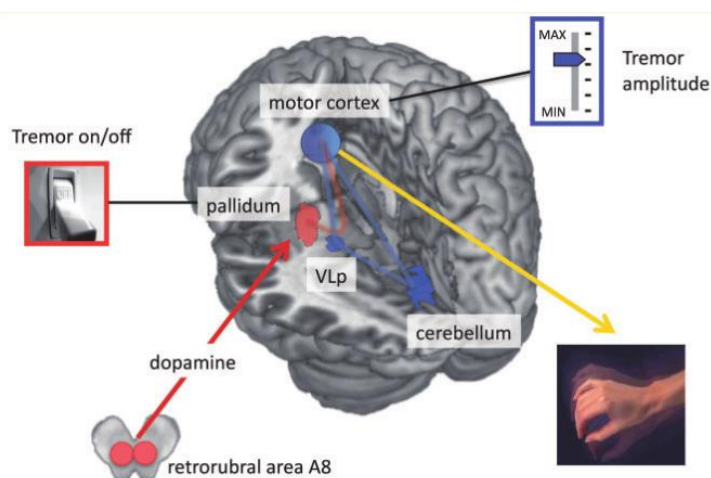
Tremor, one of the cardinal motor symptoms of PD, is defined as a rhythmic, involuntary, oscillating movement of one or more body parts (Helmich & Dirkx, 2017). Unlike other motor symptoms, tremor severity does not correlate with the degree of striatal dopamine depletion and therefore, tremor response to dopaminergic medication is subpar when compared to bradykinesia and rigidity (Helmich & Dirkx, 2017). Tremor also has many types – the classical PD tremor occurs at rest with a frequency of 4 to 6 Hz (Helmich, Toni, Deuschl, & Bloem, 2013). Many PD patients also have action tremor produced by voluntary contraction of muscle, and includes postural, isometric, and kinetic tremor (Helmich et al., 2013). In 34-60% of PD patients, action tremor can be classified as reemergent resting tremor (Helmich et al., 2013). Reemergent tremor occurs after a delay of two or more seconds after the limb affected by resting tremor assumes a new posture; it occurs at the same frequency as resting tremor and it responds to levodopa (Helmich et al., 2013). Action tremor that is not reemergent tremor occurs at a higher frequency, between 6 and 15 Hz, and it does not respond to levodopa (Helmich et al., 2013). It is possible that reemergent tremor and resting tremor in PD are caused by the same mechanisms, although this finding has not been previously tested (Helmich et al., 2013). One finding supporting this view is that in many PD patients, voluntary actions suppress resting tremor, but does not completely interrupt it (Helmich et al., 2013).

There is a consensus towards central, rather than peripheral, mechanisms being responsible for parkinsonian tremor (Helmich & Dirkx, 2017). This is supported by the fact that high-frequency DBS of both the basal ganglia and the thalamus is effective in treating tremor. Studies using intraoperative recordings have found neural oscillations in

the basal ganglia and the ventral intermediate nucleus of the thalamus (Vim) with the same frequency as tremor (Helmich & Dirkx, 2017). An important finding is that pallidal neurons are only transiently and inconsistently coherent with tremor, whereas neurons of the Vim are highly synchronous; this suggests that the thalamus contributes more to the driving force behind tremor (Helmich & Dirkx, 2017). One of the first hypotheses regarding the pathophysiology of tremor was the thalamic pacemaker theory, which states that hyperpolarized cells in the thalamus act as the tremor pacemaker (Helmich & Dirkx, 2017). The basis for this hypothesis lies in *in vitro* studies showing that slightly depolarized thalamic cells oscillate at 10 Hz, whereas hyperpolarized cells oscillate at 6 Hz. These two frequencies coincide with the frequency of physiological tremor and PD tremor, respectively (Helmich, Hallett, Deuschl, Toni, & Bloem, 2012). In the animal model, the 6 Hz oscillatory mode is associated with low threshold calcium spikes, which often follow membrane hyperpolarization. However, this pattern was not observed in the thalamus of tremor-dominant PD patients (Helmich et al., 2012). Other theories argue that the tremor pacemaker resides within the basal ganglia, but the theories remain incomplete due to strong clinical evidence showing the efficacy of Vim-DBS in treating tremor. More recent studies have been used to construct a model that integrates the role of both the basal ganglia and the cerebellothalamic circuits in tremor. The dimmer-switch model of parkinsonian resting tremor introduces the idea of dopaminergic cell death in the retrorubral field, located dorsally and caudally to the SNc.

Although loss of neurons in the SNc has become the pathological hallmark of PD, tremor-dominant patients have milder degeneration of the SNc and instead, more extensive dopaminergic cell loss in the retrorubral area (RRA) of the midbrain (Helmich & Dirkx, 2017). The exact role of the RRA in the pathogenesis of PD tremor remains elusive. However, there is evidence to show that resting tremor may result from pallidal dopamine depletion, resulting from the loss of dopaminergic projections from the RRA to the pallidum (Helmich, Janssen, Oyen, Bloem, & Toni, 2011). This pallidal dysfunction leads to pathological activity in the striato-pallidal circuit, which triggers activity in the cerebellothalamocortical circuit through the primary motor cortex to produce tremor (Helmich et al., 2011). The dimmer-switch model (*Figure 4*; Helmich, Hallett, Deuschl, Toni, & Bloem, 2012) attempts to explain the interaction between the basal ganglia and

the cerebellothalamocortical circuit in the generation and maintenance of resting tremor. Rick Helmich and colleagues used concurrent electromyography (EMG) and functional magnetic resonance imaging (fMRI) to show that the basal ganglia operates analogous to a light switch that ‘turns on’ tremor, and the cerebellothalamocortical circuit operates analogous to a light dimmer that modulates tremor amplitude (Helmich et al., 2012).



© Oxford University Press. Used with permission.

#### **Figure 4: Dimmer-switch model of PD resting tremor**

Dopaminergic cell death in the retrorubral area in tremor-dominant PD causes dopamine depletion in the pallidum (in red). This leads to a pathological signal that triggers the cerebellothalamocortical circuit (in blue) through the primary motor cortex. Therefore, the striato-pallidal circuit causes the onset of tremor (analogous to a light switch) while the cerebellothalamocortical circuit produces the tremor and controls its amplitude (analogous to a light dimmer). VLp: ventral posterolateral nucleus of the thalamus.

### 1.7 Rationale and hypothesis

As pointed out in *Figure 2*, the target region for motor symptom alleviation is ideally the sensorimotor portion of the STN, located in the dorsolateral region. Due to suboptimal placement of the DBS lead during surgery, the target can be completely missed, or stimulation of the target can also include current spread to adjacent regions, leading to adverse effects discussed above. It has been reported that lead misplacement beyond a 2-3 mm window may result in inadequate clinical benefit (Ellis et al., 2008). Furthermore, two referral centers for DBS troubleshooting reported that therapy failure in half of the evaluated leads was caused by suboptimal positioning (Schüpbach et al., 2017). Even with a theoretically optimal lead location, the functional target can vary from patient to

patient due to differences in disease phenotype or anatomical variations of the target. Current steering is a potential solution to address these issues by steering current to the optimal region in cases of suboptimal lead position, or steering current away from stimulating non-motor areas of the target or neighboring tissue which can cause adverse side effects. Technological advancements have made it possible to create non-spherical electrical field shapes by fractionating current over two or more active contacts. Different electrical field shapes can stimulate desired structures to different degrees of symptom alleviation. Therefore, an optimal electrical field shape would localize current to the desired structure and avoid unintended stimulation of neighboring anatomical structures for optimal symptom improvement. *Thus, it was hypothesized that the way the electrical field is shaped affects a patient's upper limb symptom alleviation.*

The present literature on current steering (section 1.2.5.1) all contribute to the advancement of a more individualized form of DBS therapy. Although the first two studies employed the fractionation of current over two or more contacts (Barbe et al., 2014; Timmermann et al., 2015), the method used to figure out which setting each patient was programmed with was a case-by-case scenario; the programming clinician adjusted stimulation settings continually until optimal clinical effects were observed. With the VANTAGE study (Timmermann et al., 2015), the reader is unaware of the impact that a certain current steering setting had across all patients or if one setting happened to benefit multiple patients optimally. The current thesis provides a more systemic approach that looks at the effects of current amplitude and a set of current steering settings across all patients. Detail about the current steering programs was also not revealed in the literature; the number of contacts involved, and the percentage of current received by each contact in the stimulation programs was not disclosed. In addition, information about the response of each type of motor symptom to current steering was lacking; although there was a reduction in the overall UPDRS motor score from baseline, it is unclear as to what extent each individual symptom was improved. The current thesis assesses the response of specific motor symptoms to test how one type of current configuration impacts different symptoms in the same limb.

The goal of the current thesis was to explore the effectiveness of current steering as it relates to appendicular motor symptoms of the upper limbs. These appendicular symptoms include rest tremor, postural tremor, bradykinesia and rigidity. This study tested 16 different current fractionation settings; four of these settings solely employ monopolar stimulation whereas the remaining 12 employ current steering either unilaterally or bilaterally. As touched upon earlier, the current field created by DBS systems that allow for current steering is not limited to the relatively spherical electrical field created by monopolar stimulation. Current steering can be achieved on a horizontal plane—with directional lead technology—and a vertical plane. Directional leads contain contacts that are split into three segments such that fractionation of current can be achieved in horizontal directions. The DBS system used in this study solely explored current steering in the vertical plane, as demonstrated by *Figure 3*.

### 1.7.1 Summary of objectives

Given the variations in lead position, symptom phenotype, and anatomical factors across patients, the benefits of current steering and/or monopolar stimulation will differ among patients. For this reason, the first objective tests the effectiveness of current steering settings in comparison to the monopolar settings for optimal symptom alleviation. The first objective is as follows:

- 1) Determine the optimal current fractionation setting and amplitude for each patient's upper limb symptom alleviation

The second objective tests if there is a difference in target between the optimal alleviation of hyperkinetic symptoms and hypokinetic symptoms in the same patient. As discussed, the classical model of basal ganglia function (*Figure 1*) and the prevalence of the indirect pathway over the direct one is the pathophysiological hallmark of PD hypokinetic symptoms. The model's prediction of increased STN activity is a plausible reason to target and inhibit the nucleus with DBS, possibly limiting the excessive inhibition of thalamocortical systems responsible for normal movement. Hyperkinetic symptoms, on the other hand, have a different pathophysiology relating to degeneration of the RRA and involvement of the cerebellothalamocortical circuit (*Figure 4*). Therefore, the

management of tremor could possibly involve stimulation of a different region. This means that hyperkinetic symptoms of a limb will be optimally alleviated by settings that differ from those that optimally alleviate hypokinetic symptoms. The second objective is:

- 2) Compare optimal alleviation between hyperkinetic symptoms, rest and postural tremor, and hypokinetic symptoms, rigidity and bradykinesia, in the same limb

## Chapter 2

### 2 Methods

This section outlines the methods used for the current study. Participants underwent bilateral implantation in the STN of a constant-current DBS system capable of current steering. The current steering investigation lasted approximately four weeks for each patient in which a set of clinical tasks was performed after each setting change. Study assessment tools included the UPDRS-III examination as well as motion capture technology that was used to quantify bradykinesia, postural tremor, rest tremor, and rigidity of the upper limbs.

#### 2.1 Study participants

Seven PD patients who underwent bilateral STN-DBS were included in this study analysis; *Table 1* outlines the participant demographics. This study was approved by the Human Research Ethics Board at Western University (REB #108453). The following lists the inclusion criteria for candidates of the study: (1) idiopathic PD with a 30% improvement in symptom response to levodopa treatment, assessed by the UPDRS, (2) II or IV Hoehn-Yahr stage, (3) disabling motor fluctuations with off periods and dyskinesia during on phases, (4) assessed for eligibility for the DBS procedure, (5) able to give informed consent, (6) able to visit the clinic for assessment, (7) no dementia or psychiatric abnormalities on neuropsychological testing. The following lists the exclusion criteria for candidates: (1) previous brain surgery or cardiac pacemaker, (2) moderately severe parkinsonism in the context of unstable pharmacological treatment, (3) dementia as assessed by the Diagnostic and Statistical Manual of Mental Disorders (DSM) V criteria, (4) severe psychiatric symptoms such as hallucinations and depression, (5) bad general health, (6) lack of compliance at follow-up visits. All patients in this study had implantation of the constant-current, multiple-source Vercise DBS System by Boston Scientific; however, the type of lead implanted (non-directional vs. directional) differed among patients. Note that although four out of the seven study subjects had a directional lead implanted, current steering was only investigated in the vertical plane for *all* patients.

**Table 1: Participant pool demographics**

<b>Participant ID</b>	<b>Age (yrs)</b>	<b>Sex</b>	<b>PD Duration (yrs)</b>
BSC 01	55	M	8
BSC 02	52	M	12
BSC 03	69	M	14
BSC 05	63	F	17
BSC 06	57	F	12
BSC 07	75	F	10
BSC 08	61	F	14
Mean (SD)	61.71( $\pm$ 8.10)	-	12.43( $\pm$ 2.94)

*SD: standard deviation of the mean*

## 2.2 Assessment tools

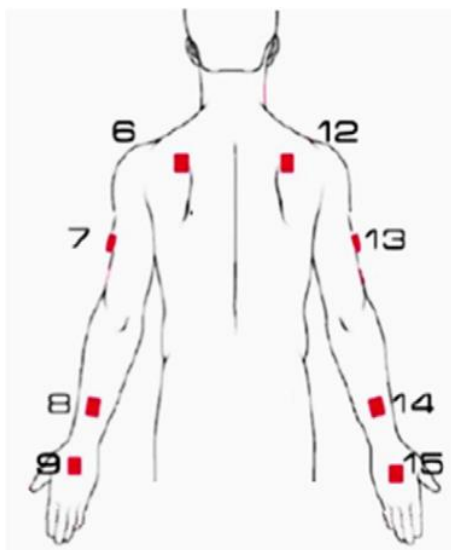
To quantify motor symptoms, a standardized clinical scale and a wearable motion capture system was used. The UPDRS is the most commonly used scale to follow the course of PD; part III of this scale is a whole-body motor evaluation that assesses the severity of certain tasks on a scale of zero to four, zero being normal and four being the most severe (see *Appendix 3*). Most literature on the clinical effects of PD use the motor UPDRS score to quantify symptoms. The problem with this clinical rating scale is that it is subjective to the rater's discretion. Although the examining neurologist or researcher undergoes the same training to administer the UPDRS, the interpretation of the severity of certain motor symptoms can vary from person to person. In addition to the UPDRS motor score, the current thesis used objective kinematic measures to track and quantify body movements similar to motion capture technology used in the entertainment industry.

### 2.2.1 Motion capture system

Research using sensor systems has gained recent interest in the biomedical field to monitor human movement. The strengths of this system include its reliability, validity, flexibility in terms of allowing assessments to be completed outside of clinic, and the ability to provide large quantities of data for assessment of clinical impact (Gilmore & Jog, 2017). The major concern with using this type of assessment technique is the ability to extract relevant features; if not properly analyzed, the sensors can detect small changes in body movement which may not be characteristic of the symptom being quantified (Gilmore & Jog, 2017). These systems usually contain 16-19 inertial measurement unit



(IMU) sensors that are located all over the body and provide information about body segments. Since the current project was only looking at upper limb movements, the wearable motion capture system in this study consisted of IMU sensors placed along the arm (according to *Figure 5*; Delrobaei, Tran, Gilmore, McIsaac, & Jog, 2016). The sensors include 3D accelerometers, 3D gyroscopes and 3D magnetometers within each unit. The relative position and orientation between adjacent sensors enable a fusion software to identify joint angles. The first study subject (BSC 01) started off using IMU sensors from the animation company Synertial Ltd. but switched to sensors from the company Xsens due to better magnetic field detection; the rest of the participants had all their study visits completed with the Xsens sensors. Data acquisition was performed at 60 Hz sampling rate using Xsens MVN 2018 software. For more details regarding the IMU hardware and fusion software, please refer to the study by Delrobaei and his colleagues in 2016 which used a similar procedure to assess PD bradykinesia using wearable technology (Delrobaei et al., 2016).



© Elsevier. Used with permission.

**Figure 5: Position of IMU sensors on the upper limbs**

Four sensors are placed on each arm, along the hand, forearm, upper arm, and shoulder, while patients engage in the clinical tasks.

### 2.3 Clinical tasks and study timeline

To evaluate upper limb bradykinesia, all participants were asked to perform a repetitive pronation-supination task in a seated position as fast and wide as possible for at least 10

seconds. The task was performed individually for each arm and repeated for a total of two trials per arm. Kinematic data was collected using the motion capture system and clinical scale data was collected using item 3.6 (pronation-supination movements of hands) of the UPDRS-III examination. This task was validated against the respective UPDRS item using an IMU-based motion capture system in a study by Delrobaei and colleagues (Delrobaei et al., 2016). To evaluate upper limb rest and postural tremor, all participants were asked to perform and repeat the following tasks for a total of two trials:

- 1) Rest tremor: while sitting, participants rested both of their forearms on the arms of a chair with their wrists hanging off the edge for at least 20 seconds.
- 2) Postural tremor: while sitting, participants fully extended their arms forward with hands pronated at shoulder height level for at least 20 seconds.

Kinematic data was collected using the motion capture system and clinical scale data was collected using item 3.17 (rest tremor amplitude) and item 3.15 (postural tremor of the hands) of the UPDRS-III examination. The two tasks were validated against the respective UDPRS-III items using an IMU-based motion capture system in a second study by Delrobaei and colleagues (Delrobaei et al., 2018). Rigidity of the upper limbs was only evaluated using item 3.3 (rigidity) of the UPDRS-III examination.

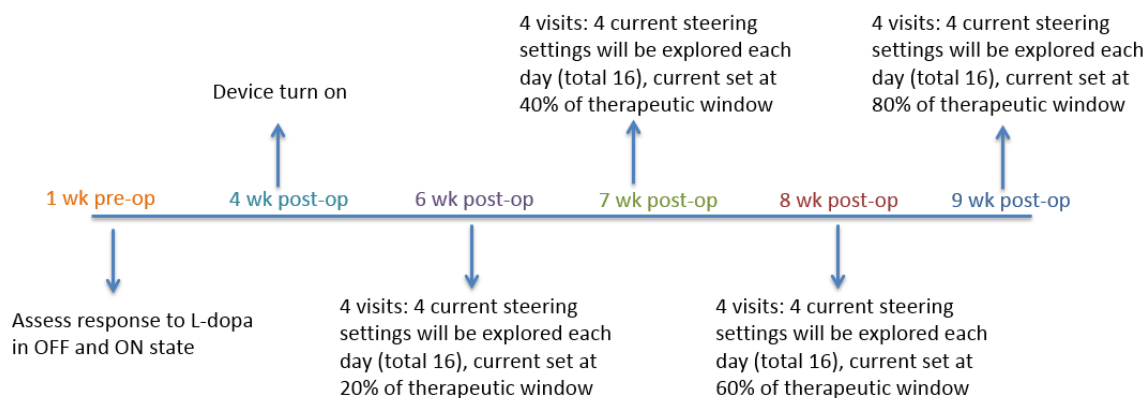


### Figure 6: Study timeline

Pre-assessment occurs within a week before the DBS surgery. Device turn-on occurs at least four weeks post-operation. The current steering investigation begins at least six weeks post-operation and lasts for a duration of four weeks.

As outlined on the timeline in *Figure 6*, study participants were first assessed within one week prior to their DBS surgery to determine their response to levodopa medication. Patients arrived at this visit off any form of levodopa medication for 12+ hours; kinematic and UPDRS-III data were collected in the medication-off state according to the clinical tasks mentioned above. Patients were then instructed to take 135% of their usual levodopa dose and wait approximately 45 minutes for maximal effect of the medication; kinematic and UPDRS-III data were collected in the medication-on state. At least four weeks after their DBS surgery, device turn-on occurs. During this visit, a standard monopolar review of the bottom (ventral) four contacts on the right and left leads was performed by stimulating each contact individually and increasing current amplitude in increments of 0.5 mA. An efficacy threshold (minimum amplitude at which improvement in symptoms occur) and adverse effect threshold (amplitude at which the patient begins to experience side effects) were used to determine a therapeutic window of current for each contact. The best contact is one with both a large therapeutic window, and one that requires the least amount of current to produce symptom benefit. The best and next best contact was determined for each patient for current fractionation to occur. Most patients went home from their device turn-on visit on a monopolar stimulation at a minimal level of current (~0.5 mA), with the best contact that was identified on each side of the brain. All patients were programmed with a frequency of 130 Hz for the entire duration of the study and all patients were programmed with a pulse width of 60  $\mu$ s, except BSC 01 who was programmed with 90  $\mu$ s. The choice for stimulation frequency and pulse width as 130 Hz and 60  $\mu$ s was based on majority of literature showing these values to be clinically effective.

At least two weeks after device turn-on, or six weeks post-operation, the month long current steering investigation began. Prior to the investigation, all patients except for the first (BSC 01) underwent a multipolar review of the contacts to confirm that the second-best contact was still the most effective when paired with the best contact. The current steering investigation happened over four consecutive weeks for all patients except for BSC 08, who had a week gap in the middle of the testing period. Each week consisted of four consecutive visits to the lab; 16 settings were explored in one week with four settings tested each day. The 16 different current fractionations are listed in *Table 2*. The

settings were randomized across patients such that each patient did not receive the same order of settings within the week. The same set of 16 settings was repeated in the same order for each patient in the following weeks at increasing amplitudes. During the first of the four weeks, the amplitude was set at 20% of the patient's therapeutic window (TW) according to the following equation:

$$\text{Week \#1 Amplitude} = \text{Lower limit of TW} + (0.20 \times \text{TW}) \quad (1)$$

The same method was used to calculate the amplitude for week #2, week #3, and week #4 at 40%, 60%, and 80% of each patient's therapeutic window, respectively. Note that for BSC 08 only, the amplitude was set at 60% of the therapeutic window at week #4 instead of week #3, and 80% of the therapeutic window at week #3 instead of week #4. However, for simplification, 'Week 3' indicated on *Tables 6-13* signifies a testing amplitude that was 60% of the therapeutic window for *all* patients, and likewise 'Week 4' signifies a testing amplitude that was 80% of the therapeutic window for *all* patients. The following settings were not tested at the respective week's amplitude for the mentioned participants: setting 13 at week 4 amplitude for BSC 03, setting 13 at week 3 and 4 amplitude for BSC 07. The reason for not testing was due to unmanageable dyskinesia that caused discomfort to both participants and interfered with testing equipment.

Patients arrived each day off any levodopa medication for 12+ hours. After each current steering setting was programmed, a 25-minute wait period was given to allow for the stimulation to take effect. Kinematic and UPDRS-III data was collected after each setting change while the patient performed the clinical tasks mentioned above. At the end of each day following the four setting changes, the patient went home with a baseline setting. During the first week of the current steering investigation, patients went home with a baseline setting that fractionated current equally between the best and next best contact (50%-50% split) on the left and right leads, at a minimal amplitude of current. At the end of the week, patients went home with a setting from the 16 tested settings that provided the greatest clinical benefit according to a *total-body* UPDRS-III score, at the week's testing amplitude; this became the new baseline setting with which the patients returned the following week. At the end of the four weeks, patients concluded the study

by going home on the setting and corresponding amplitude that was optimal across all weeks, again according to a total-body UPDRS-III score (*Table 5*).

**Table 2: Current fractionation settings**

Setting Number	Left STN	Right STN
<b>1</b>	A: 100% B: 0%	A: 100% B: 0%
<b>2</b>	A: 100% B: 0%	A: 70% B: 30%
<b>3</b>	A: 100% B: 0%	A: 50% B: 50%
<b>4</b>	A: 100% B: 0%	A: 0% B: 100%
<b>5</b>	A: 70% B: 30%	A: 100% B: 0%
<b>6</b>	A: 70% B: 30%	A: 70% B: 30%
<b>7</b>	A: 70% B: 30%	A: 50% B: 50%
<b>8</b>	A: 70% B: 30%	A: 0% B: 100%
<b>9</b>	A: 50% B: 50%	A: 100% B: 0%
<b>10</b>	A: 50% B: 50%	A: 70% B: 30%
<b>11</b>	A: 50% B: 50%	A: 50% B: 50%
<b>12</b>	A: 50% B: 50%	A: 0% B: 100%
<b>13</b>	A: 0% B: 100%	A: 100% B: 0%
<b>14</b>	A: 0% B: 100%	A: 70% B: 30%
<b>15</b>	A: 0% B: 100%	A: 50% B: 50%
<b>16</b>	A: 0% B: 100%	A: 0% B: 100%

*STN: subthalamic nucleus; A and B represent the best two contacts at the left and right STN; setting numbers in red indicate settings where current steering occurs either unilaterally or bilaterally; the remaining four settings employ bilateral monopolar stimulation.*

### 2.3.1 Feature extraction

Joint angles were obtained from the four IMUs placed along the wrist, elbow, and shoulder of each arm (*Figure 5*). For bradykinesia assessment, the following features were extracted from each joint angle to analyze upper limb motion: standard deviation of the signal (STD), angular velocity (Vel), and variability in terms of time (Time\_Var) and amplitude (Amp\_Var). Joint angle signals were extracted and analyzed for three arm joints to examine wrist rotation relative to the elbow, elbow rotation relative to the shoulder, and shoulder rotation relative to the fixed back reference. For more information regarding the feature extraction process, please refer to section 2.3 of the study published by Delrobaei and his team (Delrobaei et al., 2016). An improvement in bradykinesia would show increases in STD and Vel, and decreases in Time\_Var and Amp\_Var. From

this, the bradykinesia index (BKI) calculation can be derived to quantify bradykinesia for the repetitive pronation-supination task:

$$BKI = \sqrt{\frac{\text{Time}_{\text{Var}} * \text{Amp}_{\text{Var}}}{\text{STD} * \text{VEL}}} \quad (1)$$

The BKI can be calculated individually at each joint involved in generating the arm rotation such that a BKI for the wrist ( $BKI_{\text{Wrist}}$ ), elbow ( $BKI_{\text{Elbow}}$ ), and shoulder ( $BKI_{\text{Shoulder}}$ ), is computed. In the referenced study (Delrobaei et al., 2016), a total arm BKI was calculated according to equation (2) below. However, for the current thesis  $BKI_{\text{Shoulder}}$  was omitted because shoulder rotation was much slower in the participants relative to wrist and elbow rotation and thus total arm BKI was not an accurate reflection of their bradykinetic state. In addition, joint angle signals for the wrist and elbow are combined; the reason for the combined signal is because the relative position of the forearm sensor to the hand and upper arm sensors affects the individual joint angle signals from the wrist and elbow. Therefore, instead of using  $BKI_{\text{Wrist}}$  and  $BKI_{\text{Elbow}}$  that are calculated using joint angles from the wrist and elbow, respectively, the combined signal was used to calculate a total forearm BKI ( $BKI_{\text{Forearm}}$ ) that better reflects the patient's upper limb bradykinetic state (equation (3)).

$$BKI_{\text{Arm}} = \sqrt[3]{BKI_{\text{Wrist}} * BKI_{\text{Elbow}} * BKI_{\text{Shoulder}}} \quad (2)$$

$$BKI_{\text{Arm}} = BKI_{\text{Forearm}} = \sqrt{\frac{\text{Time}_{\text{Var}} * \text{Amp}_{\text{Var}}}{\text{STD} * \text{VEL}}} \quad (3)$$

For tremor assessment, the list of measured joint angles for the right and left arm is displayed in *Table 3*. A tremor severity score (TSS) was calculated at each joint so tremor severity could be quantified for the total arm. To calculate this score, signals containing angular displacements of all arm joints were band-pass filtered from 4 Hz to 20 Hz to eliminate non-tremor movements. The higher end of the filtering range was set at 20 Hz because some forms of action tremor fall between frequencies of 6 Hz and 15 Hz. The root-mean-square (RMS) of each filtered signal associated with each joint was calculated

as the TSS for that joint. The RMS of all joints associated with each limb's TSS was calculated as the TSS for that limb. Therefore, the TSS for each arm is calculated according to equation (4).

**Table 3: List of joint angles for tremor assessment**

<b>Body part</b>	<b>Segment</b>	<b>Motion</b>
Right arm	Right wrist	Flexion/extension Ulnar/radial Pronation/supination
	Right elbow	Flexion/extension Pronation/supination
	Right shoulder	Flexion/extension Abduction/adduction Rotation
Left arm	Left wrist	Flexion/extension Ulnar/radial Pronation/supination
	Left elbow	Flexion/extension Pronation/supination
	Left shoulder	Flexion/extension Abduction/adduction Rotation

$$TSS = RMS [F_{4-20Hz}(J_i)] \quad (4)$$

$J_i$  is the  $i^{\text{th}}$  joint movement; the maximum number of joint movements involved in the calculation for each arm is eight (see *Table 3*).  $F_{4-20Hz}$  represents signals filtered from 4 Hz to 20 Hz, and RMS represents the root-mean-square of all joints forming the signal. For more information regarding the TSS calculation, refer to section 2.4 in the study published by Delrobaei and his colleagues who used the same procedure for monitoring whole-body tremor using wearable technology (Delrobaei et al., 2018).

## 2.4 Data analysis

To determine each patient's weekly optimal setting from kinematic data, raw BKI and TSS values were normalized to a minimum and maximum. The values used for normalization were determined using kinematic data from two neurologists who mimicked the motor performance of a healthy participant when performing the clinical tasks to obtain a minimum BKI and TSS, and that of a severe PD patient to obtain a

maximum BKI and TSS. MATLAB R2017b was used to create 3D scatter plots with bradykinesia values (expressed as a percentage) from each setting plotted on the x-axis, postural tremor values (expressed as a percentage) plotted on the y-axis, and rest tremor values (expressed as a percentage) plotted on the z-axis. The 3D graphs also included kinematic values from each patient's baseline visit which occurred prior to DBS surgery in the medication-off, stimulation-off (OFF) state. The Euclidean distance (ED) of each data point to the center of the graph was calculated according to equation (5); the optimal setting had the smallest ED to the center (represents the minimum of the normalized values).

$$ED = \sqrt{(x_2 - x_1)^2 + (y_2 - y_1)^2 + (z_2 - z_1)^2} \quad (5)$$

A non-parametric Wilcoxon matched-pairs signed rank test was used to compare the ED of the OFF state of patients with the ED of the optimal setting determined from all four weeks. Statistical significance was set at  $p < .05$  (two-sided). Statistics were conducted using GraphPad Prism 7.

To compare UPDRS-III scores across settings for each patient, raw scores from items 3.15 (postural tremor of hands), 3.17 (rest tremor amplitude), 3.3 (rigidity), and 3.6 (pronation-supination movements of hands) were converted to z-scores according to the following equation:

$$Z = \frac{(x - \mu)}{\sigma} \quad (6)$$

x represents the raw item score from 0 to 4,  $\mu$  represents the mean of the item score for all patients at each week,  $\sigma$  represents the standard deviation of the mean. Microsoft Excel 2016 was used to plot the z-scores on radar charts. A chi-squared test was used to assess the types of settings that made up instances where simultaneous optimal alleviation of hyperkinetic and hypokinetic symptoms occurred in the same limb, as well as instances where only optimal alleviation of hyperkinetic or hypokinetic symptoms occurred in a limb. Degrees of freedom was set at 1 and statistical significance was set at



$p < .05$ . Statistics were conducted using guidelines outlined in *Statistical Methods Sixth Edition* (Cochran & Snedecor, 1974).

#### 2.4.1 Electrode localization

Patients in this study underwent post-operative computed tomography (CT) scans that showed the final lead location. Pre-operative MRI scans were co-registered to post-operative CT scans using NiftyReg software, and MER data was brought into the same space to show localization of the DBS lead at the STN. MER electrode coordinates were extracted from the StealthStation planning machine according to the surgical plan. MER data of each patient was used to reconstruct the microelectrode tracks on the MRI/CT fusion and was visualized with 3D Slicer (*Appendix 4*).

## Chapter 3

### 3 Results

This chapter presents the results of seven PD participants who underwent bilateral STN-DBS and an approximate month-long current steering investigation post-operation.

#### 3.1 Study participants: clinical outcomes

Initially, eight PD participants were recruited; however, BSC 04 was forced to drop out of the study due to a failed psychological assessment prior to receiving DBS surgery. As outlined in *Table 1* in the Methods section, three males and four females met the inclusion and exclusion criteria. The mean age of the participants was  $61.71 \pm 8.10$  years and the mean disease duration was  $12.43 \pm 2.94$  years. As mentioned above, each patient underwent a contact review prior to the current steering investigation to identify the best two contacts on each side of the brain, i.e. the optimal stimulation sites. Results from the contact review as well as the amplitude ranges defining the therapeutic window of each patient are presented below.

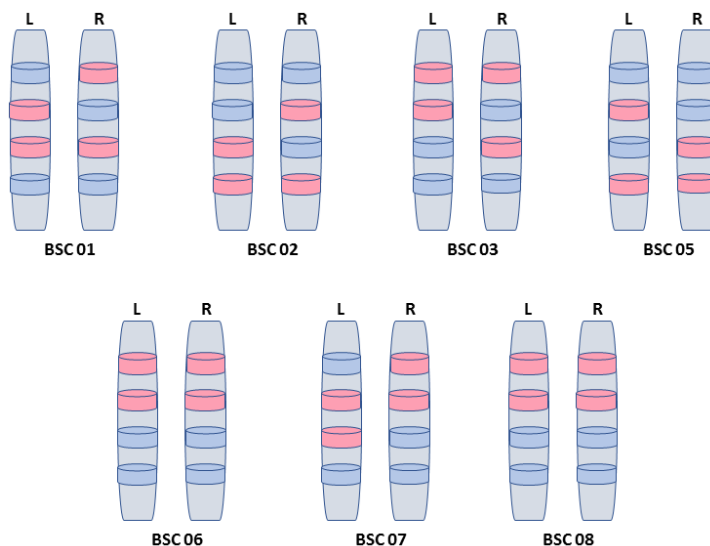


**Figure 7: Optimal stimulation sites**

Simulation of the left and right lead with the bottom four contacts on each lead (shown as rings) displayed for each patient; contacts in pink represent the two best contacts on each lead chosen for current fractionation. Size of the lead and contacts are not to scale. L; lead implanted in the left subthalamic nucleus; R: lead implanted in the right subthalamic nucleus.

**Table 4: Lower and upper amplitude limits of the therapeutic window**

Participant ID	Therapeutic Window at Left STN		Therapeutic Window at Right STN	
	Lower Limit (mA)	Upper Limit (mA)	Lower Limit (mA)	Upper Limit (mA)
BSC 01	2	6	0.75	6
BSC 02	1	3.5	1	3
BSC 03	1	4.5	1	5
BSC 05	0.5	3	0.5	3.5
BSC 06	1.5	3.5	1	4
BSC 07	1.5	3.4	1.5	5.6
BSC 08	1.5	4	1.5	3
Mean (SD)	1.29 ( $\pm 0.49$ )	3.99 ( $\pm 1.01$ )	1.04 ( $\pm 0.37$ )	4.3 ( $\pm 1.24$ )

*SD: standard deviation of the mean; STN: subthalamic nucleus; current amplitude values are displayed in milliamperes(mA); lower limit defined by minimum amplitude at which symptom improvement occurs; upper limit defined by maximum amplitude patient can withstand before experiencing adverse side effects.*

Recall that at the end of the current steering investigation, patients went home with a setting that was optimal among the four weeks, as measured by a whole-body UPDRS-III score. The whole-body UPDRS-III score takes into consideration speech, facial expression, rest tremor of the head and the upper and lower limbs, postural tremor of the upper limbs, rigidity of the neck and the upper and lower limbs, bradykinetic state assessed by finger taps, hand and arm movements and arising from a chair, leg agility, posture and postural stability, gait and whole-body bradykinesia (*Appendix 3*). This setting showed a consistent improvement of whole-body symptoms at each week's amplitude. Patients went home at the end of the study with this setting paired with the amplitude of the week at which the setting caused optimal symptom improvement. *Table 5* lists this setting for each patient.

**Table 5: Optimal setting at study conclusion according to whole-body UPDRS score**

<b>Participant ID</b>	<b>Optimal Setting</b>
BSC 01	14
BSC 02	8
BSC 03	2
BSC 05	<b>4</b>
BSC 06	2
BSC 07	8
BSC 08	10

*Setting 4: bilateral monopolar*

### 3.2 Objective #1 results

The first objective was to determine the optimal current fractionation setting and amplitude for each patient's upper limb symptom alleviation. To quantify symptoms for this objective, kinematic data from IMU sensors was used to quantify upper limb rest tremor, upper limb postural tremor and upper limb bradykinesia while participants were engaged in the three seated tasks outlined in section 2.4. 3D scatter plots were created to determine the optimal setting for the three symptoms, defined by the setting having the smallest Euclidean distance to the center of the graph (refer to section 2.5 for data analysis method). *Figures 8-14* show panels created for each patient that display 3D graphs for each week.

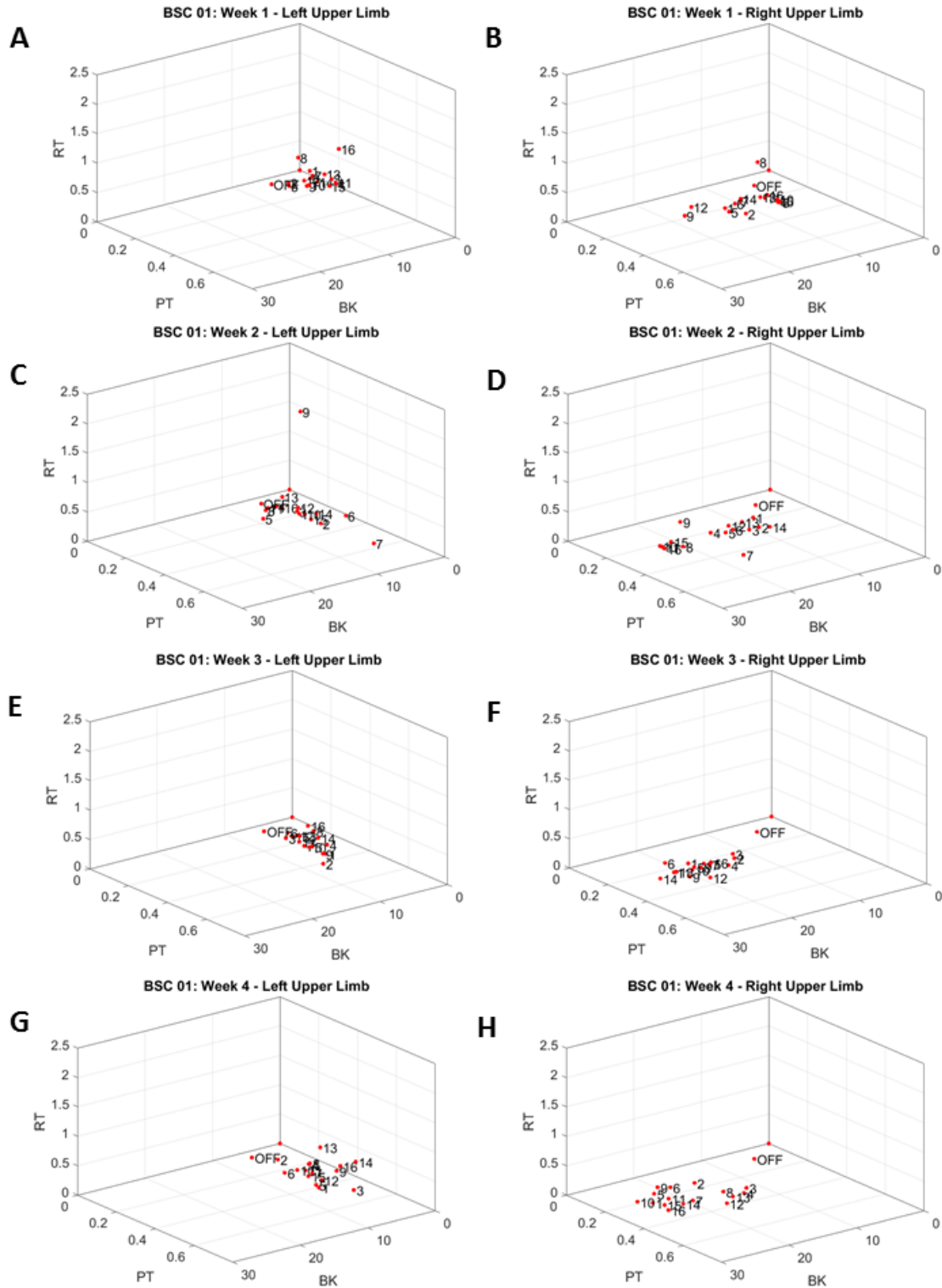


**Figure 8: 3D graphs of kinematic data for BSC 01**

3D visualizations of kinematic parameters measured at baseline (OFF) and during 16 current fractionation settings tested at each week on BSC 01. Bradykinesia (BK) is represented on the x-axis, postural tremor (PT) is represented on the y-axis, and rest

tremor (RT) is represented on the z-axis. Current amplitude at week 1 (A and B) was set to 2.8 mA on the left lead and 1.8 mA on the right lead. Current amplitude at week 2 (C and D) was set to 3.6 mA on the left lead and 2.8 mA on the right lead. Current amplitude at week 3 (E and F) was set to 4.4 mA on the left lead and 3.9 mA on the right lead. Current amplitude at week 4 (G and H) was set to 4.8 mA on the left lead and 4.4 mA on the right lead. Plotted values are normalized percentages.

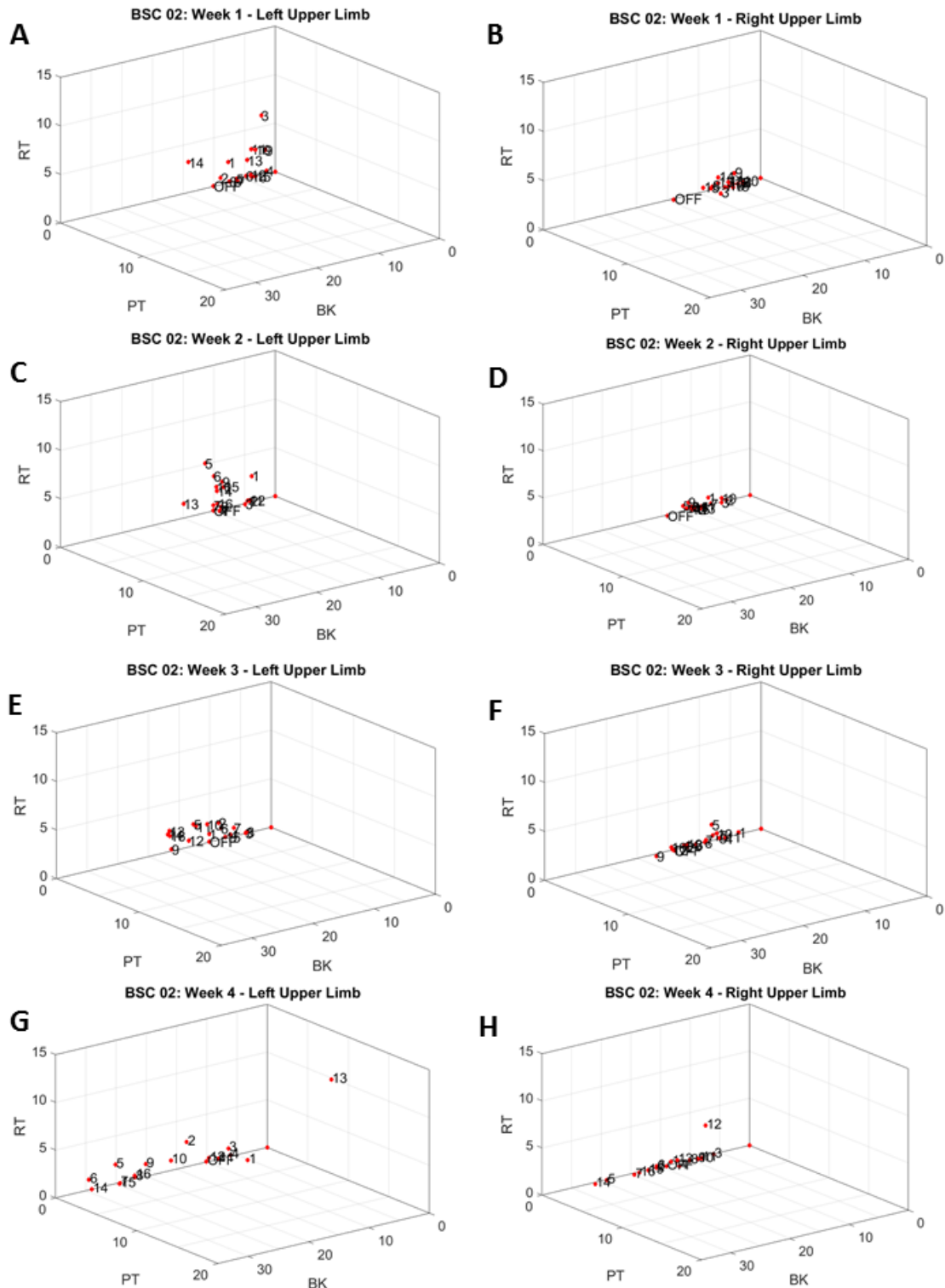


**Figure 9: 3D graphs of kinematic data for BSC 02**

3D visualizations of kinematic parameters measured at baseline (OFF) and during 16 current fractionation settings tested at each week on BSC 02. Bradykinesia (BK) is represented on the x-axis, postural tremor (PT) is represented on the y-axis, and rest tremor (RT) is represented on the z-axis. Current amplitude at week 1 (A and B) was set

to 1.5 mA on the left lead and 1.4 mA on the right lead. Current amplitude at week 2 (C and D) was set to 2 mA on the left lead and 1.8 mA on the right lead. Current amplitude at week 3 (E and F) was set to 2.5 mA on the left lead and 2.2 mA on the right lead. Current amplitude at week 4 (G and H) was set to 3 mA on the left lead and 2.6 mA on the right lead. Plotted values are normalized percentages.



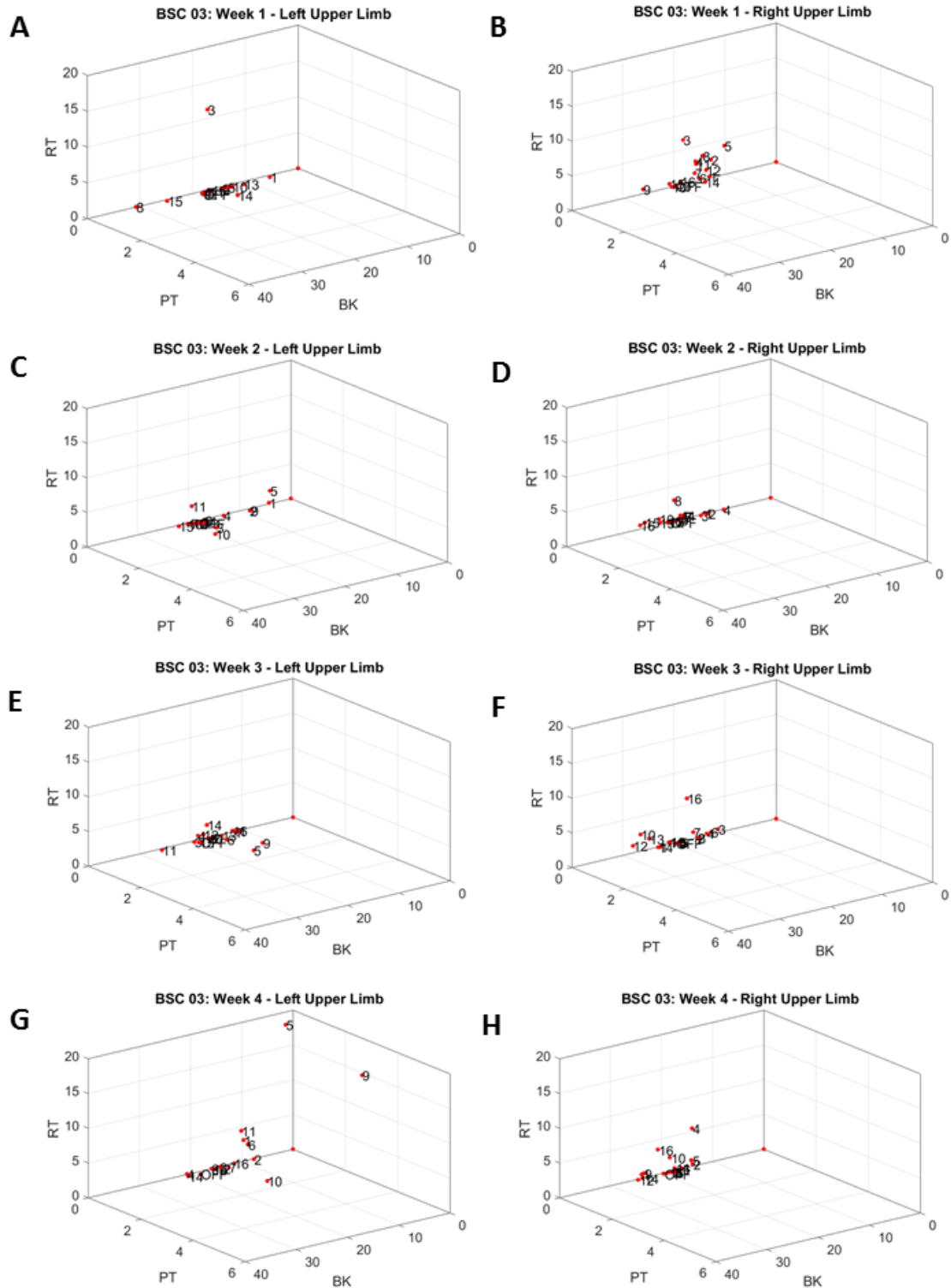


**Figure 10: 3D graphs of kinematic data for BSC 03**

3D visualizations of kinematic parameters measured at baseline (OFF) and during 16 current fractionation settings tested at each week on BSC 03. Bradykinesia (BK) is represented on the x-axis, postural tremor (PT) is represented on the y-axis, and rest tremor (RT) is represented on the z-axis. Current amplitude at week 1 (A and B) was set

to 1.7 mA on the left lead and 1.8 mA on the right lead. Current amplitude at week 2 (C and D) was set to 2.4 mA on the left lead and 2.6 mA on the right lead. Current amplitude at week 3 (E and F) was set to 3.1 mA on the left lead and 3.4 mA on the right lead. Current amplitude at week 4 (G and H) was set to 3.8 mA on the left lead and 4.2 mA on the right lead. Plotted values are normalized percentages.

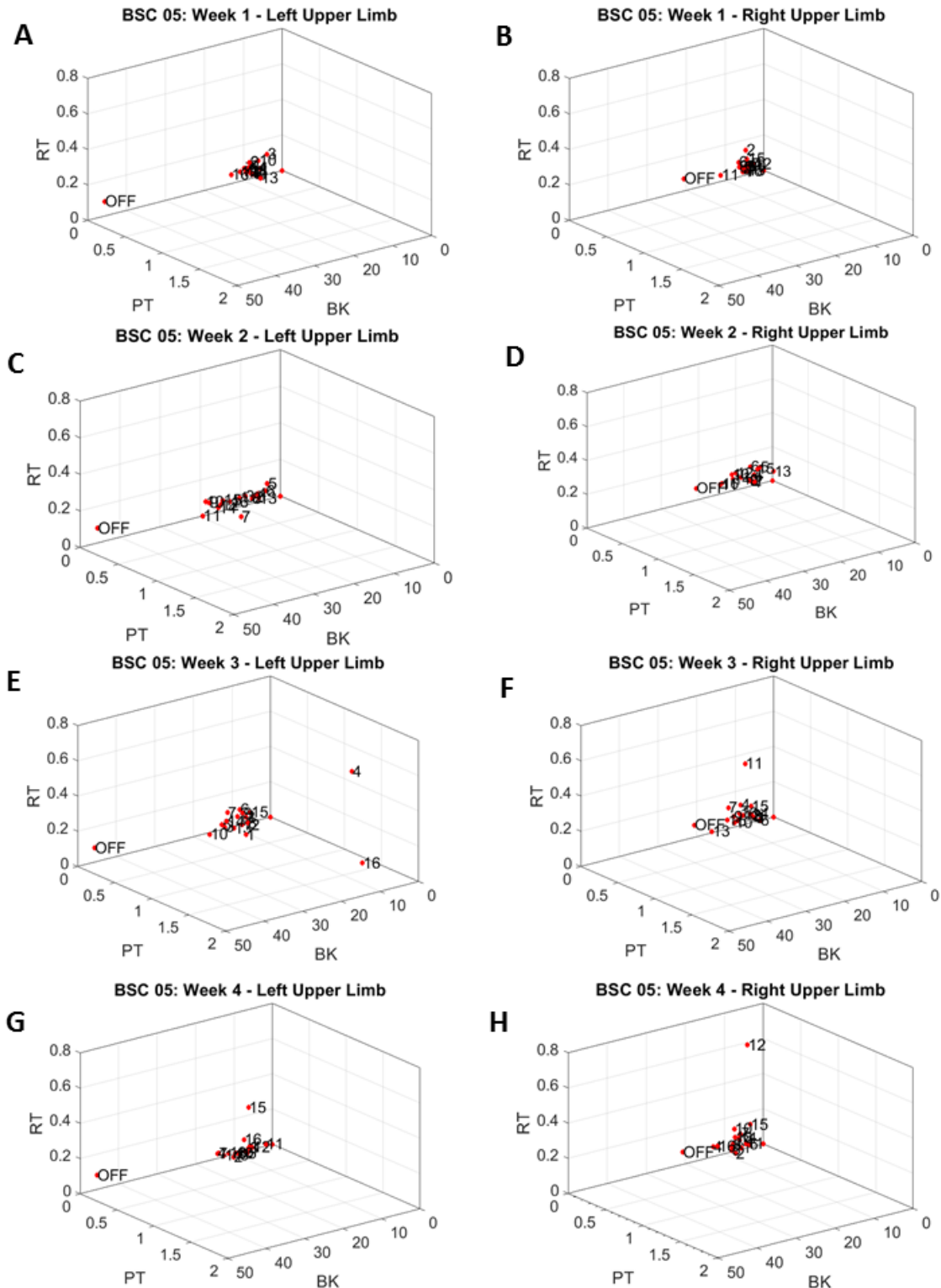


**Figure 11: 3D graphs of kinematic data for BSC 05**

3D visualizations of kinematic parameters measured at baseline (OFF) and during 16 current fractionation settings tested at each week on BSC 05. Bradykinesia (BK) is represented on the x-axis, postural tremor (PT) is represented on the y-axis, and rest tremor (RT) is represented on the z-axis. Current amplitude at week 1 (A and B) was set

to 1 mA on the left lead and 1.1 mA on the right lead. Current amplitude at week 2 (C and D) was set to 1.5 mA on the left lead and 1.7 mA on the right lead. Current amplitude at week 3 (E and F) was set to 2 mA on the left lead and 2.3 mA on the right lead. Current amplitude at week 4 (G and H) was set to 2.5 mA on the left lead and 2.9 mA on the right lead. Plotted values are normalized percentages.

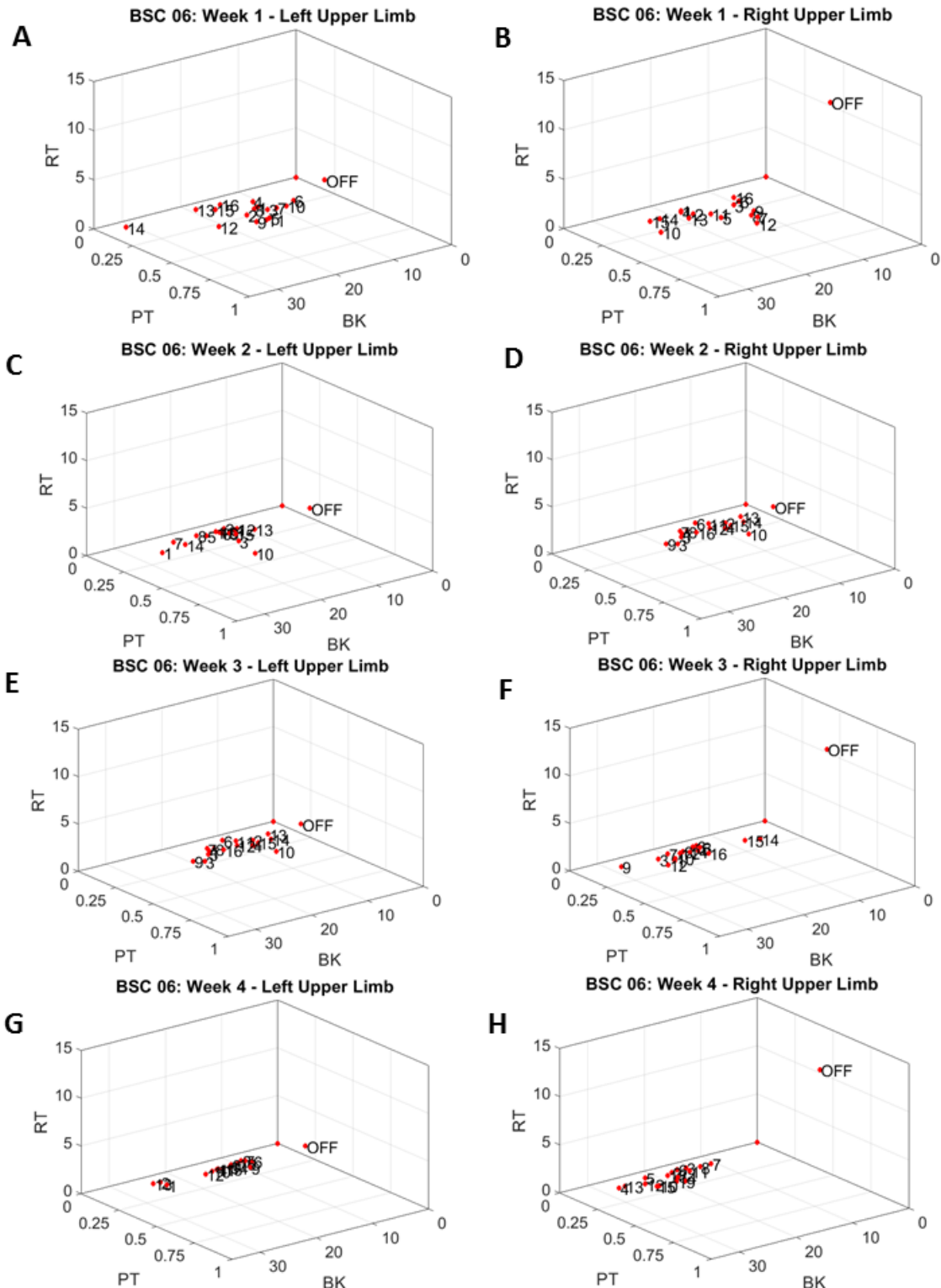


**Figure 12: 3D graphs of kinematic data for BSC 06**

3D visualizations of kinematic parameters measured at baseline (OFF) and during 16 current fractionation settings tested at each week on BSC 06. Bradykinesia (BK) is represented on the x-axis, postural tremor (PT) is represented on the y-axis, and rest tremor (RT) is represented on the z-axis. Current amplitude at week 1 (A and B) was set

to 1.9 mA on the left lead and 1.6 mA on the right lead. Current amplitude at week 2 (C and D) was set to 2.3 mA on the left lead and 2.2 mA on the right lead. Current amplitude at week 3 (E and F) was set to 2.7 mA on the left lead and 2.8 mA on the right lead. Current amplitude at week 4 (G and H) was set to 3.1 mA on the left lead and 3.4 mA on the right lead. Plotted values are normalized percentages.

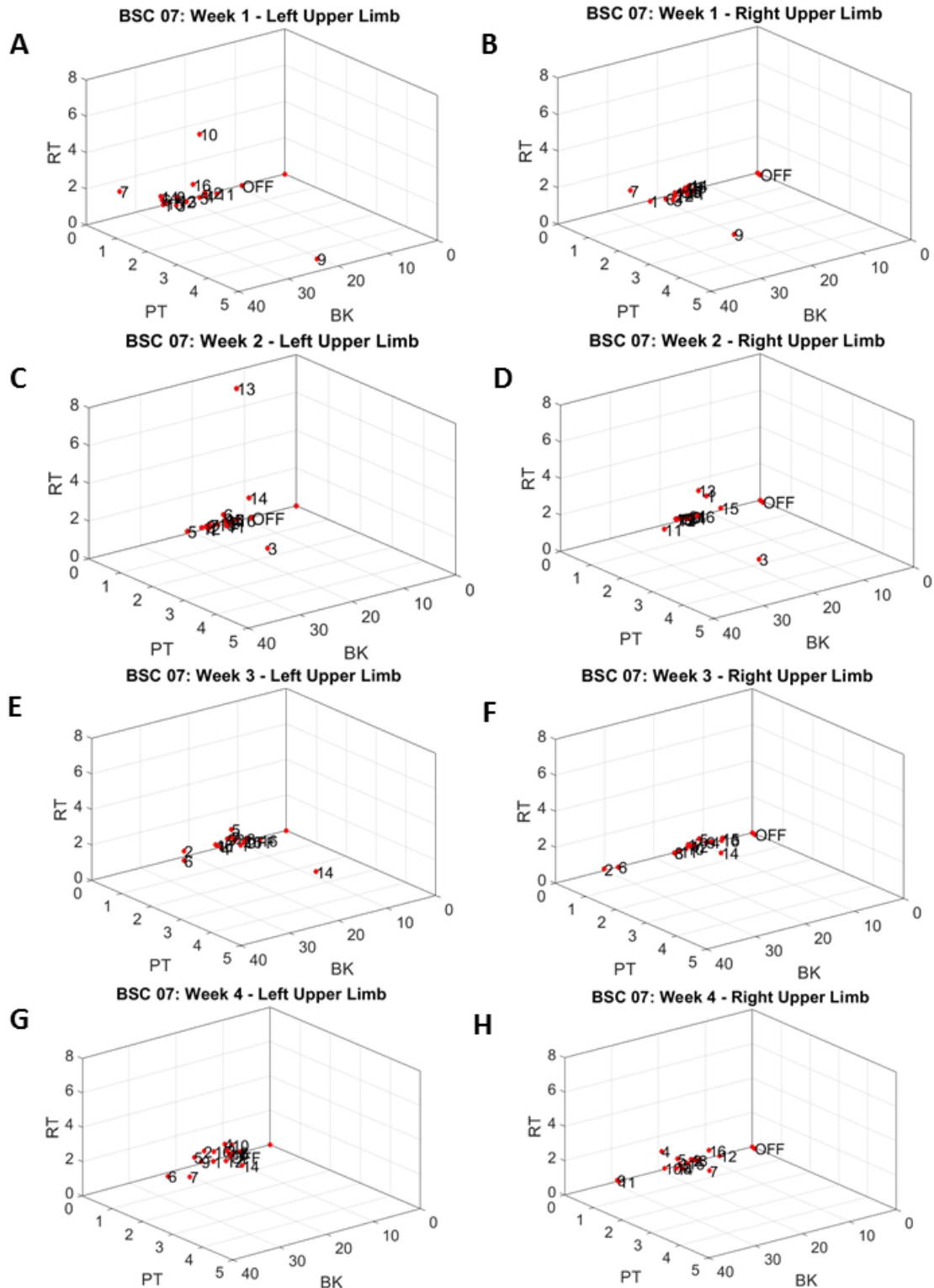


**Figure 13: 3D graphs of kinematic data for BSC 07**

3D visualizations of kinematic parameters measured at baseline (OFF) and during 16 current fractionation settings tested at each week on BSC 07. Bradykinesia (BK) is represented on the x-axis, postural tremor (PT) is represented on the y-axis, and rest tremor (RT) is represented on the z-axis. Current amplitude at week 1 (A and B) was set

to 1.9 mA on the left lead and 2.3 mA on the right lead. Current amplitude at week 2 (C and D) was set to 2.2 mA on the left lead and 3.1 mA on the right lead. Current amplitude at week 3 (E and F) was set to 2.6 mA on the left lead and 3.9 mA on the right lead. Current amplitude at week 4 (G and H) was set to 3.0 mA on the left lead and 4.7 mA on the right lead. Plotted values are normalized percentages.



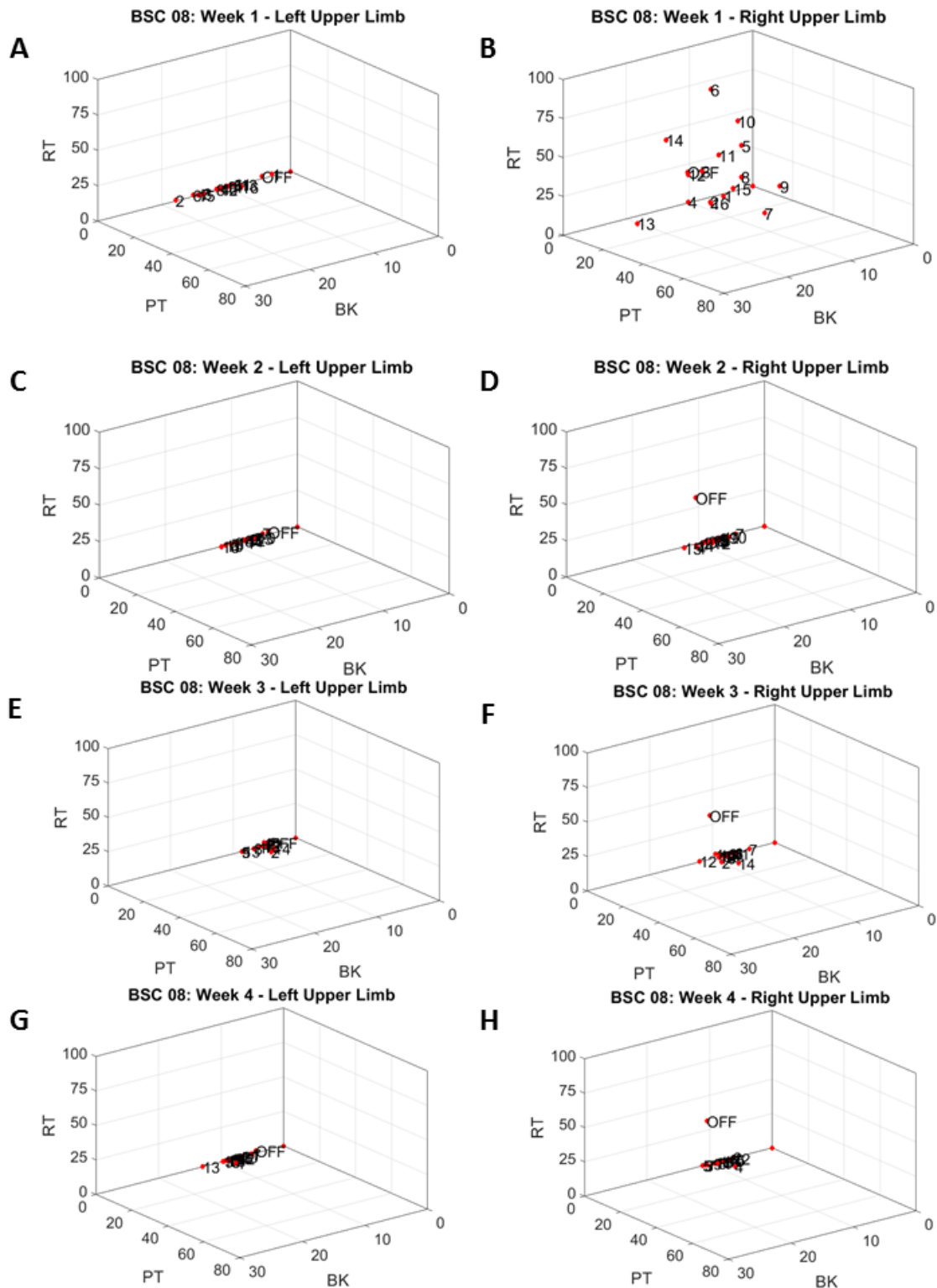


**Figure 14: 3D graphs of kinematic data for BSC 08**

3D visualizations of kinematic parameters measured at baseline (OFF) and during 16 current fractionation settings tested at each week on BSC 08. Bradykinesia (BK) is represented on the x-axis, postural tremor (PT) is represented on the y-axis, and rest tremor (RT) is represented on the z-axis. Current amplitude at week 1 (A and B) was set

to 2 mA on the left lead and 1.8 mA on the right lead. Current amplitude at week 2 (C and D) was set to 2.5 mA on the left lead and 2.1 mA on the right lead. Current amplitude at week 3 (E and F) was set to 3.5 mA on the left lead and 2.7 mA on the right lead. Current amplitude at week 4 (G and H) was set to 3.0 mA on the left lead and 2.4 mA on the right lead. Plotted values are normalized percentages.

*Table 6* summarizes the findings from *Figures 8-14* where the optimal setting, for upper limb alleviation of rest tremor, postural tremor and bradykinesia, of each week for all patients was found by calculating the Euclidean distance from the data point of each setting to the center of the 3D graph; the optimal setting had the smallest Euclidean distance to the center. The settings listed in *Table 6* are grouped according to the use of current steering either unilaterally (settings in green/purple), bilaterally (settings in red), or the absence of current steering, i.e. a bilateral monopolar stimulation (bolded settings). Settings in green have current steering occurring at the STN that is contralateral to the limb being affected (i.e. left STN for right limb, right STN for left limb) whereas settings in purple have current steering occurring at the STN that is ipsilateral to the affected limb (i.e. left STN for left limb, right STN for right limb). The highlighted settings for each patient indicate the optimal setting across all four weeks, at the corresponding week's amplitude.

*Figure 15* shows the results of a two-tailed Wilcoxon matched-pairs signed rank test (non-parametric) to determine whether there is a significant difference between the Euclidean distances of each patient's OFF data point to the center of the 3D graph and the Euclidean distances of each patient's optimal setting (highlighted settings in *Table 6*) to the center. Significance was found between the two groups for the left ( $n = 7$ ,  $p = 0.0156$ ) and right ( $n = 7$ ,  $p = 0.0313$ ) upper limb.

**Table 6: Optimal settings for upper limb rest tremor, postural tremor and bradykinesia determined by kinematic data**

	BSC 01		BSC 02		BSC 03		BSC 05		BSC 06		BSC 07		BSC 08	
	L	R	L	R	L	R	L	R	L	R	L	R	L	R
<b>Week 1</b>	11	11	4	6	1	5	1	12	6	16	11	14	1	1
<b>Week 2</b>	14	14	2	2	1	4	6	13	13	4	14	15	7	7
<b>Week 3</b>	8	2	8	1	1	3	4	6	13	14	16	15	7	12
<b>Week 4</b>	8	3	3	3	2	2	11	6	6	7	8	12	3	7

*L: left upper limb; R: right upper limb; settings in red represent the occurrence of bilateral current steering, bolded settings are monopolar setting, settings in green employ current steering at the STN contralateral to the limb, settings in purple employ current steering at the STN ipsilateral to the limb; highlighted settings represent the setting of each upper limb that was optimal across all weeks. Week 1 settings were optimal at 20% of each patient's therapeutic window. Week 2 settings were optimal at 40% of each patient's therapeutic window. Week 3 settings were optimal at 60% of each patient's therapeutic window. Week 4 settings were optimal at 80% of each patient's therapeutic window.*

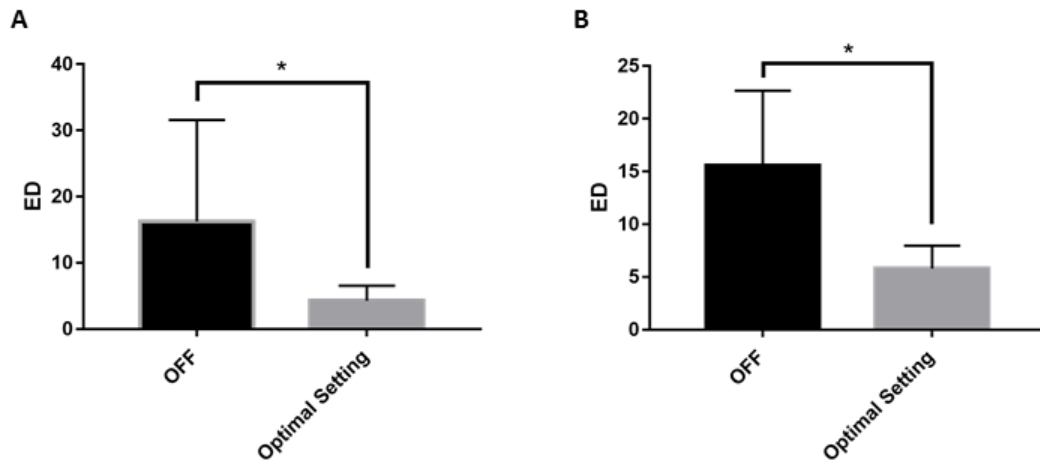


**Figure 15: Euclidean distances (EDs) of optimal settings for alleviation of rest tremor, postural tremor and bradykinesia in the left and right upper limbs of patients with Parkinson's disease**

A statistically significant difference was revealed between the EDs of the OFF group and the EDs of the optimal settings for the A) left upper limb ( $n = 7$ ,  $p = 0.0156^*$ ) and B) right upper limb ( $n = 7$ ,  $p = 0.0313^*$ ) of patients with Parkinson's disease. Results are reported as the mean  $\pm$  SD. A two-tailed, Wilcoxon matched-pairs signed rank test was completed. ED: Euclidean distance.

### 3.3 Objective #2 results

To compare the responses of hyperkinetic symptoms and hypokinetic symptoms of the upper limbs to each current fractionation setting, UPDRS-III subscores were converted to z-scores and graphed on radar charts (refer to section 2.5 for data analysis method). Items 3.15 (postural tremor of hands) and 3.17 (rest tremor amplitude) defined hyperkinetic symptoms and items 3.3 (rigidity) and 3.6 (bradykinesia: pronation-supination movements of hands) defined hypokinetic symptoms (see *Appendix 3*). Panels of radar charts for each patient are displayed in *Figures 16-22*.

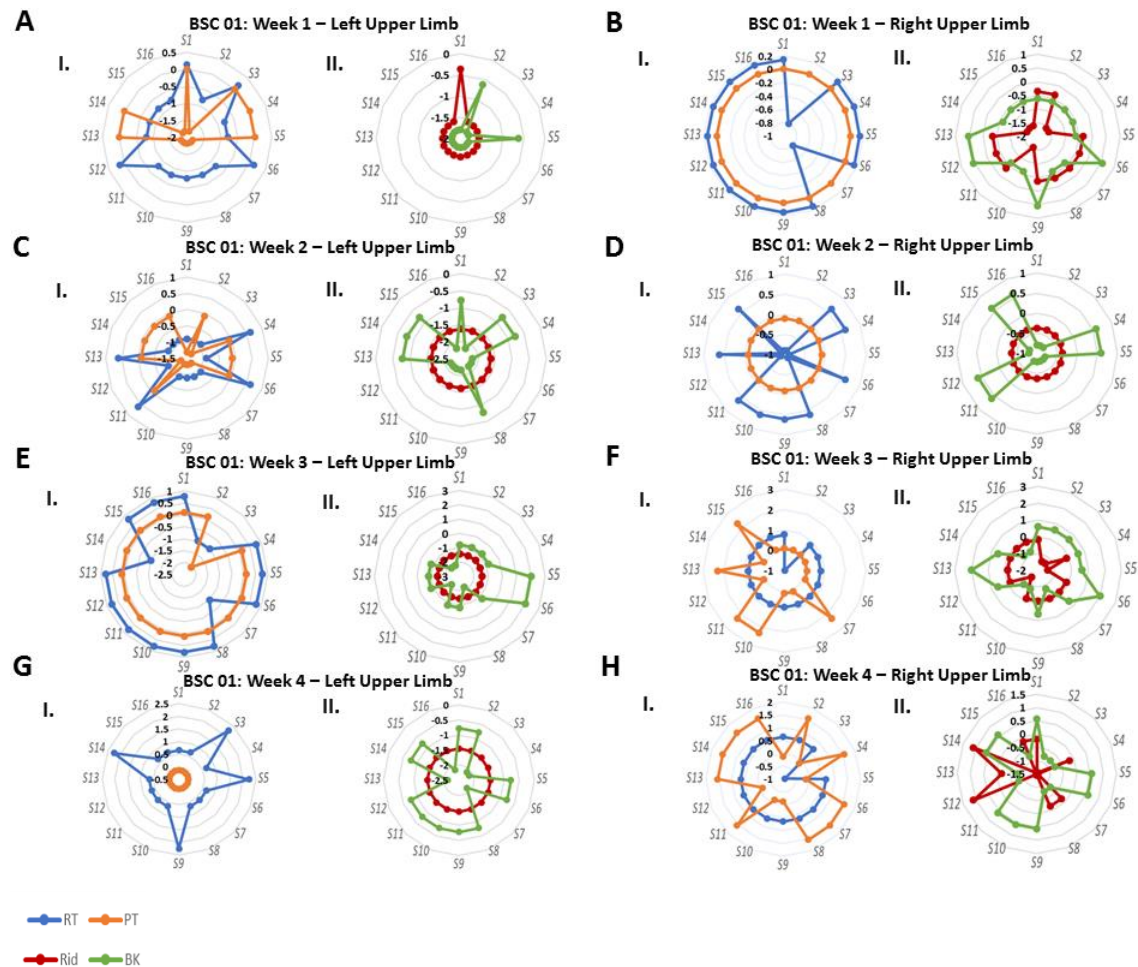


**Figure 16: Radar charts of UPDRS-III subscores for BSC 01**

Visual representations showing the effect of 16 current fractionation settings (labeled around the circumference of each radar chart) on upper limb symptoms. A-H show results at each week for the left and right upper limb of BSC 01; the left chart displays rest tremor (RT) and postural tremor (PT) and the right chart displays rigidity (Rid) and

bradykinesia (BK). The left charts in A-H all display hyperkinetic (RT and PT) symptoms and the right charts in A-H all display hypokinetic (Rid and BK) symptoms. Graphed values are z-scores calculated from raw scores for UPDRS item 3.15, item 3.17, item 3.3, and item 3.6, representing postural tremor, rest tremor, rigidity, and bradykinesia, respectively. Distance from the center represents symptom severity. Current amplitude at week 1 (A and B) was set to 2.8 mA on the left lead and 1.8 mA on the right lead. Current amplitude at week 2 (C and D) was set to 3.6 mA on the left lead and 2.8 mA on the right lead. Current amplitude at week 3 (E and F) was set to 4.4 mA on the left lead and 3.9 mA on the right lead. Current amplitude at week 4 (G and H) was set to 4.8 mA on the left lead and 4.4 mA on the right lead. UPDRS: Unified Parkinson's Disease Rating Scale.

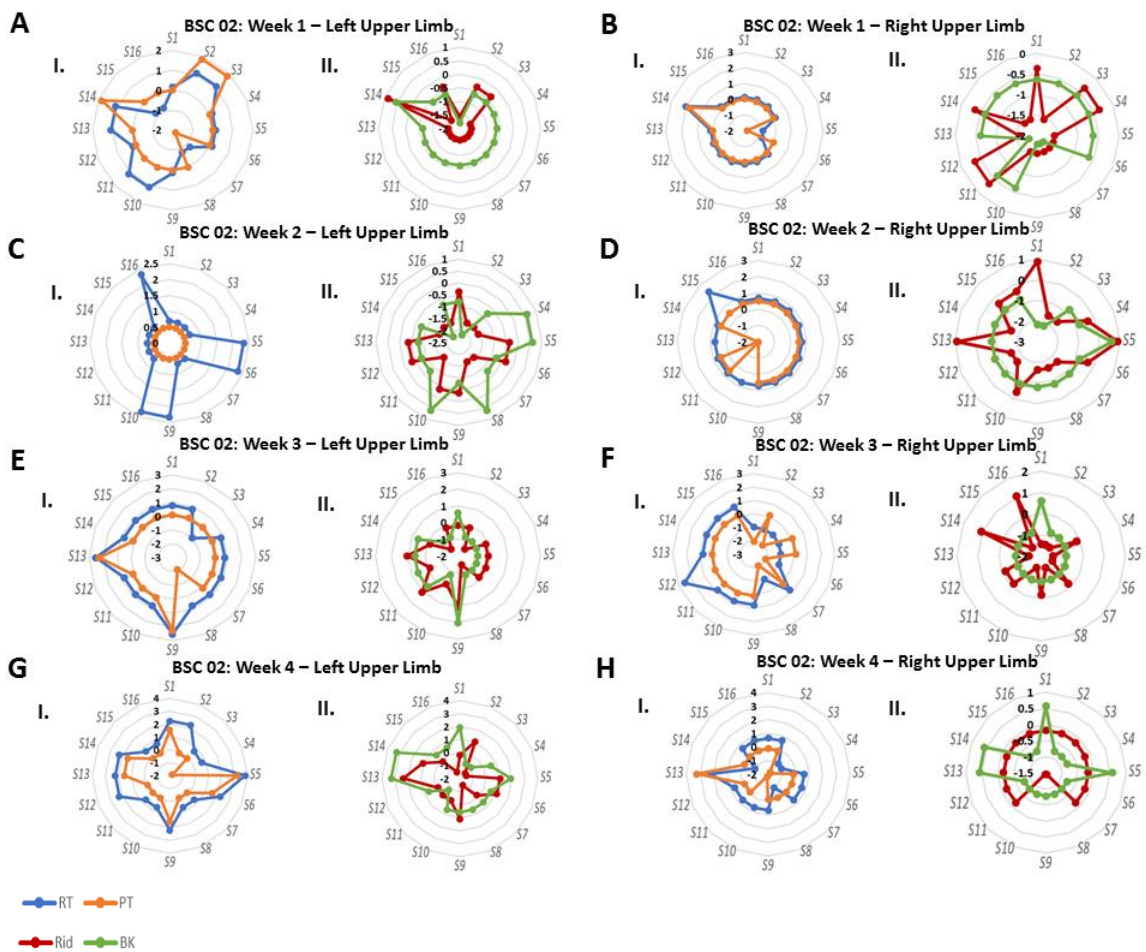


**Figure 17: Radar charts of UPDRS-III subscores for BSC 02**

Visual representations showing the effect of 16 current fractionation settings (labeled around the circumference of each radar chart) on upper limb symptoms. A-H show results at each week for the left and right upper limb of BSC 02; the left chart displays rest tremor (RT) and postural tremor (PT) and the right chart displays rigidity (Rid) and bradykinesia (BK). The left charts in A-H all display hyperkinetic (RT and PT) symptoms and the right charts in A-H all display hypokinetic (Rid and BK) symptoms. Graphed values are z-scores calculated from raw scores for UPDRS item 3.15, item 3.17,

item 3.3, and item 3.6, representing postural tremor, rest tremor, rigidity, and bradykinesia, respectively. Distance from the center represents symptom severity. Current amplitude at week 1 (A and B) was set to 1.5 mA on the left lead and 1.4 mA on the right lead. Current amplitude at week 2 (C and D) was set to 2 mA on the left lead and 1.8 mA on the right lead. Current amplitude at week 3 (E and F) was set to 2.5 mA on the left lead and 2.2 mA on the right lead. Current amplitude at week 4 (G and H) was set to 3 mA on the left lead and 2.6 mA on the right lead. UPDRS: Unified Parkinson's Disease Rating Scale.

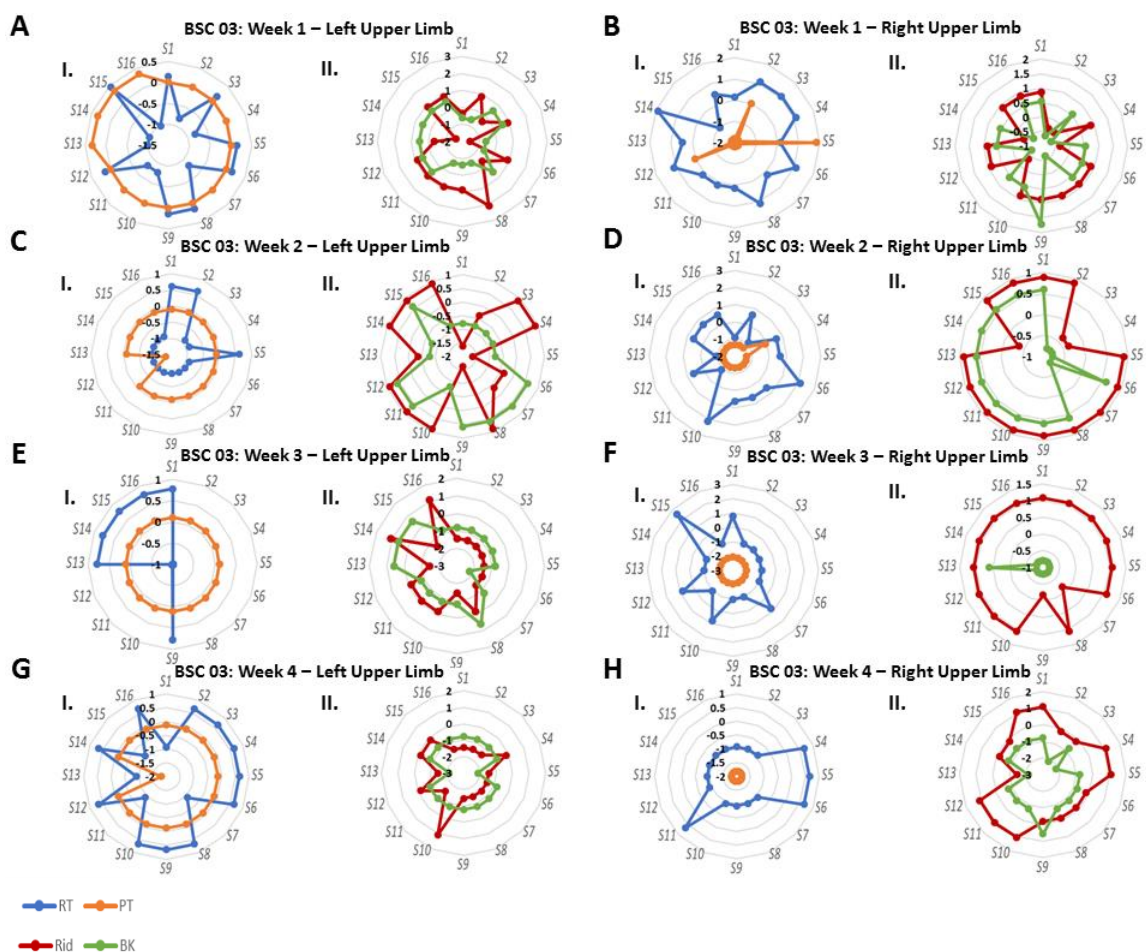


**Figure 18: Radar charts of UPDRS-III subscores for BSC 03**

Visual representations showing the effect of 16 current fractionation settings (labeled around the circumference of each radar chart) on upper limb symptoms. A-H show results at each week for the left and right upper limb of BSC 03; the left chart displays rest tremor (RT) and postural tremor (PT) and the right chart displays rigidity (Rid) and bradykinesia (BK). The left charts in A-H all display hyperkinetic (RT and PT) symptoms and the right charts in A-H all display hypokinetic (Rid and BK) symptoms. Graphed values are z-scores calculated from raw scores for UPDRS item 3.15, item 3.17, item 3.3, and item 3.6, representing postural tremor, rest tremor, rigidity, and bradykinesia, respectively. Distance from the center represents symptom severity. Current amplitude at week 1 (A and B) was set to 1.7 mA on the left lead and 1.8 mA on the right lead. Current amplitude at week 2 (C and D) was set to 2.4 mA on the left lead

and 2.6 mA on the right lead. Current amplitude at week 3 (E and F) was set to 3.1 mA on the left lead and 3.4 mA on the right lead. Current amplitude at week 4 (G and H) was set to 3.8 mA on the left lead and 4.2 mA on the right lead. UPDRS: Unified Parkinson's Disease Rating Scale.

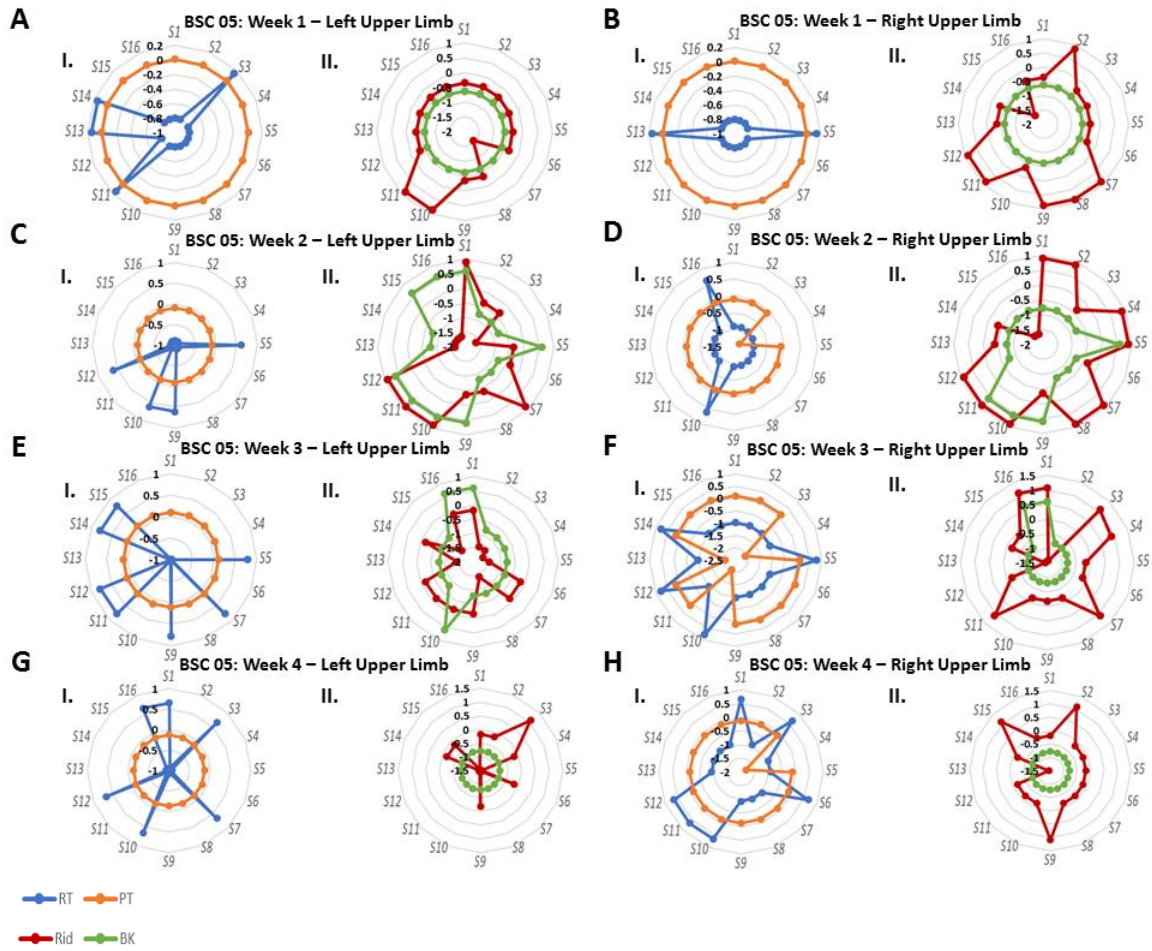


**Figure 19: Radar charts of UPDRS-III subscores for BSC 05**

Visual representations showing the effect of 16 current fractionation settings (labeled around the circumference of each radar chart) on upper limb symptoms. A-H show results at each week for the left and right upper limb of BSC 05; the left chart displays rest tremor (RT) and postural tremor (PT) and the right chart displays rigidity (Rid) and bradykinesia (BK). The left charts in A-H all display hyperkinetic (RT and PT) symptoms and the right charts in A-H all display hypokinetic (Rid and BK) symptoms. Graphed values are z-scores calculated from raw scores for UPDRS item 3.15, item 3.17, item 3.3, and item 3.6, representing postural tremor, rest tremor, rigidity, and bradykinesia, respectively. Distance from the center represents symptom severity. Current amplitude at week 1 (A and B) was set to 1 mA on the left lead and 1.1 mA on the right lead. Current amplitude at week 2 (C and D) was set to 1.5 mA on the left lead and 1.7 mA on the right lead. Current amplitude at week 3 (E and F) was set to 2 mA on the left lead and 2.3 mA on the right lead. Current amplitude at week 4 (G and H) was set to 2.5 mA on the left lead and 2.9 mA on the right lead. UPDRS: Unified Parkinson's Disease Rating Scale.

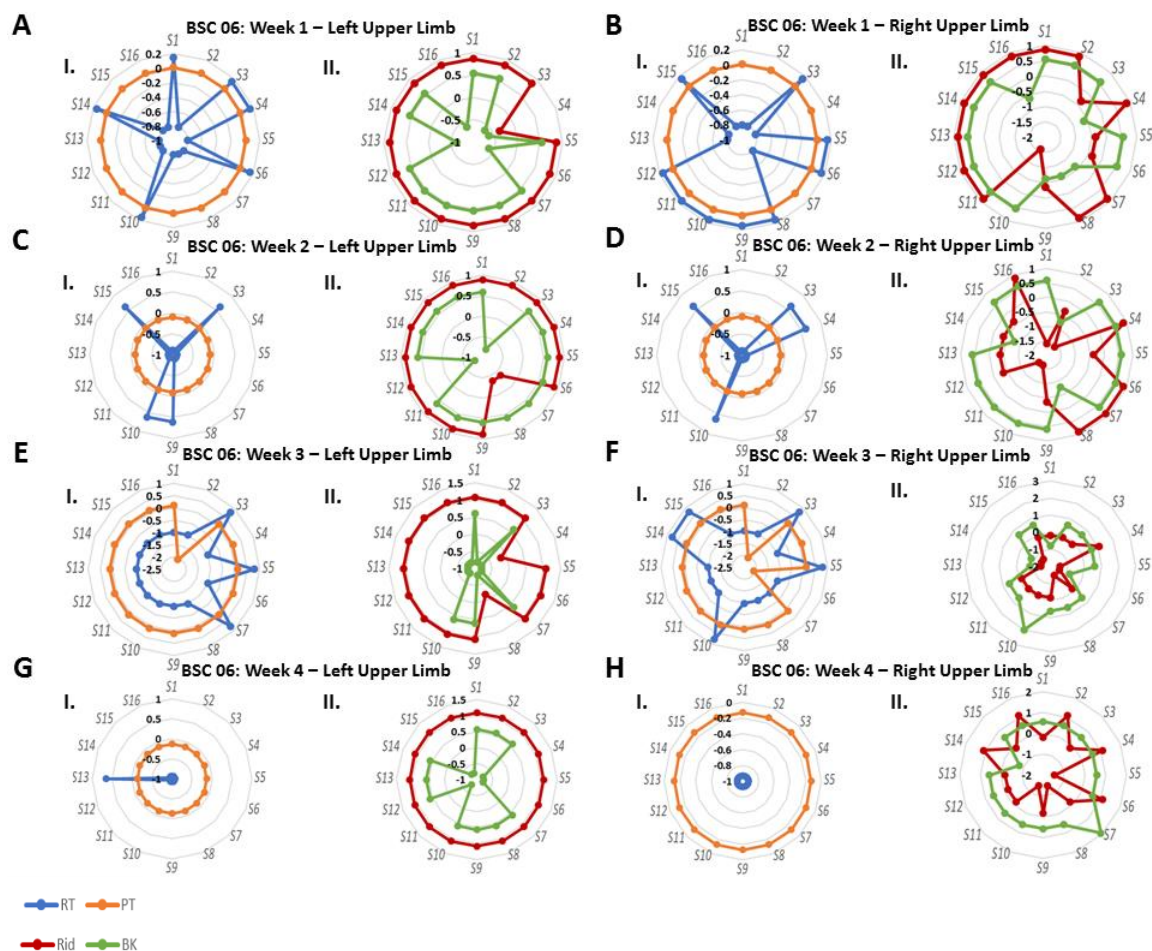


**Figure 20: Radar charts of UPDRS-III subscores for BSC 06**

Visual representations showing the effect of 16 current fractionation settings (labeled around the circumference of each radar chart) on upper limb symptoms. A-H show results at each week for the left and right upper limb of BSC 06; the left chart displays rest tremor (RT) and postural tremor (PT) and the right chart displays rigidity (Rid) and bradykinesia (BK). The left charts in A-H all display hyperkinetic (RT and PT) symptoms and the right charts in A-H all display hypokinetic (Rid and BK) symptoms. Graphed values are z-scores calculated from raw scores for UPDRS item 3.15, item 3.17, item 3.3, and item 3.6, representing postural tremor, rest tremor, rigidity, and bradykinesia, respectively. Distance from the center represents symptom severity. Current amplitude at week 1 (A and B) was set to 1.9 mA on the left lead and 1.6 mA on the right lead. Current amplitude at week 2 (C and D) was set to 2.3 mA on the left lead and 2.2 mA on the right lead. Current amplitude at week 3 (E and F) was set to 2.7 mA on the left lead and 2.8 mA on the right lead. Current amplitude at week 4 (G and H) was set to 3.1 mA on the left lead and 3.4 mA on the right lead. UPDRS: Unified Parkinson's Disease Rating Scale.



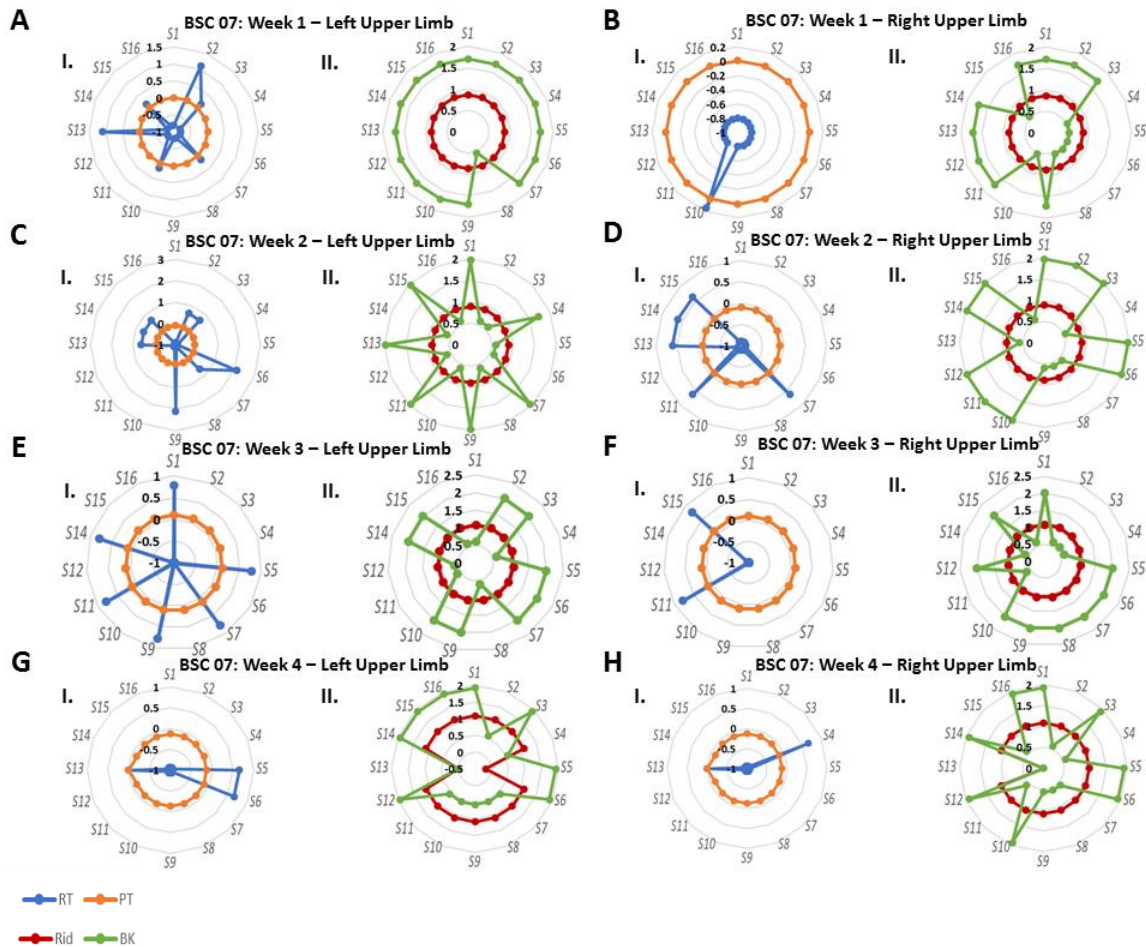


**Figure 21: Radar charts of UPDRS-III subscores for BSC 07**

Visual representations showing the effect of 16 current fractionation settings (labeled around the circumference of each radar chart) on upper limb symptoms. A-H show results at each week for the left and right upper limb of BSC 07; the left chart displays rest tremor (RT) and postural tremor (PT) and the right chart displays rigidity (Rid) and bradykinesia (BK). The left charts in A-H all display hyperkinetic (RT and PT) symptoms and the right charts in A-H all display hypokinetic (Rid and BK) symptoms. Graphed values are z-scores calculated from raw scores for UPDRS item 3.15, item 3.17, item 3.3, and item 3.6, representing postural tremor, rest tremor, rigidity, and bradykinesia, respectively. Distance from the center represents symptom severity. Current amplitude at week 1 (A and B) was set to 1.9 mA on the left lead and 2.3 mA on the right lead. Current amplitude at week 2 (C and D) was set to 2.2 mA on the left lead and 3.1 mA on the right lead. Current amplitude at week 3 (E and F) was set to 2.6 mA on the left lead and 3.9 mA on the right lead. Current amplitude at week 4 (G and H) was set to 3.0 on the left lead and 4.7 on the right lead. UPDRS: Unified Parkinson's Disease Rating Scale.

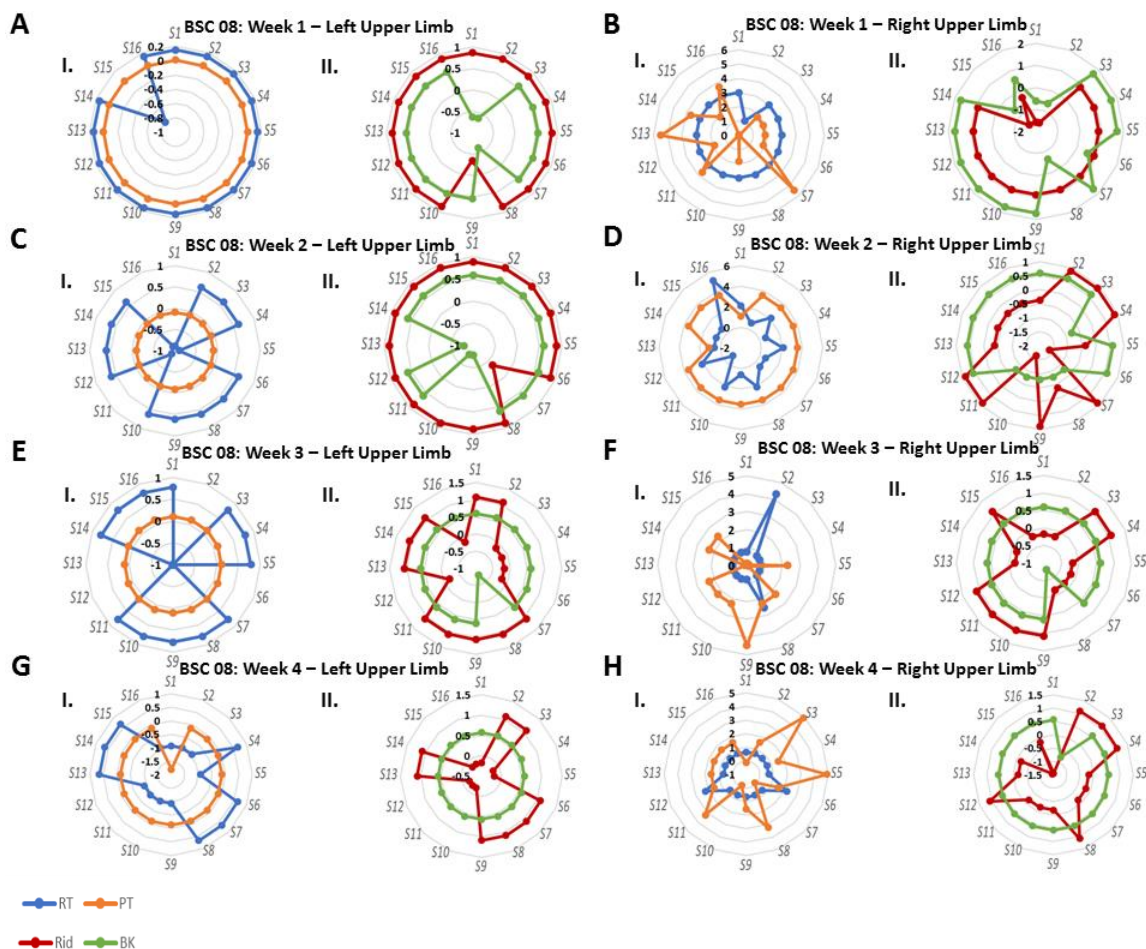


**Figure 22: Radar charts of UPDRS-III subscores for BSC 08**

Visual representations showing the effect of 16 current fractionation settings (labeled around the circumference of each radar chart) on upper limb symptoms. A-H show results at each week for the left and right upper limb of BSC 08; the left chart displays rest tremor (RT) and postural tremor (PT) and the right chart displays rigidity (Rid) and bradykinesia (BK). The left charts in A-H all display hyperkinetic (RT and PT) symptoms and the right charts in A-H all display hypokinetic (Rid and BK) symptoms. Graphed values are z-scores calculated from raw scores for UPDRS item 3.15, item 3.17, item 3.3, and item 3.6, representing postural tremor, rest tremor, rigidity, and bradykinesia, respectively. Distance from the center represents symptom severity. Current amplitude at week 1 (A and B) was set to 2 mA on the left lead and 1.8 mA on the right lead. Current amplitude at week 2 (C and D) was set to 2.5 mA on the left lead and 2.1 mA on the right lead. Current amplitude at week 3 (E and F) was set to 3.5 mA on the left lead and 2.7 mA on the right lead. Current amplitude at week 4 (G and H) was set to 3 mA on the left lead and 2.4 mA on the right lead. UPDRS: Unified Parkinson's Disease Rating Scale.

The radar charts were used to determine optimal settings for hyperkinetic symptoms and hypokinetic symptoms according to the UPDRS-III subscores. For example, looking at display A)I. in *Figure 22* showing the hyperkinetic radar chart of rest tremor (blue connected line) and postural tremor (orange connected line), setting 15 is the only setting that has the coordinate for rest tremor at the center of the graph; therefore, setting 15, when compared to the rest of the settings, is optimal for hyperkinetic symptom alleviation in the left upper limb of BSC 08 at week 1. A summary of these optimal settings for hyperkinetic and hypokinetic symptoms for each patient at each week is displayed in *Tables 7-10*. The tables also highlight in red which settings were optimal in each patient's upper limbs for alleviation of both hyperkinetic and hypokinetic symptoms. Put another way, the settings in red are optimal for hyperkinetic *and* hypokinetic symptom alleviation in the *same* limb.

**Table 7: Week 1 optimal settings determined by UPDRS-III subscores**

	Hyperkinetic	
	L	R
BSC 01	S2, S7, S8, S9, S10, S11, S15, S16	S2, S7
BSC 02	S7	S5
BSC 03	S2, S4, S7, S10, S11, S13, S14, S16	S15
BSC 05	S1, S2, S4, S5, S6, S7, S8, S9, S10, S12, S15, S16	S1, S2, S3, S4, S6, S7, S8, S9, S10, S11, S12, S14, S15, S16
BSC 06	S2, S5, S7, S8, S9, S11, S12, S13, S15, S16	S1, S2, S4, S7, S13, S14, S16
BSC 07	S1, S4, S5, S6, S8, S9, S11, S12, S14, S16	S1, S2, S3, S4, S5, S6, S7, S8, S9, S11, S12, S13, S14, S15, S16
BSC 08	S15	S2
	Hypokinetic	
	L	R
BSC 01	S3, S4, S6, S7, S8, S9, S10, S11, S12, S13, S14, S15, S16	S3, S4, S10, S14, S15, S16
BSC 02	S1	S7, S8, S9
BSC 03	S5	S2
BSC 05	S7	S15
BSC 06	S4, S13, S16	S9, S10
BSC 07	S8	S4, S5, S6, S7, S8, S10, S15
BSC 08	S1, S2, S8, S9	S1, S2, S15

UPDRS: Unified Parkinson's Disease Rating Scale; L: left upper limb; R: right upper limb; optimal settings for hyperkinetic symptoms (top) and hypokinetic symptoms (bottom) determined by UPDRS item scores for the left and right upper limb of all patients at week 1; settings in red indicate optimal settings for both hyperkinetic and hypokinetic symptoms, in the same patient for the same limb.

**Table 8: Week 2 optimal settings determined by UPDRS-III subscores**

	Hyperkinetic	
	L	R
BSC 01	S3, S7, S8, S9, S10, S12	S1, S2, S5, S7, S12, S14, S16
BSC 02	S1, S2, S3, S4, S7, S8, S11, S12, S13, S14, S15	S10, S13
BSC 03	S12	S1, S3, S11, S13
BSC 05	S1, S2, S3, S4, S6, S7, S8, S11, S13, S14, S15, S16	S4
BSC 06	S1, S2, S4, S5, S6, S7, S8, S11, S12, S13, S14, S16	S1, S2, S5, S6, S7, S8, S9, S11, S12, S13, S14, S16
BSC 07	S1, S4, S5, S8, S10, S11, S12, S16	S1, S2, S3, S4, S5, S6, S8, S9, S10, S12, S16
BSC 08	S1, S5, S11, S16	S13
	Hypokinetic	
	L	R
BSC 01	S2, S5, S6, S7, S9, S10, S11, S12, S16	S1, S2, S3, S6, S7, S8, S9, S10, S13, S14
BSC 02	S2, S15	S2
BSC 03	S1, S5	S3, S4
BSC 05	S4, S13	S15
BSC 06	S2, S7, S8, S12	S1, S2, S3, S10, S11, S14
BSC 07	S2, S3, S5, S6, S8, S10, S12, S14, S16	S7, S8, S9, S13, S16
BSC 08	S7, S9, S10, S13	S10

UPDRS: Unified Parkinson's Disease Rating Scale; L: left upper limb; R: right upper limb; optimal settings for hyperkinetic symptoms (top) and hypokinetic symptoms (bottom) determined by UPDRS item scores for the left and right upper limb of all patients at week 2; settings in red indicate optimal settings for both hyperkinetic and hypokinetic symptoms, in the same patient for the same limb.

**Table 9: Week 3 optimal settings determined by UPDRS-III subscores**

	Hyperkinetic	
	L	R
BSC 01	S3	S2
BSC 02	S3, S8	S1, S3, S6, S8
BSC 03	S2, S3, S4, S5, S6, S7, S8, S10, S11, S12	S2, S3, S4, S5, S6, S8, S9, S11, S13, S14, S16
BSC 05	S1, S2, S3, S4, S6, S8, S10, S13, S16	S4, S13
BSC 06	S2	S2, S6
BSC 07	S2, S3, S4, S6, S8, S10, S12, S15, S16	S1, S2, S3, S4, S5, S6, S7, S8, S9, S10, S12, S14, S16
BSC 08	S2, S6, S12, S13	S1, S3, S4, S6, S13, S16
	Hypokinetic	
	L	R
BSC 01	S8, S11, S15, S16	S11
BSC 02	S3, S8, S15	S2, S3, S5, S6, S8, S10, S13, S15
BSC 03	S6	S7, S9
BSC 05	S2, S3, S4, S5, S8, S13, S15	S2, S13
BSC 06	S4, S8	S6, S13, S14
BSC 07	S1, S4, S8, S11, S12, S16	S2, S3, S4, S11, S14, S16
BSC 08	S3, S4, S5, S6, S8, S12, S16	S8

UPDRS: Unified Parkinson's Disease Rating Scale; L: left upper limb; R: right upper limb; optimal settings for hyperkinetic symptoms (top) and hypokinetic symptoms (bottom) determined by UPDRS item scores for the left and right upper limb of all patients at week 3; settings in red indicate optimal settings for both hyperkinetic and hypokinetic symptoms, in the same patient for the same limb.

**Table 10: Week 4 optimal settings determined by UPDRS-III subscores**

	Hyperkinetic	
	L	R
BSC 01	S1, S2, S4, S6, S7, S8, S10, S11, S12, S13, S15, S16	S1, S3, S4, S5, S9, S10, S12
BSC 02	S4	S3, S4
BSC 03	S1, S7, S11, S15	S1, S2, S3, S7, S8, S9, S10, S12, S14, S15, S16
BSC 05	S2, S4, S5, S6, S8, S9, S11, S13, S14, S15	S4
BSC 06	S1, S2, S3, S4, S5, S6, S7, S8, S9, S10, S11, S12, S14, S15, S16	S1, S2, S3, S4, S5, S6, S7, S8, S9, S10, S11, S12, S13, S14, S15, S16
BSC 07	S1, S2, S3, S4, S7, S8, S9, S10, S11, S12, S14, S15, S16	S1, S2, S3, S5, S6, S7, S8, S9, S10, S11, S12, S14, S15, S16
BSC 08	S1	S1, S7, S10
	Hypokinetic	
	L	R
BSC 01	S3, S4, S7, S13, S16	S2, S3
BSC 02	S3	S8, S9, S10
BSC 03	S5	S2
BSC 05	S5, S7, S8, S10, S11, S12, S16	S1, S3, S4, S5, S6, S7, S8, S10, S11, S12, S14, S16
BSC 06	S4, S5, S6, S11, S15, S16	S5, S8, S10
BSC 07	S2, S4, S5, S7, S8, S9, S10, S11	S2, S4, S7, S8, S9, S11, S15
BSC 08	S1, S4, S5, S10, S11, S12, S15, S16	S1, S15

UPDRS: Unified Parkinson's Disease Rating Scale; L: left upper limb; R: right upper limb; optimal settings for hyperkinetic symptoms (top) and hypokinetic symptoms (bottom) determined by UPDRS item scores for the left and right upper limb of all patients at week 4; settings in red indicate optimal settings for both hyperkinetic and hypokinetic symptoms, in the same patient for the same limb.

A further analysis was done to determine the types of settings that occurred in instances, involving all patients, where there was simultaneous optimal alleviation of hyperkinetic and hypokinetic symptoms in the same limb (settings in red in *Tables 7-10*). *Table 11* shows this breakdown as the proportion of instances at each week, involving all patients, that contained settings employing bilateral current steering (group 1), bilateral monopolar stimulation (group 2), current steering at the contralateral STN (group 3), and current steering at the ipsilateral STN (group 4). Recall that current steering at the contralateral STN refers to settings that have a current fractionation other than a 0%-100% split at the STN that is contralateral to the limb being tested. Likewise, current steering at the ipsilateral STN refers to settings that have a current fractionation other than a 0%-100% split at the STN that is ipsilateral to the limb being tested. A chi-square assessment of the values in *Table 11* with degrees of freedom of 1 ( $df = 1$ ) and alpha level of significance of 0.05 returned statistical significance ( $p < 0.05$ ) between group 3 and group 4 when the number of occurrences in each group were totaled for all four weeks.

*Table 12* breaks down the types of settings that made up instances, involving all patients, where only optimal hyperkinetic symptom alleviation in a limb was achieved, using the same four groups to categorize the settings. A chi-square assessment of the values in *Table 12* returned statistical significance between group 2 and group 3 ( $df = 1, p < 0.05$ )

at week 2 for the left upper limb and between group 2 and group 4 ( $df = 1, p < 0.05$ ) at week 2 for the right upper limb.

*Table 13* breaks down the types of settings that made up instances, involving all patients, where only optimal hypokinetic symptom alleviation in a limb was achieved. A chi-square assessment of the values in *Table 13* returned no statistical significance between any two groups at each week ( $df = 1, p > 0.05$ ).

**Table 11: Chi-square assessment of instances involving settings that optimally alleviate hyperkinetic and hypokinetic symptoms in the same limb**

	Total Instances	Group 1 - Bilateral	Group 2 - Monopolar	Group 3 - Contralateral	Group 4 - Ipsilateral
<b>Week 1 - L</b>	<b>11</b>	4	3	1	3
<b>Week 1 - R</b>	<b>8</b>	2	1	2	3
<b>Week 2 - L</b>	<b>17</b>	4	3	3	7
<b>Week 2 - R</b>	<b>12</b>	2	3	2	5
<b>Week 3 - L</b>	<b>14</b>	2	4	3	5
<b>Week 3 - R</b>	<b>11</b>	2	3	2	4
<b>Week 4 - L</b>	<b>21</b>	7	7	2	5
<b>Week 4 - R</b>	<b>13</b>	3	2	4	4
<b>Total</b>	<b>107</b>	<b>26</b>	<b>26</b>	<b>19<sup>a</sup></b>	<b>36<sup>a</sup></b>

*STN: Subthalamic nucleus; L: left upper limb; R: right upper limb. Group 1 contains instances where the setting employed bilateral current steering. Group 2 contains instances where the setting employed bilateral monopolar stimulation. Group 3 contains instances where the setting employed current steering at the STN contralateral to the testing limb. Group 4 contains instances where the setting employed current steering at the STN ipsilateral to the testing limb. A chi-square test was performed using degrees of freedom (df) of 1 and alpha of 0.05. There was a statistically significant difference between the total number of occurrences in group 3 (current steering at the STN contralateral to the limb) and the total number of occurrences in group 4 (current steering at the STN ipsilateral to the limb) across all weeks ( $df = 1, p < 0.05^a$ ).*

**Table 12: Chi-square assessment of instances involving settings that optimally alleviate only hyperkinetic symptoms in a limb**

	Total Instances	Group 1 - Bilateral	Group 2 - Monopolar	Group 3 - Contralateral	Group 4 - Ipsilateral
<b>Week 1 - L</b>	<b>39</b>	10	9	9	11
<b>Week 1 - R</b>	<b>33</b>	7	10	10	6
<b>Week 2 - L</b>	<b>20</b>	9	13 <sup>a</sup>	4 <sup>a</sup>	11
<b>Week 2 - R</b>	<b>14</b>	6	10 <sup>a</sup>	8	2 <sup>a</sup>
<b>Week 3 - L</b>	<b>22</b>	7	4	8	3
<b>Week 3 - R</b>	<b>28</b>	6	10	6	6
<b>Week 4 - L</b>	<b>35</b>	8	8	12	7
<b>Week 4 - R</b>	<b>41</b>	10	11	10	10
<b>Total</b>	<b>232</b>	<b>63</b>	<b>52</b>	<b>63</b>	<b>54</b>

STN: Subthalamic nucleus; L: left upper limb; R: right upper limb. A chi-square test was performed using degrees of freedom (df) of 1 and alpha of 0.05. Group 1 contains instances where the setting employed bilateral current steering. Group 2 contains instances where the setting employed bilateral monopolar stimulation. Group 3 contains instances where the setting employed current steering at the STN contralateral to the testing limb. Group 4 contains instances where the setting employed current steering at the STN ipsilateral to the testing limb. There was a statistically significant difference between group 2 (bilateral monopolar stimulation) and group 3 (current steering at the STN contralateral to the limb) at week 2 for the left upper limb ( $df = 1, p < 0.05^a$ ) and between group 2 (bilateral monopolar stimulation) and group 4 (current steering at the STN ipsilateral to the limb) at week 2 for the right upper limb ( $df = 1, p < 0.05^a$ ).

**Table 13: Chi-square assessment of instances involving settings that optimally alleviate only hypokinetic symptoms in a limb**

	Total Instances	Group 1 - Bilateral	Group 2 - Monopolar	Group 3 - Contralateral	Group 4 - Ipsilateral
<b>Week 1 - L</b>	<b>13</b>	1	5	3	4
<b>Week 1 - R</b>	<b>15</b>	4	3	4	4
<b>Week 2 - L</b>	<b>15</b>	5	3	4	3
<b>Week 2 - R</b>	<b>14</b>	5	3	3	3
<b>Week 3 - L</b>	<b>18</b>	4	5	4	5
<b>Week 3 - R</b>	<b>12</b>	4	2	1	5
<b>Week 4 - L</b>	<b>13</b>	2	3	3	5
<b>Week 4 - R</b>	<b>17</b>	5	3	6	3
<b>Total</b>	<b>117</b>	<b>30</b>	<b>27</b>	<b>28</b>	<b>32</b>

STN: Subthalamic nucleus; L: left upper limb; R: right upper limb. Group 1 contains instances where the setting employed bilateral current steering. Group 2 contains instances where the setting employed bilateral monopolar stimulation. Group 3 contains instances where the setting employed current steering at the STN contralateral to the testing limb. Group 4 contains instances where the setting employed current steering at the STN ipsilateral to the testing limb. A chi-square test was performed using degrees of freedom (df) of 1 and alpha of 0.05. There was no statistical significant difference between any two values at each week ( $df = 1, p > 0.05$ ).

## Chapter 4

### 4 Discussion

The current study aimed at determining the effectiveness of current steering in the alleviation of appendicular motor symptoms of the upper limbs. It was hypothesized that the way the electrical field was shaped will affect a patient's upper limb symptom alleviation. The electrical field was shaped using 16 different current fractionation settings, four of which were bilateral monopolar settings and the remaining 12 having employed current steering either unilaterally or bilaterally. This section will discuss the results from the two objectives, present limitations and future directions of the study, and end with concluding remarks.

#### 4.1 Discussion of objective #1

The first objective was to determine the setting and amplitude that optimally alleviates each patient's upper limb symptoms. Given the variations in lead position, symptom phenotype, and anatomical factors across patients, it was predicted that the benefits of current steering and/or monopolar stimulation will differ among patients. Kinematic data was used to quantify postural tremor, rest tremor, and bradykinesia, from which weekly optimal settings were computed for the left and right upper limb of the seven patients (*Table 6*). A notable observation from *Table 6* is that the optimal settings change from week to week for most patients. Recall that the two contacts chosen on each lead to deliver current from stayed consistent across the study for all patients (*Figure 7*), and the only variable that changed from week to week was the current amplitude. Thus, it can be said that current amplitude influences the electrical field shape created by the current fractionation setting. This is supported by a review of the technical features of DBS systems which states that the current distribution, and therefore the electric stimulation field, can be altered by the electrode design, the polarity and proportion of current coming from each contact, and the amplitude of current (Amon & Alesch, 2017). Another observation is that at week 4, all the optimal settings employed current steering either unilaterally or bilaterally. This may suggest that at higher amplitudes, there is a larger spread of current to neighboring structures and steering the current away from these



structures is needed for optimal symptom alleviation. This phenomenon is supported by the case study alluded to in section 1.2.5.1; further increasing amplitude on the monopolar stimulation through contact #2 induced dyskinesia and was not sufficient to control the patient's tremor (Barbe et al., 2014). As a result, the stimulation field was adjusted to a 'tear drop shape' by shifting stimulation toward a more proximal contact and amplitude was slowly increased for improvement in motor symptoms without causing dyskinesia (Barbe et al., 2014).

*Table 6* also highlights 14 optimal settings, at the corresponding week's amplitude, that optimally alleviated each patient's left and right upper limb symptoms among the four weeks. Symptom alleviation at the 14 optimal states was significantly different from symptoms quantified at the OFF state of all patients (*Figure 15*). This suggests that at the optimal setting and amplitude, the electrical field shape was able to localize the current to the target region in the STN. Eight out of the 14 optimal settings employed current steering either unilaterally or bilaterally whereas the remaining six were bilateral monopolar settings. As previously mentioned, monopolar settings create a relatively spherical electrical field (Barbe et al., 2014). Therefore, we can assume that the optimal states that involved a bilateral monopolar setting were able to create a spherical electrical field around the active contact on both sides of the brain, at a specific amplitude, that was able to stimulate the target region. Likewise, it can be assumed that the optimal states that involved the use of current steering either unilaterally or bilaterally created an electrical field shape, that was non-spherical and extended over two active contacts, which was able to stimulate the target region. This suggests that the active contacts of the leads that employed current steering was not within the *optimal* target region since optimal alleviation could not be achieved with monopolar stimulation. Failure of the active contacts to be within the target region could be due to the many reasons that lead to suboptimal lead position in the brain (section 1.2.6) or anatomical factors that vary from patient to patient, resulting in differences in functional target. It can be challenging to study the variations in anatomy of basal ganglia nuclei across patients, which is usually approached in two ways: in vivo imaging studies and postmortem studies. One MRI study on 148 healthy adults ranging in age from 18 to 77 years old showed a bilateral age-related shrinkage (in volume) of the head of the caudate nucleus and the putamen in

both sexes (Gunning-Dixon, Head, McQuain, Acker, & Raz, 1998). In the same study, a mild bilateral age-related shrinkage of the globus pallidus was only observed in men. Although this study did not look at the size of the STN, the implications of age-related changes in the neostriatum of healthy adults can be extended to a sample of diseased patients. Variations in the shape or size of the STN across PD patients can affect optimal anatomical targeting during DBS. A postmortem study measured the centers and borders of the STN in relation to the anterior commissure-posterior commissure (AC-PC) line in 12 postmortem brains of patients who died of non-neurological diseases, ranging from 29 to 84 years of age (den Dunnen & Staal, 2005). The study showed that with a relatively constant length of the AC-PC line, the center of the STN tends to move 3.9 mm cranially, 2.6 mm laterally and 0.2 mm anteriorly with increasing age. This change is thought to be caused by the loss of neurons, however the extent to which neuronal loss occurs in the STN at different ages is unknown (den Dunnen & Staal, 2005). Again, the age-related changes can be applied to PD patients whose subthalamic nuclei can vary in shape and spatial position, affecting optimal target determination during DBS. Within limits, current steering may address this issue by allowing stimulation to be directed toward the functional target, even if lead position is seemingly optimal based on pre-operative MRI and stereotactic atlases.

#### 4.1.1 Involvement of the ipsilateral STN

Some weekly optimal settings involved current steering at the STN that was ipsilateral to the limb of interest (settings in purple in *Table 6*). This phenomenon is of interest because conventionally it is known that movement of limbs is controlled by the contralateral side of the brain. Specifically, upper limb muscles are mainly under the control of crossed corticospinal projections originating from contralateral motor areas, including the basal ganglia (Davare, Duque, Vandermeeren, Thonnard, & Olivier, 2007). This idea puts to question why shaping of the electrical field is necessary at the ipsilateral STN if the target region of a limb is the contralateral STN. Previous studies involving unilateral STN DBS also suggest a similar finding; mild but sufficient improvement is observed in the extremities ipsilateral to the stimulating electrode. For instance, Tabbal et al. used objective kinematic measures to show improvement in ipsilateral motor function in 52

PD patients who underwent unilateral STN DBS at a median of 8.7 months before testing (Tabbal et al., 2008). Investigating the reasons for ipsilateral clinical benefit from unilateral DBS may help to explain the need for targeted stimulation of not only the STN contralateral to the limb, but also the ipsilateral STN. A potential explanation for this phenomenon lies in the effects of brain lateralization on motor control.

#### 4.1.2 Lateralization of motor control

Specific brain functions are mainly controlled by one hemisphere, a phenomenon known as lateralization (or hemispheric dominance); the right hemisphere is dominant for spatial cognition, body schema, proprioceptive control, and action inhibition, whereas the left hemisphere is dominant for verbal processing and motor control (Lizarraga et al., 2017). In 90% of humans that are right-handed, the left-sided dominance of motor control is clear, whereas in left-handed and ambidextrous humans, brain asymmetries are less obvious and it is unclear which hemisphere is dominant (Lizarraga et al., 2017). Although the mechanism of lateralization for motor control is unknown, it has been proposed that the left hemisphere controls limb trajectory and timing aspects of ballistic and sequential movements, whereas the right hemisphere controls final limb position and posture (Lizarraga et al., 2017). Additionally, the right inferior frontal cortex and STN contribute to motor inhibition through suppression of thalamocortical signals. This idea of lateralization can therefore be used to explain why stimulation parameters also affect the STN that is ipsilateral to the targeted limb. In a right-handed PD patient with left-sided dominance, stimulation of potentially lateralized motor circuits in the left hemisphere could be necessary for optimal symptom alleviation in both the right and left upper limbs. In addition, if the active contacts on the right lead are in proximity to potentially lateralized circuits that contribute to motor inhibition as mentioned above, current steering could address this issue by avoiding stimulation to these areas in the right hemisphere for optimal symptom alleviation of both the right and left upper limbs. Furthermore, Walker et al. used intraoperative microelectrode recordings of the STN in patients with advanced idiopathic PD during unilateral DBS of the contralateral STN to show that therapeutic 160 Hz unilateral stimulation results in increased activity in the contralateral STN (Walker et al., 2011). This shows that unilateral STN stimulation

activates bilateral basal ganglia networks, further adding to the idea that stimulation parameters need to be tailored to the left and right nuclei for optimal symptom alleviation of a limb, to avoid under- or overstimulation of potentially lateralized motor circuits.

#### 4.2 Discussion of objective #2

The second objective compared the optimal alleviation of hyperkinetic symptoms, which include upper limb rest and postural tremor, to optimal alleviation of hypokinetic symptoms, which include upper limb rigidity and bradykinesia; it was predicted that hyperkinetic symptoms will be optimally alleviated by settings that differ from those that optimally alleviate hypokinetic symptoms in the same limb. UPDRS-III subscores were used to quantify postural tremor, rest tremor, rigidity and bradykinesia, from which weekly optimal settings were computed for the left and right upper limb of the seven patients (*Tables 7-10*).

There were 107 instances where the same setting was able to optimally alleviate hyperkinetic and hypokinetic symptoms of a limb (*Table 11*). There were 232 instances where a setting was able to only optimally alleviate the hyperkinetic symptoms of a limb (*Table 12*). Finally, there were 117 instances where a setting was able to only optimally alleviate the hypokinetic symptoms of a limb (*Table 13*). These results suggest that there are spatially separate regions for the alleviation of hyperkinetic and hypokinetic regions; however, the settings involved in the instances of simultaneous optimal alleviation of hyperkinetic and hypokinetic symptoms created electrical field shapes, at the corresponding week's amplitude, that were potentially able to target both regions. Although the sensorimotor STN is conventionally used as the target for many DBS surgeries for PD, as was the case for patients in this study, the tripartite functional organization (*Figure 2*) is an oversimplification and may even be a topic of debate among proponents. Alkemade and Forstmann argue that the current hypothesis of the three subdivisions is based on low numbers of clinical observations and primate tracing studies, and support a view that the topological organization within the nucleus does not contain strict anatomical boundaries (Alkemade & Forstmann, 2014). Even if one holds the assumption of functional specialization, the segregated sensorimotor, associative, and limbic regions show substantial areas of overlap (Accolla et al., 2016). Therefore, the

exact location of leads within the STN for optimal control of different symptoms is continuously being studied.

#### 4.2.1 Optimal tremor control

Current hypotheses regarding tremor generation in PD point to abnormal synchronization of neuronal firing in the basal ganglia thalamocortical loop (*Figure 4*). Although resting tremor usually responds successfully to STN-DBS, severe tremor and coexisting essential tremor may progressively worsen with time (Mirza et al., 2017). Ventral intermediate nucleus of the thalamus (Vim) DBS has been shown to suppress tremor more effectively in tremor-dominant PD; however, proximal postural tremor, distal intention tremor and some cerebellar outflow tremor is difficult to be well controlled by even Vim DBS (Xie, Bernard, & Warnke, 2012). To address these issues, the posterior subthalamic area (PSA) has been proposed as a target site because of promising results in tremor suppression. The PSA consists of the zona incerta (Zi) and the prelemniscal radiation (Raprl), and is bounded anteriorly by the posterior border of the STN and superiorly by the ventral thalamic nuclei (Xie et al., 2012). The caudal Zi is an effective target for all forms of tremor because of its unique GABAergic connections with the basal ganglia and cerebellar thalamocortical loops (Xie et al., 2012). Given that the STN is relatively small with its 5.9 mm x 3.7 mm x 5 mm dimensions and current spread is estimated to be 2-3 mm from the electrode for intensities of 2-3 mA, stimulation of neighboring structures seems probable (Alkemade et al., 2017; Jankovic & Tolosa, 2015). Looking at the breakdown of settings that only optimally alleviated hyperkinetic symptoms (*Table 12*), we see that approximately 78% of the 232 total instances employed current steering either unilaterally or bilaterally; the electrical field shapes created by these settings, at the corresponding week's amplitude, could have potentially steered current to the caudal Zi for tremor suppression, especially in patients that had significant postural tremor. At week 2, there is a significant difference between instances that contained bilateral monopolar settings and settings that employed current steering at the STN contralateral ( $df = 1, p < 0.05$ ) and ipsilateral ( $df = 1, p < 0.05$ ) to the limb of interest. The greater number of occurrences involving bilateral monopolar settings may have contributed to

spherical electrical fields surrounding the active contacts for local stimulation in the STN for optimal suppression of resting tremor.

#### 4.2.2 Optimal control of rigidity and bradykinesia

Rigidity and bradykinesia respond well to both STN and GPi DBS, however the exact location within these nuclei for optimal control needs further investigation (Mirza et al., 2017). There is evidence to show that stimulation of the Raprl could reduce rigidity as well as contralateral tremor (Xie et al., 2012). The Raprl is a fiber bundle that lies posterior to the STN, separated from it by the Zi; it consists of fibers that project to the thalamus as well as ascending cerebellothalamic fibers (Xie et al., 2012). A study by Velasco et al. on 10 PD patients who underwent unilateral Raprl electrical stimulation showed significant improvement in tremor and rigidity, with mild improvement in bradykinesia (Velasco et al., 2001). Additionally, another study showed chronic Raprl electrical stimulation induced a significant decrease in tremor and rigidity in 14 PD patients (Jimenez et al., 2000). The aforementioned studies are of importance to the results seen in *Table 11* showing 107 instances where the same setting worked to optimally alleviate hyperkinetic and hypokinetic symptoms in the same limb. The electrical field shapes created by these settings, at the corresponding week's amplitude, may have potentially reached the Raprl where optimal control of tremor (hyperkinetic) and rigidity (hypokinetic) can be achieved. Given that the Raprl is a non-spherical fiber bundle, it can be difficult to optimally capture with spherical stimulation geometries (Schüpbach et al., 2017); this can explain why approximately 76% of the 107 instances of simultaneous optimal alleviation of hyperkinetic and hypokinetic symptoms employed current steering either unilaterally or bilaterally. There was also a significant difference between instances involving settings that employed current steering at the STN ipsilateral to the limb and those that employed current steering at the STN contralateral to the limb ( $df = 1, p < 0.05$ ). The greater number of instances involving current steering at the ipsilateral STN could point towards the effects of lateralization discussed in section 4.1.2, where lateralized motor circuits controlling hyperkinetic and hypokinetic symptoms could have potentially been the target of stimulation.

### 4.3 Implications and clinical relevance

The current study's findings can be used to contribute to the advancement of PD symptom management. To start off, the optimal settings outlined in *Table 6* are the result of an objective quantification using an IMU-based sensor system, as opposed to a relatively subjective interpretation using UPDRS-III subscores. From these results, it can be concluded that implanting a constant-current DBS system that is capable of current steering is potentially more beneficial to the patient than implanting a voltage-controlled single source system given that more than half the 14 optimal settings employed current steering either unilaterally or bilaterally. Factors such as suboptimal lead positioning, differences in functional target due to symptom heterogeneity, and anatomical variations between patients cannot be predicted before surgery to guarantee that a patient will optimally benefit from a monopolar setting creating a spherical electrical field around the active contact. Therefore, having the flexibility to program a uniform, non-spherical electrical field allows the patient to receive optimal treatment despite the external factors mentioned above. Although the optimal settings in *Table 6* were only quantified for the upper limb, the findings can be extended to whole-body quantification; from the optimal settings determined by a whole-body UPDRS-III score that each patient went home with at the study conclusion (*Table 5*), only one patient went home with a bilateral monopolar stimulation. Furthermore, the results of the second objective provide insight into the use of current steering in alleviating PD symptom subtypes. The fact that there were more instances where settings were able to optimally alleviate only hyperkinetic symptoms of a limb (*Table 12*) or only hypokinetic symptoms of a limb (*Table 13*), compared to instances where the same setting was able to optimally alleviate hyperkinetic and hypokinetic symptoms of a limb (*Table 11*) shows that there are different electrical field shapes, and by extension potentially different targets, for optimal alleviation of different symptom subtypes. Therefore, clinical follow-up could focus on using similar programming parameters in subsets of patients based on similar symptom phenotype; future studies are needed to support this.

#### 4.4 Limitations

One of the most prominent limitations of this study is the low sample size; an n-value of seven is not an accurate representation of the PD population as there are varying disease phenotypes that extend well beyond the tested sample. In addition, statistical power could be increased with a larger sample size to have more conclusive outcomes. Another prominent limitation is that there is not a testable way to show how the geometry of the electric field inside the brain is being changed by current steering; a close alternative would be mapping electric field simulations on post-operative MRI scans that show localization of electrodes within the STN. Using ultra-high resolution 7 T MRI to show which area within the nucleus is being targeted can also be used to corroborate the understanding of functional subdivision in the STN. Other limitations of the study were constraints of time and feasibility, such as being able to test only 16 different settings, not being able to replicate a testing session at a different time point, and the lack of age-matched healthy control data. The different possibilities of current fractionation are infinite (e.g. current can be fractionated between two contacts using an 80%-20% split, 60%-40% split, 55-45% split, etc.), but due to the constraints of time and preventing patient fatigue, a maximum of four settings were tested each day. Being able to replicate patient performance at a setting and amplitude at a different time point and extending to a longitudinal study that follows the course of treatment over a few months, can increase the reproducibility of the study. Normalization of kinematic values for this study was achieved using data from neurologists who were used as healthy participants and who also mimicked performance of a severe PD patient; using values from age-matched healthy controls and advanced PD patients with severe motor symptoms could increase the validity of the study.

#### 4.5 Future directions

To address some of the limitations in this study, future studies could look at the correlation between the use of current steering in optimal symptom alleviation and electrode localization in the STN using imaging techniques. A deeper investigation into different electrical field shapes can also be explored by testing different combinations of current fractionation, and even investigating the effects of current steering in horizontal



directions. The latter would require implanting directional leads for DBS and contributing to the limited literature on the utility and effectiveness of steering the stimulation field in the plane perpendicular to the lead. Another follow-up study would be to look at the effects of current steering on axial symptoms and perform a comparison to see if there are settings that work optimally for appendicular and axial symptom improvement.

Additionally, closely monitoring disease phenotype pre- and post-DBS treatment could have significant clinical implications. Categorizing patients according to their symptoms such as being tremor-dominant or bradykinesia-dominant and looking at the effects of current steering on these subsets of patients can eliminate some of the programming challenges clinicians face during patient follow-up.

#### 4.6 Conclusion

In summary, the current thesis showed that manipulating the shape of the electrical field in PD patients who underwent STN-DBS using current steering affected the degree of upper limb symptom alleviation. Kinematic data was used to show that the use of current steering in optimal upper limb symptom alleviation is highly individualized and is not only patient-dependent but also limb-dependent. Current steering may address issues of lead misplacement and possible anatomical differences by directing the stimulation field to the target region. This study also used UPDRS-III subscores to contribute to the growing evidence for areas that individually control tremor and hypokinetic symptoms. Current steering may also contribute to instances of simultaneous alleviation of hyperkinetic and hypokinetic symptoms by shaping the electrical field to optimally capture areas that control both symptom subtypes. Limitations of this study include a low sample size and being unable to detect which subarea of the STN was being stimulated by the different settings. Future directions should be aimed at mapping electric field simulations on high resolution MRI scans that show electrode location so that more robust conclusions about functional targets can be made.

## Bibliography

- Accolla, E. A., Herrojo Ruiz, M., Horn, A., Schneider, G.-H., Schmitz-Hübsch, T., Draganski, B., & Kühn, A. A. (2016). Brain networks modulated by subthalamic nucleus deep brain stimulation. *Brain*, *139*(9), 2503–2515. <https://doi.org/10.1093/brain/aww182>
- Alkemade, A., De Hollander, G., Keuken, M. C., Schäfer, A., Ott, D. V. M., Schwarz, J., ... Forstmann, B. U. (2017). Comparison of T2\*-weighted and QSM contrasts in Parkinson's disease to visualize the STN with MRI. *PLoS ONE*, *12*(4), 1–13. <https://doi.org/10.1371/journal.pone.0176130>
- Alkemade, A., & Forstmann, B. U. (2014). Do we need to revise the tripartite subdivision hypothesis of the human subthalamic nucleus (STN)? Response to Alkemade and Forstmann. *NeuroImage*, *95*, 326–329. <https://doi.org/10.1016/j.neuroimage.2015.01.038>
- Amon, A., & Alesch, F. (2017). Systems for deep brain stimulation: review of technical features. *Journal of Neural Transmission*, *124*(9), 1083–1091. <https://doi.org/10.1007/s00702-017-1751-6>
- Baradaran, N., Tan, S. N., Liu, A., Ashoori, A., Palmer, S. J., Wang, Z. J., ... McKeown, M. J. (2013). Parkinson's disease rigidity: Relation to brain connectivity and motor performance. *Frontiers in Neurology*, *4* JUN(June). <https://doi.org/10.3389/fneur.2013.00067>
- Barbe, M. T., Maarouf, M., Alesch, F., & Timmermann, L. (2014). Multiple source current steering - a novel deep brain stimulation concept for customized programming in a Parkinson's disease patient. *Parkinsonism and Related Disorders*, *20*(4), 471–473. <https://doi.org/10.1016/j.parkreldis.2013.07.021>
- Bejjani, B. P., Gervais, D., Arnulf, I., Papadopoulos, S., Demeret, S., Bonnet, A. M., ... Agid, Y. (2000). Axial parkinsonian symptoms can be improved: The role of levodopa and bilateral subthalamic stimulation. *Journal of Neurology Neurosurgery and Psychiatry*, *68*(5), 595–600. <https://doi.org/10.1136/jnnp.68.5.595>
- Benabid, A. L., Chabardes, S., Mitrofanis, J., & Pollak, P. (2009). Deep brain stimulation of the subthalamic nucleus for the treatment of Parkinson's disease. *The Lancet Neurology*, *8*(1), 67–81. [https://doi.org/10.1016/S1474-4422\(08\)70291-6](https://doi.org/10.1016/S1474-4422(08)70291-6)
- Berardelli, A. (2001). Pathophysiology of bradykinesia in Parkinson's disease. *Brain*, *124*(11), 2131–2146. <https://doi.org/10.1093/brain/124.11.2131>
- Beurrier, C., Bioulac, B., Audin, J., & Hammond, C. (2001). High-frequency stimulation produces a transient blockade of voltage-gated currents in subthalamic neurons. *J Neurophysiol*, *85*(4), 1351–1356. <https://doi.org/10.1152/jn.2001.85.4.1351>
- Bikson, M., Lian, J., Hahn, P. J., Stacey, W. C., Sciortino, C., & Durand, D. M. (2001). Suppression of epileptiform activity by high frequency sinusoidal fields in rat hippocampal slices. *The Journal of Physiology*, *531*(1), 181–191. <https://doi.org/10.1111/j.1469-7793.2001.0181j.x>

- Broggi, G., Franzini, A., Marras, C., Romito, L., & Albanese, A. (2003). Surgery of Parkinson's disease: Inclusion criteria and follow-up. *Neurological Sciences*, 24(SUPPL. 1), 38–40. <https://doi.org/10.1007/s100720300037>
- Bronte-Stewart, H., Barberini, C., Koop, M. M., Hill, B. C., Henderson, J. M., & Wingeier, B. (2009). The STN beta-band profile in Parkinson's disease is stationary and shows prolonged attenuation after deep brain stimulation. *Experimental Neurology*, 215(1), 20–28. <https://doi.org/10.1016/j.expneurol.2008.09.008>
- Cochran, W. G., & Snedecor, G. W. (1974). *Statistical Methods: Sixth Edition* (6th ed.). Iowa State University Press.
- Connolly, B. S., & Lang, A. E. (2014). Pharmacological treatment of Parkinson disease: A review. *JAMA - Journal of the American Medical Association*, 311(16), 1670–1683. <https://doi.org/10.1001/jama.2014.3654>
- Davare, M., Duque, J., Vandermeeren, Y., Thonnard, J. L., & Olivier, E. (2007). Role of the ipsilateral primary motor cortex in controlling the timing of hand muscle recruitment. *Cerebral Cortex*, 17(2), 353–362. <https://doi.org/10.1093/cercor/bhj152>
- Delrobaei, M., Memar, S., Pieterman, M., Stratton, T. W., McIsaac, K., & Jog, M. (2018). Towards remote monitoring of Parkinson's disease tremor using wearable motion capture systems. *Journal of the Neurological Sciences*, 384(August 2017), 38–45. <https://doi.org/10.1016/j.jns.2017.11.004>
- Delrobaei, M., Tran, S., Gilmore, G., McIsaac, K., & Jog, M. (2016). Characterization of multi-joint upper limb movements in a single task to assess bradykinesia. *Journal of the Neurological Sciences*, 368(September), 337–342. <https://doi.org/10.1016/j.jns.2016.07.056>
- DeMaagd, G., & Philip, A. (2015). Parkinson's Disease and Its Management: Part 1: Disease Entity, Risk Factors, Pathophysiology, Clinical Presentation, and Diagnosis. *P & T: A Peer-Reviewed Journal for Formulary Management*, 40(8), 504–532. Retrieved from <http://www.ncbi.nlm.nih.gov/pubmed/26236139> <http://www.pubmedcentral.nih.gov/articlerender.fcgi?artid=PMC4517533>
- den Dunnen, W. F. A., & Staal, M. J. (2005). Anatomical alterations of the subthalamic nucleus in relation to age: A postmortem study. *Movement Disorders*, 20(7), 893–898. <https://doi.org/10.1002/mds.20417>
- Dostrovsky, J. O., Levy, R., Wu, J. P., Hutchison, W. D., Tasker, R. R., & Lozano, A. M. (2000). Microstimulation-Induced Inhibition of Neuronal Firing in Human Globus Pallidus. *Journal of Neurophysiology*, 84(1), 570–574. <https://doi.org/10.1152/jn.2000.84.1.570>
- Ellis, T. M., Foote, K. D., Fernandez, H. H., Sudhyadhom, A., Rodriguez, R. L., Zeilman, P., ... Okun, M. S. (2008). Reoperation for suboptimal outcomes after deep brain stimulation surgery. *Neurosurgery*, 63(4), 754–760. <https://doi.org/10.1227/01.NEU.0000325492.58799.35>
- Eusebio, A., & Brown, P. (2009). Synchronisation in the beta frequency-band - The bad boy of parkinsonism or an innocent bystander? *Experimental Neurology*, 217(1), 1–

3. <https://doi.org/10.1016/j.expneurol.2009.02.003>

- Fasano, A., & Lozano, A. M. (2015). Deep brain stimulation for movement disorders: 2015 and beyond. *Current Opinion in Neurology*, 28(4), 423–436. <https://doi.org/10.1097/WCO.0000000000000226>
- Filali, M., Hutchison, W. D., Palter, V. N., Lozano, A. M., & Dostrovsky, J. O. (2004). Stimulation-induced inhibition of neuronal firing in human subthalamic nucleus. *Experimental Brain Research*, 156(3), 274–281. <https://doi.org/10.1007/s00221-003-1784-y>
- Gilmore, G., & Jog, M. (2017). Future Perspectives: Assessment Tools and Rehabilitation in the New Age. In *Movement Disorders Rehabilitation* (pp. 155–182). Springer, Cham. [https://doi.org/https://doi.org/10.1007/978-3-319-46062-8\\_10](https://doi.org/https://doi.org/10.1007/978-3-319-46062-8_10)
- Gunning-Dixon, F. M., Head, D., McQuain, J., Acker, J. D., & Raz, N. (1998). Differential aging of the human striatum: a prospective MR imaging study. *American Journal of Neuroradiology*, 19(September), 1501–1507.
- Hamani, C., Saint-Cyr, J. A., Fraser, J., Kaplitt, M., & Lozano, A. M. (2004). The subthalamic nucleus in the context of movement disorders. *Brain*, 127(1), 4–20. <https://doi.org/10.1093/brain/awh029>
- Helmich, R. C., & Dirks, M. F. (2017). Pathophysiology and Management of Parkinsonian Tremor. *Seminars in Neurology*, 37(2), 127–134. <https://doi.org/10.1055/s-0037-1601558>
- Helmich, R. C., Hallett, M., Deuschl, G., Toni, I., & Bloem, B. R. (2012). Cerebral causes and consequences of parkinsonian resting tremor: A tale of two circuits? *Brain*, 135(11), 3206–3226. <https://doi.org/10.1093/brain/aws023>
- Helmich, R. C., Janssen, M. J. R., Oyen, W. J. G., Bloem, B. R., & Toni, I. (2011). Pallidal dysfunction drives a cerebellothalamic circuit into Parkinson tremor. *Annals of Neurology*, 69(2), 269–281. <https://doi.org/10.1002/ana.22361>
- Helmich, R. C., Toni, I., Deuschl, G., & Bloem, B. R. (2013). The pathophysiology of essential tremor and parkinson's tremor. *Current Neurology and Neuroscience Reports*, 13(9). <https://doi.org/10.1007/s11910-013-0378-8>
- Herzog, J., Fietzek, U., Hamel, W., Morsnowski, A., Steigerwald, F., Schrader, B., ... Volkman, J. (2004). Most effective stimulation site in subthalamic deep brain stimulation for Parkinson's disease. *Movement Disorders*, 19(9), 1050–1054. <https://doi.org/10.1002/mds.20056>
- Jankovic, J., & Tolosa, E. (2015). Deep-Brain Stimulation for Movement Disorders. In *Parkinson's Disease and Movement Disorders* (6th ed., p. 657). Wolters Kluwer.
- Jimenez, F., Velasco, F., Velasco, M., Brito, F., Morel, C., Marquez, I., & Perez, M. L. (2000). Subthalamic prelemniscal radiation stimulation for the treatment of Parkinson's disease: Electrophysiological characterization of the area. *Archives of Medical Research*, 31(3), 270–281. [https://doi.org/10.1016/S0188-4409\(00\)00066-7](https://doi.org/10.1016/S0188-4409(00)00066-7)
- Kopell, B. H., Machado, A., & Butson, C. (2009). Stimulation Technology in Functional Neurosurgery. *Textbook of Stereotactic and Functional Neurosurgery*, 1401–1425.

[https://doi.org/10.1007/978-3-540-69960-6\\_84](https://doi.org/10.1007/978-3-540-69960-6_84)

- Laxton, A. W., Dostrovsky, J. O., & Lozano, A. M. (2009). Stimulation Physiology in Functional Neurosurgery. In *Textbook of Stereotactic and Functional Neurosurgery* (pp. 1384–1396). <https://doi.org/10.1007/978-3-540-69960-6>
- Lizarraga, K. J., Luca, C. C., De Salles, A., Gorgulho, A., Lang, A. E., & Fasano, A. (2017). Asymmetric neuromodulation of motor circuits in Parkinson's disease: The role of subthalamic deep brain stimulation. *Surgical Neurology International*, 8. <https://doi.org/10.4103/sni.sni>
- Louis, E. D., Tang, M. X., & Cote, L. (1999). Progression of Parkinsonian Signs in Parkinson Disease, 56, 334–337. <https://doi.org/10.1001/archneur.56.3.334>
- Magrinelli, F., Picelli, A., Tocco, P., Federico, A., Roncari, L., Smania, N., ... Tamburin, S. (2016). Pathophysiology of Motor Dysfunction in Parkinson's Disease as the Rationale for Drug Treatment and Rehabilitation. *Parkinson's Disease*, 2016. <https://doi.org/10.1155/2016/9832839>
- McIntyre, C. C., & Anderson, R. W. (2016). Deep brain stimulation mechanisms: the control of network activity via neurochemistry modulation. *Journal of Neurochemistry*, 139, 338–345. <https://doi.org/10.1111/jnc.13649>
- Mirza, S., Yazdani, U., Dewey III, R., Patel, N., Dewey, R. B., Miocinovic, S., & Chitnis, S. (2017). Comparison of Globus Pallidus Interna and Subthalamic Nucleus in Deep Brain Stimulation for Parkinson Disease: An Institutional Experience and Review. *Parkinson's Disease*, 2017, 1–15. <https://doi.org/10.1155/2017/3410820>
- Montgomery Jr., E. B. (2017). Principles of Electrophysiology. In *Deep Brain Stimulation Programming* (Second, pp. 17–43). Oxford University Press.
- Nonnekes, J., Timmer, M. H. M., Vries, N. M. De, & Rascol, O. (2016). Unmasking Levodopa Resistance in Parkinson's Disease, 31(11), 1602–1609. <https://doi.org/10.1002/mds.26712>
- Obeso, J. A., Rodriguez-Oroz, M. C., Rodriguez, M., Lanciego, J. L., Artieda, J., Gonzalo, N., & Olanow, C. W. (2000). Pathophysiology of the basal ganglia in Parkinson's disease. *Trends in Neurosciences*, 23(Box 1), S8–S19. [https://doi.org/10.1016/S1471-1931\(00\)00028-8](https://doi.org/10.1016/S1471-1931(00)00028-8)
- Rizek, P., Kumar, N., & Jog, M. S. (2016). An update on the diagnosis and treatment of Parkinson disease. *CMAJ: Canadian Medical Association Journal*, 1157–1165. <https://doi.org/http://dx.doi.org.proxy1.lib.uwo.ca/10.1503/cmaj.151179>
- Rodriguez-Oroz, M. C., Jahanshahi, M., Krack, P., Litvan, I., Macias, R., Bezard, E., & Obeso, J. A. (2009). Initial clinical manifestations of Parkinson's disease: features and pathophysiological mechanisms. *The Lancet Neurology*, 8(12), 1128–1139. [https://doi.org/10.1016/S1474-4422\(09\)70293-5](https://doi.org/10.1016/S1474-4422(09)70293-5)
- Romanelli, P., Bronte-Stewart, H., Heit, G., Schaal, D. W., & Esposito, V. (2004). The functional organization of the sensorimotor region of the subthalamic nucleus. *Stereotactic and Functional Neurosurgery*, 82(5–6), 222–229. <https://doi.org/10.1159/000082778>

- Schüpbach, W. M. M., Chabardes, S., Matthies, C., Pollo, C., Steigerwald, F., Timmermann, L., ... Schuurman, P. R. (2017). Directional leads for deep brain stimulation: Opportunities and challenges. *Movement Disorders*, 32(10), 1371–1375. <https://doi.org/10.1002/mds.27096>
- Steigerwald, F., Müller, L., Johannes, S., Matthies, C., & Volkmann, J. (2016). Directional deep brain stimulation of the subthalamic nucleus: A pilot study using a novel neurostimulation device. *Movement Disorders*, 31(8), 1240–1243. <https://doi.org/10.1002/mds.26669>
- Tabbal, S. D., Ushe, M., Mink, J. W., Revilla, F. J., Wernle, A. R., Hong, M., ... Perlmutter, J. S. (2008). Unilateral subthalamic nucleus stimulation has a measurable ipsilateral effect on rigidity and bradykinesia in parkinson disease. *Experimental Neurology*, 211(1), 234–242. <https://doi.org/10.1016/j.expneurol.2008.01.024>
- Tewari, A., Jog, R., & Jog, M. S. (2016). The Striatum and Subthalamic Nucleus as Independent and Collaborative Structures in Motor Control. *Frontiers in Systems Neuroscience*, 10(March), 1–13. <https://doi.org/10.3389/fnsys.2016.00017>
- Timmermann, L., Jain, R., Chen, L., Maarouf, M., Barbe, M. T., Allert, N., ... Alesch, F. (2015). Multiple-source current steering in subthalamic nucleus deep brain stimulation for Parkinson's disease (the VANTAGE study): A non-randomised, prospective, multicentre, open-label study. *The Lancet Neurology*, 14(7), 693–701. [https://doi.org/10.1016/S1474-4422\(15\)00087-3](https://doi.org/10.1016/S1474-4422(15)00087-3)
- Velasco, F., Jimenez, F., Perez, M. L., Carrillo-Ruiz, J. D., Velasco, A. L., Ceballos, J., & Velasco, M. (2001). Electrical stimulation of the prelemniscal radiation in the treatment of parkinson's disease: An old target revised with new techniques. *Neurosurgery*, 49(2), 293–306. <https://doi.org/10.1097/00006123-200108000-00009>
- Wagle Shukla, A., Zeilman, P., Fernandez, H., Bajwa, J. A., & Mehanna, R. (2017). DBS Programming: An Evolving Approach for Patients with Parkinson's Disease. *Parkinson's Disease*, 2017. <https://doi.org/10.1155/2017/8492619>
- Walker, H. C., Watts, R. L., Schrandt, C. J., Huang, H., Guthrie, S. L., Guthrie, B. L., & Montgomery, E. B. J. (2011). Activation of subthalamic neurons by contralateral subthalamic deep brain stimulation in Parkinson disease. *Neurophysiological*, 105(3), 1112–1121. <https://doi.org/10.1152/jn.00266.2010>
- Xie, T., Bernard, J., & Warnke, P. (2012). Post subthalamic area deep brain stimulation for tremors: a mini-review. *Translational Neurodegeneration*, 1(1), 20. <https://doi.org/10.1186/2047-9158-1-20>
- Yoon, M., & Munz, M. (1999). Placement of deep brain stimulators into the subthalamic nucleus. *Stereotact Funct Neurosurg*, 72, 145–149. <https://doi.org/DOI:10.1159/000029717>

# Appendices

## Appendix 1: Letter of Information and Consent



London Movement Disorders Center



London Health  
Sciences Centre

---

### Letter of Information and Consent

**Study Title:** The use of whole-body kinematic technology for optimizing current steering deep brain stimulation in Parkinson's disease patients

**Principal investigator:** Dr. Mandar Jog, London Health Science Movement Disorders Clinic, UWO

**Protocol Version:** 8.0

**Protocol Date:** 1/June/2018

**Participant Number:** BSC - \_\_\_ \_\_

In this Consent document, "you" always refers to the study participant. Participants of this study must be able to give informed consent and cannot have a substitute decision maker (SDM) (i.e. someone who makes the decision of participation on behalf of a participant).

This consent form explains the research study you are invited to join. Please ask the study doctor or the study staff to explain any words or facts that you do not understand. You should keep a signed copy of this consent form. You may wish to discuss this study with your family and friends before making your decision. If you decide to take part in the research study, you must sign this form before you have anything done for this research study.

---

### Introduction

We are inviting you to voluntarily participate in a research project designed to assess the use of a new method in the practice of a surgical procedure known as deep brain stimulation (DBS). This procedure allows electrical signals to be sent to brain areas related to control of body movement – one area being the subthalamic nucleus (STN). The device being implanted in the STN is part of the routine DBS therapy; therefore, the surgery and clinical management of your DBS device will not be changed. However, during the research visits of this study, we will be exploring a new method of delivering current to the appropriate brain region.

During DBS, electrodes are placed deep in the brain and are connected to a programmable stimulator device. Similar to a heart pacemaker, the stimulator uses electric pulses to help regulate the amount of stimulation delivered to the electrodes. The doctor controls the stimulator settings with a wireless device and stimulation settings can be adjusted as a patient's condition changes over time. The surgical procedure to implant the electrodes will have been clearly explained to you by your surgeon and neurologist, and you will have already signed a separate consent form for this operation as part of the treatment of your Parkinson's disease (PD).

Currently, the delivery of current is directed toward the same brain region for all patients. A new DBS technique has broadened our ability to control and thus, investigate different programming settings of the stimulator device. Through stimulating different regions in the brain, this investigation can help us to determine the best location to deliver current, for each patient. The ability to change where and how much current is being delivered is called current-steering. This study seeks to investigate current-steering with the use of your DBS device to determine the effectiveness of this new programming technique.

## Background

DBS of the STN is a therapy for individuals who are no longer responding to Levodopa (the current drug used to treat PD) as well as they were at the start of their treatment. The purpose of the method of DBS is to stimulate target brain structures while minimizing the stimulation of surrounding regions. The success of DBS therapy is reliant on 3 main aspects: 1) proper patient selection, 2) accurate placement of the electrode lead within the brain, 3) effective selection of stimulator settings of the DBS device. The precise location of the electrode lead and the stimulator settings contribute equally to the therapeutic effect for the patient. However, if the electrode is misplaced within the brain tissue, corrective surgery possesses an added risk for the patient.

The DBS device being used for this study will allow the current to enter the patient's brain through multiple contact points. The device used in this study is not new; however, current steering or the ability to control the amount of current delivered at each contact point is a new technique. The technique of current steering will be investigated in this study. The current steering feature of DBS devices has not been extensively researched. Current steering allows for a more personalized treatment of PD. The ability to direct the current to the optimal location for each patient is a very promising approach to improve the therapeutic success of DBS.

In this study, we attempt to use our lab expertise to investigate the current steering technique. The STN is composed of many different types of brain cells that respond differently to electrical stimulation. It is hypothesized that PD symptom relief is highly dependent on the location of DBS electrical stimulation. Therefore, it is predicted that current steering can change the area of brain tissue being stimulated, and a notable change in PD motor and perceptual features will result as different types of STN brain cells can be targeted. The objectives of the study are:

1. Investigate whether using current steering settings during DBS to direct the current to an optimal location within the brain tissue has any direct effect on PD motor and perceptual symptoms.
2. Determine if there are common settings of the programmable DBS device that are best for treating symptom improvement among all patients.

We are looking to investigate current steering in 16 persons that have undergone STN-DBS recruited from the Movement Disorders Clinic at London Health Sciences Centre (LHSC). This study will require you to come to the research lab 4 days a week for a month post-operation.



## Study Funding

The study is funded in part by Boston Scientific who manufacture the DBS device being used in the current study. Other funding is coming from a research grant from Movement Disorders Center at London Health Sciences Centre (LHSC).

## Inclusion and Exclusion criteria

If you decide to join, you will be asked to sign this consent form and you must agree to follow the instructions given by the research staff during the study. You may not participate in this study if you participated in another clinical research project less than 4 weeks ago. Based on your screening information, the study doctor will determine if you are eligible to join this study.

Inclusion criteria:

1. Diagnosed Idiopathic Parkinson Disease with excellent response to levodopa medication
2. A score of between II-IV on the Hoehn-Yahr scale
3. Severe motor fluctuations with disabling off periods and dyskinesia during on phases
4. Assessed for eligibility for the DBS procedure
5. Able to give informed consent
6. Able to visit the clinic for assessment
7. No dementia or psychiatric abnormalities.

Exclusion criteria:

1. Any previous brain surgery or a cardiac pacemaker
2. If your medication routine is unstable and/or you take levodopa containing medications less than 3 times a day.
3. Any diagnosis of dementia, severe cognitive disturbances or severe psychiatric symptoms (in particular hallucinations and depression) as assessed by DSM criteria
4. Any hip or joint replacements (unless well treated as assessed by the study team)
5. Lack of compliance at follow-up.
6. *Additional exclusion criteria for perceptual test:* Severe visual impairment determined from visual testing (i.e., convergence insufficiency)

## Study Tools

The study will make use of several technological devices to objectively measure all motor symptoms associated with Parkinson's disease. The whole-body mobility is assessed using a motion capture suit which houses several motion sensors that track all body movements. You will be dressed in a lightweight, stretchable, and breathable suit over your regular clothing. You will also wear a head sensor attached to a lightweight cap, as well as fingerless gloves and shoe attachments with hand and foot sensors. The total weight of the suit is 1.5 kg. Walking will be assessed using a pressure sensor carpet walkway. You will be required to walk across the carpet so that the system can capture your walking patterns in various ways. Your speech will also be recorded using a head mounted microphone and a digital recording device. To assess the perceptual capabilities of the PD subjects, a computational virtual reality environment and haptics-enabled robots (such as the KINARM Exoskeleton and End-Point robots) may be used.

You will also complete standard clinical scales at each visit that are used to monitor motor and non-motor features of Parkinson's disease (Table 1.)

**Table 1.** Clinical scales used at every visit.

<b>Clinical Scale</b>	<b>Description</b>
<b>The Unified Parkinson's Disease Rating Scale (UPDRS)</b>	A widely used clinical scale used to measure the impairment and disability associated with Parkinson Disease
<b>The Montreal Cognitive Assessment (MoCA)</b>	A brief 30-question test which assesses different types of cognitive abilities such as short-term memory and concentration.
<b>Freezing of Gait Questionnaire (FOG-Q)</b>	A 6 item questionnaire used to monitor freezing of gait in Parkinson's disease
<b>Activities-specific Balance Confidence (ABC) Scale</b>	A 16 item scale that measures one's confidence in maintaining their balance when completing specific activities
<b>Beck's Depression Inventory</b>	A 21 item questionnaire used to measure affect related to depression

All visits will be recorded with a video camera for data analysis purposes only. The recorded videos will be coded and not linked to your personal information. You may opt-out from these recordings by selecting an option on page 10 of this letter.

## Study Procedure and Design

This is a trial seeking to optimize a patients' DBS device programming using objective and quantitative data that will be obtained from kinematic technology such as the motion capture suit and the carpet walkway.

Participants will then undergo DBS implantation into the STN on both sides of the brain with the Boston Scientific DBS device. Patients will be given at least 4 weeks to recover from the operation; for instance, from week 0 to week 4. At least 6 weeks post-operation, each participant will undergo a 4-week titration regime to determine the effect that current steering has on their primary motor symptoms. Classic hallmark PD symptoms will be assessed using the kinematic technology.

### *Visit 1: 1 week before surgery*

Study participants will be seen one week prior to the DBS surgery to assess their response to the levodopa medication. You will arrive at the research laboratory after being OFF levodopa medications for 12 hours. Full body mobility assessments will be conducted in your OFF state using the motion capture suit, carpet walkway and the speech recorder. Following these assessments, you will be asked to take 135% of your usual levodopa medication. For example, if the patient usually takes 100mg of levodopa for the treatment of their PD, 135% of that would be 135mg. During the wait time for the medication to take into effect, clinical rating scales for movement difficulties and other difficulties

(depression, memory etc.) will be completed (outlined in Table 1.). Once the levodopa medication has taken effect a full body mobility assessment will be conducted in your ON state using the motion capture suit, carpet walkway and the speech recorder.

***Visit 2: at least 4 weeks post-surgery***

At least 4 weeks post-operation a Movement Disorder Neurologist will turn on the patients' device.

***\*\*Note: The next visit sessions will occur over 1 consecutive month, with 4 visits each week\*\****

***Visit 3-6: at least 6 weeks post-surgery***

During these visits 16 current steering paradigms will be explored, 4 each day. These setting paradigms will be randomized for each participant so the same settings are not presented in the same order for each person. Your device will also be set to 20% more of the therapeutic amplitude (current) you will be at clinically. After each current steering setting is implemented, a 30-minute wait period will be allowed for the setting to take effect. Full body assessments will be performed for each setting change as well as the UPDRS. At the end of each day, following the 4 setting changes, your DBS device will be returned to the original setting you came in with. At the end of the week you will be turned to a setting that was found to be most beneficial. You will then be asked to return the following week.

***Visit 7-10: at least 7 weeks post-surgery***

This visit will be the exact same as visits 3-6 except the amplitude (current) of the device will be increased by 40% of the baseline setting.

***Visit 12-15: at least 8 weeks post-surgery***

This visit will be the exact same as visits 3-6 except the amplitude (current) of the device will be increased by 60%.

***Visit 16-19: at least 9 weeks post-surgery***

This visit will be the exact same as visits 3-6 except the amplitude (current) of the device will be increased by 80%.

***Visit 20(optional): at least 12<sup>th</sup> week post-surgery***

During this visit, the subject's various perceptual capabilities will be measured. The subject will be asked to perform two-forced alternative choice perceptual tasks while sitting down. These tasks will be displayed on a computer monitor and the patient will be asked to provide verbal responses to questions asked during the tasks. The perceptual tasks will involve tasks to test for temporal perception, displacement perception and velocity perception (an example is when two objects are shown on a monitor and the participant is asked to tell which object is moving faster or further). Alternatively, the subjects may carry out proprioceptive perceptive tests (such as temporal, displacement and velocity perception) using a haptics-enabled device (such as the KINARM Exoskeleton and End-Point robots). An example of a task involves the subject comparing two speeds of passive movement (powered by the haptics device), and verbally answering which of the compared speeds they perceive to be faster.

## Study Tasks

Patients will perform various tasks during the programming sessions including:

1. **Relaxed position (20 Seconds):** The participants are asked to rest their arms in neutral position while: back hunched forward, both forearms on legs, and hands hanging loose between legs. The participants hold this position for 20 seconds.
2. **Supported Posture (20 seconds):** The participants are asked to rest their arms in neutral position on the arm rests of a chair. The participants hold this position for 20 seconds.
3. **Pronated Posture (20 seconds):** While sitting, participants fully extend their arms forward with hands in pronation at shoulder height level. The participants hold this position for 20 seconds.
4. **Supinated Posture (20 seconds):** While sitting, participants fully extend their arms forward with hands in supination at shoulder height level. The participants hold this position for 20 seconds.
5. **Pronation-supination (20 seconds):** Same position as posture, participants are asked to turn hands one at a time and as fast as possible so that their palms face up and down alternatively. The participants keep this motion for 20 seconds.
6. **Normal walking (90 seconds):** consists of rising from a chair and walking around a 25 meter track 5 times at a preferred normal pace.
7. **Fast walking (90 seconds):** consists of rising from a chair and walking around a 25 meter track 5 times at a fast as possible pace.
8. **Backwards walking (90 seconds):** consists of rising from a chair, turning around and walking down the 7 meter long gait carpet. Once off the carpet the patient turns around and walks backwards across the carpet back into the starting chair.
9. **180 Degrees Turn (60 seconds):** while standing, the participant is asked to turn left/right 180 degrees on the spot to face the back. After a few seconds, they are asked to return to the original position. This task is performed for 8 turns.
10. **Speech recording (120 seconds):** a microphone will be taped to the patients' cheekbone and speech tasks will be carried out.
11. **UPDRS (5 minutes):** this clinical rating scale will be carried out to assess motor symptom severity after each setting change.
12. **Visual Temporal Perception (about 30 minutes):** Patients will perform a 2-Alternative-Forced-Choice task composed of approximately 160 trials. In each trial, comparisons between the time of shapes flashing on the screen (i.e., the first shape appears, disappears for varying amount of time [this time changes between trials and shapes compared in trials] then reappears again briefly before disappearing permanently. This is followed by another shape flashing on the screen. The subject will be asked which time duration between the shape disappearing and reappearing was faster (or if they were the same) between the two compared shapes in each trial.
13. **Visual Displacement Perception (about 30 minutes):** Patients will Perform a 2 Alternative Forced Choice task composed of approximately 160 trials. In each trial a shape at a certain point displayed on a computer monitor will displace to twice, the subject must answer which displacement was greater, or if their displaced was of the same magnitude.

- 
14. **Visual Velocity Perception (about 40 minutes):** Patients will perform a 2-Alternative-Forced-Choice task composed of approximately 200 trials. In each trial two shapes will be moving in opposite directions on a computer monitor for 10 seconds, the subject must answer which velocity was greater, or that the velocities are the same speed.
15. **Proprioceptive Temporal Perception (about 30 minutes):** Patients will perform a 2-Alternative-Forced-Choice task composed of approximately 160 trials. In each trial, subjects should compare the difference in time between the release of force applied from the haptics device (i.e., in each trial, the device will apply force, remove force for a set time, apply force again, remove force a second time, reapply force, end of trial). The subject will be asked which time duration between the removal of the force applied to the patient and the force being reapplied was longer (or if they were the same) between the two compared pauses in force for each trial.
16. **Proprioceptive Displacement Perception (about 30 minutes):** Patients will perform a 2-Alternative-Forced-Choice task composed of approximately 160 trials. In each trial the subject's limb will begin at a starting point and be passively displaced twice from this starting point. The subject should compare the proprioceptive displacements and verbally answer which displacement they felt was greater, or that the displacements were the same.
17. **Proprioceptive Velocity Perception (about 40 minutes):** Patients will perform a 2-Alternative-Forced-Choice task composed of approximately 200 trials. In each trial the haptic device will passively move the patient's limb at a certain velocity for around 7 seconds, and then move their limb again for around 7 seconds. The subject will then compare the speeds of the limb movements, and verbally respond which speed they perceived to be greater, or that they perceived the speed to be the same.
18. **Visual Shape Perception (about 30 minutes):** Patients will perform a 2-Alternative-Forced-Choice task composed of approximately 150 trials. Each trial will consist of sequential (visual) presentation of two rectangles. The subject will compare the length of the two rectangles, and indicate which rectangle they perceive to be bigger in length by selecting one of the two options, shown in the monitor at the end of each trial, using the haptic device.
19. **Proprioceptive Shape Perception (about 30 minutes):** Patients will perform a 2-Alternative-Forces-Choice task composed of approximately 150 trials. Each trial will consist of a sequential (haptic) presentation of two rectangles. The subject will be able to haptically explore the length of the rectangle by moving the haptic device along its edge. The subject will then compare the length of the two rectangles, and indicate which rectangle they perceive to be bigger in length by selecting one of the two options, shown in the monitor at the end of each trial, using the haptic device.
20. **Combined Visual-Proprioceptive Shape Perception (about 30 minutes):** Patients will perform a 2-Alternative-Forced-Choice task composed of approximately 150 trials. Each trial will consist of a sequential (visual and haptic both) presentation of two rectangles. In these trials, subjects will simultaneously look at and haptically explore the length of the rectangle. In one of the two presentations, the visually and haptically specified length of the rectangle will be the same, whereas in the other presentation the visually and haptically specified length of the rectangle may differ. The subject will compare the length of the rectangles, and indicate which rectangle they perceive to be bigger in length by selecting one of the two options, shown in the monitor at the end of each trial, using the haptic device.

Each task will be performed twice with the exception of tasks 6, 7, 9-11. The total amount of time for the motor testing sessions is approximately 20 minutes with appropriate rest periods. Perceptual tests will be done when the DBS system is turned off, and again when it is turned on during one day of experimenting.

## Possible Risks and Harms

This study has some risks that we know about. There is also a possibility of risks that we do not know about and have not been seen in study participants to date. Please call the study doctor if you have any side effects even if you do not think it has anything to do with this study.

Risks are grouped according to two categories; a brief overview is provided for *standard of care risks* which your doctor will have discussed with you in greater detail. The second group is risks related to *participation in this research study*:

### *Study Related Risks*

**Withholding of medication:** You may have transient worsening of parkinsonian symptoms following overnight withdrawal of antiparkinsonian medications. However, this should be no different from the procedure performed as part of the routine clinical assessment before and after surgery. You may get tired during the procedure. You will be OFF medications about 12 times total throughout the study.

**Risks of Current Steering:** You may experience worsening of motor symptoms during the setting changes at the research visits. Some common side effects patients report during settings changes are:

1. Worsening of motor features associated with Parkinson's disease
2. Tingling and numbness in limbs
3. Dizziness and lightheadedness
4. Upset stomach
5. Blurred vision
6. Slurred speech

While these symptoms do not usually occur it is important to monitor for them. The study team understands the common side effects and will monitor them throughout the study. Should you be experiencing any of these symptoms, or others, please let the study team know.

**Risks associated with study tools:** The full body suit is a light weight and fully portable technology for collecting information about your mobility. There is a minimal risk associated with wearing such a suit as the system only uses simple sensors that are attached to the suit. Some study participants may experience discomfort such as itching and sweating in their body while wearing the suit. Some study participants may experience minor emotional distress with completing the scales and questionnaires. Scales will be administered by an experienced researcher trained in administering items in a sensitive manner. You will be allowed rest periods as necessary during the scales and questionnaires to facilitate comfort.

## Possible Benefits

You may not directly benefit from the study, but the information obtained may lead to new knowledge on movement disorders and may lead to new treatment for movement disorders.

## **Compensation**

You will not be compensated for participating in this research study, however you will be reimbursed for parking expenses and potential travel costs.

## **Confidentiality**

### ***Personal Health Information***

If you agree to join this study, the study doctor and his/her study team will look at your personal health information and collect only the information they need for the study. Personal health information is any information that could be used to identify you and includes your:

1. Name
2. Address
3. Partial Date of birth
4. New or existing medical records that includes types, dates and results of medical tests or procedures
5. Telephone Number

### ***Research Information in Clinical Records***

If you participate in this study, information about you from this research project may be stored in your hospital file and in the LHSC computer system. The study team can tell you what information about you will be stored electronically and if you have any concerns about this, or have any questions, please contact the laboratory at

The following people may come to the hospital to look at the study records and at your personal health information to check that the information collected for the study is correct and to make sure the study is following proper laws and guidelines:

1. Representatives of Lawson Health Research Institute (LHRI) including the LHRI Research Ethics Board
2. Representatives of the University of Western Ontario Health Sciences Research Ethics Board.
3. The study sponsor or its representatives'/partner companies (Canadian Institutes of Health Research and Boston Scientific)
4. Representatives of Health Canada or other regulatory bodies (groups of people who oversee research studies) outside of Canada, such as the United States Food and Drug Administration.

The information that is collected for the study will be kept in a locked and secure area by the study doctor for 25 years. Only the study team or the people or groups listed below will be allowed to look at your records. Your participation in this study also may be recorded in your medical record at this hospital.

Following completion of the study, identifiable videos and photographs will be stored using a code number only and will never leave University Hospital. The videos and photographs will remain stored in a secure location and will not be viewed by anyone outside the study team without your

permission. If these videos are used for scientific presentations or education purposes, you will not be identified as all personal identifiers (such as your face) will be blurred or blackened out. All videos and photographs will be destroyed after the study is complete.

Your signed consent, which will have your name on it, will not be stored with the data collected from the study and will not be connected to the data collected. The master list with your contact information on it will also be stored separately from the data collected to avoid linking your personal information to your data recordings. Consent forms and the master list will be stored in a secure location in the Movement Disorders Laboratory of Dr. Jog at University Hospital.

### **Voluntary participation**

Participation in this study is voluntary. You may refuse to participate, refuse to answer any questions or withdraw from the study at any time with no effect on your future care. You will be able to withdraw from the study at any point in time. However, to protect the integrity of the study the data collected up to the point of your withdrawal will remain a part of the study. You will not have the option of withdrawing your data once it has been collected even if you choose to withdraw from the study. No new information will be collected without your permission.

### **Alternatives to study participation**

The alternative to study participation is to continue on your current course of medication and disease management under the direction of Dr. Mandar Jog.

### **Withdrawal from the study by the investigator**

The investigator may decide to take you off the study if he feels your continued participation would impair your wellbeing or if the measuring devices are causing discomfort. The investigator may also decide to terminate your participation if compliance at follow-up is deemed insufficient.

### **Rights as a Participant**

If you are harmed as a direct result of taking part in this study, all necessary medical treatment will be made available to you at no cost. By signing this form you do not give up any of your legal rights against the investigators, sponsor or involved institutions for compensation, nor does this form relieve the investigators, sponsor or involved institutions of their legal and professional responsibilities.

### **Persons to Contact with Questions**



For more information about this research study, or if you believe that you may have a research related injury or experienced any side effects as a result of participating in this study you may call Dr. Mandar Jog at \_\_\_\_\_ If you have questions about the conduct of the study or your rights as a research participant, you may call Dr. David Hill, Scientific Director, Lawson Health Research Institute at \_\_\_\_\_

### **Publication**

If the results of the study are published, your name will not be used. If you would like to receive a copy of any potential study results, please contact Dr. Mandar Jog at \_\_\_\_\_

You do not waive any legal rights by signing the consent form. You will receive a copy of the letter of information for your records.

## **Patient Consent Form**

**Study Title:** The use of whole-body kinematic technology for optimizing current steering deep brain stimulation in Parkinson's disease patients

**Principal Investigator:** Dr. Mandar Jog, MD

**Medical Personnel:**

Dr. Mandar Jog, MD – Neurologist

Ms. Heather Russell – Clinic Nurse

I have read the Letter of Information, have had the nature of the study explained to me and I agree to participate. All questions have been answered to my satisfaction.

- I give permission for my visits to be recorded on camera for data analysis purposes only
- I do not give permission for my visits to be recorded on camera

_____ <b>Signature of Study Participant</b>	_____ <b>Printed Name</b>	_____ <b>Date</b>
_____ <b>Signature of Investigator</b>	_____ <b>Printed Name</b>	_____ <b>Date</b>
_____ <b>Signature of Person Obtaining Consent</b>	_____ <b>Printed Name</b>	_____ <b>Date</b>

## Appendix 2: Ethics Approval Notice



**Western  
Research**

Research Ethics

**Western University Health Science Research Ethics Board  
HSREB Amendment Approval Notice**

**Principal Investigator:** Dr. Mandar Jog  
**Department & Institution:** Schulich School of Medicine and Dentistry\Clinical Neurological Sciences,London Health Sciences Centre

**Review Type:** Full Board  
**HSREB File Number:** 108453  
**Study Title:** The Use of Whole-Body Kinematic Technology for Optimizing Current Steering Deep Brain Stimulation in Parkinson's disease Patients

**HSREB Amendment Approval Date:** September 25, 2017  
**HSREB Expiry Date:** October 20, 2017

**Documents Approved and/or Received for Information:**

Document Name	Comments	Version Date
Revised Western University Protocol	Received September 15, 2017	
Revised Letter of Information & Consent	Received August 23, 2017	

The Western University Health Science Research Ethics Board (HSREB) has reviewed and approved the amendment to the above named study, as of the HSREB Initial Approval Date noted above.

HSREB approval for this study remains valid until the HSREB Expiry Date noted above, conditional to timely submission and acceptance of HSREB Continuing Ethics Review.

The Western University HSREB operates in compliance with the Tri-Council Policy Statement Ethical Conduct for Research Involving Humans (TCPS2), the International Conference on Harmonization of Technical Requirements for Registration of Pharmaceuticals for Human Use Guideline for Good Clinical Practice Practices (ICH E6 R1), the Ontario Personal Health Information Protection Act (PHIPA, 2004), Part 4 of the Natural Health Product Regulations, Health Canada Medical Device Regulations and Part C, Division 5, of the Food and Drug Regulations of Health Canada.

Members of the HSREB who are named as Investigators in research studies do not participate in discussions related to, nor vote on such studies when they are presented to the REB.

The HSREB is registered with the U.S. Department of Health & Human Services under the IRB registration number IRB 00000940.

\_\_\_\_\_ in behalf of Dr. Joseph Gilbert, HSREB Chair

EO: Erika Basile \_\_\_ Grace Kelly \_\_\_ Katelyn Harris \_\_\_ Nicola Morphet \_\_\_ Karen Gopaul \_\_\_ Patricia Sargeant \_\_\_

## Appendix 3: Unified Parkinson's Disease Rating Scale Part 3

### UPDRS Part 3

#### III. Motor Examination

##### 3.1 Speech

0: Normal: No speech problems.

1: Slight: Loss of modulation, diction or volume, but still all words easy to understand.

2: Mild: Loss of modulation, diction, or volume, with a few words unclear, but the overall sentences easy to follow.

3: Moderate: Speech is difficult to understand to the point that some, but not most, sentences are poorly understood.

4: Severe: Most speech is difficult to understand or unintelligible.

Speech

##### 3.2 Facial Expression

0: Normal: Normal facial expression.

1: Slight: Minimal masked facies manifested only by decreased frequency of blinking.

2: Mild: In addition to decreased eye-blink frequency, Masked facies present in the lower face as well, namely fewer movements around the mouth, such as less spontaneous smiling, but lips not parted.

3: Moderate: Masked facies with lips parted some of the time when the mouth is at rest.

4: Severe: Masked facies with lips parted most of the time when the mouth is at rest.

Facial Expression

##### 3.17 Tremor at Rest

Extremity ratings

0: Normal: No tremor.

1: Slight.:  $\leq 1$  cm in maximal amplitude.

2: Mild:  $> 1$  cm but  $< 3$  cm in maximal amplitude.

3: Moderate: 3 - 10 cm in maximal amplitude.

4: Severe:  $> 10$  cm in maximal amplitude.

Lip/Jaw ratings

2: Mild:  $> 1$  cm but  $\leq 2$  cm in maximal amplitude.

3: Moderate:  $> 2$  cm but  $\leq 3$  cm in maximal amplitude.

4: Severe:  $> 3$  cm in maximal amplitude

Face/lip	RUE	LUE	RLE	LLE

##### 3.15 Action or Postural Tremor of hands

0: Normal: No tremor.

1: Slight: Tremor is present but less than 1 cm in amplitude.

2: Mild: Tremor is at least 1 but less than 3 cm in amplitude.

3: Moderate: Tremor is at least 3 but less than 10 cm in amplitude.

4: Severe: Tremor is at least 10 cm in amplitude.

RUE	LUE

**3.3 Rigidity** (passive movement of major joints)

0: Normal: No rigidity.

1: Slight: Rigidity only detected with activation maneuver.

2: Mild: Rigidity detected without the activation maneuver, but full range of motion is easily achieved.

3: Moderate: Rigidity detected without the activation maneuver; full range of motion is achieved with effort.

4: Severe: Rigidity detected without the activation maneuver and full range of motion not achieved.

Neck	RUE	LUE	RLE	LLE

**3.4 Finger taps** (patient taps thumb with index finger)

0: Normal: No problems.

1: Slight: Any of the following: a) the regular rhythm is broken with one or two interruptions or hesitations of the tapping movement; b) slight slowing; c) the amplitude decrements near the end of the 10 taps.

2: Mild: Any of the following: a) 3 to 5 interruptions during tapping; b) mild slowing; c) the amplitude decrements midway in the 10-tap sequence.

3: Moderate: Any of the following: a) more than 5 interruptions during tapping or at least one longer arrest (freeze) in ongoing movement; b) moderate slowing; c) the amplitude decrements starting after the 1st tap.

4: Severe: Cannot or can only barely perform the task because of slowing, interruptions or decrements

RUE	LUE

**3.5 Hand movements** (patient opens and closes hands)

0: Normal: No problem.

1: Slight: Any of the following: a) the regular rhythm is broken with one or two interruptions or hesitations of the movement; b) slight slowing; c) the amplitude decrements near the end of the task.

2: Mild: Any of the following: a) 3 to 5 interruptions during the movements; b) mild slowing; c) the amplitude decrements midway in the task.

3: Moderate: Any of the following: a) more than 5 interruptions during the movement or at least one longer arrest (freeze) in ongoing movement; b) moderate slowing; c) the amplitude decrements starting after the 1st open-and-close sequence.

4: Severe: Cannot or can only barely perform the task because of slowing, interruptions or decrements.

RUE	LUE

**3.6 Rapid alternative movements of hands** (pronation-supination movements of hands)

0: Normal: No problems.

1: Slight: Any of the following: a) the regular rhythm is broken with one or two interruptions or hesitations of the movement; b) slight slowing; c) the amplitude decrements near the end of the sequence.

RUE	LUE

2: Mild: Any of the following: a) 3 to 5 interruptions during the movements; b) mild slowing; c) the amplitude decrements midway in the sequence.

3: Moderate: Any of the following: a) more than 5 interruptions during the movement or at least one longer arrest (freeze) in ongoing movement; b) moderate slowing c) the amplitude decrements starting after the 1st supination-pronation sequence.

4: Severe: Cannot or can only barely perform the task because of slowing, interruptions or decrements.

**3.8 Leg agility** (patient taps heel on the ground in rapid succession picking up entire leg)

0: Normal: No problems.

1: Slight: Any of the following: a) the regular rhythm is broken with one or two interruptions or hesitations of the movement; b) slight slowing; c) amplitude decrements near the end of the task.

2: Mild: Any of the following: a) 3 to 5 interruptions during the movements; b) mild slowness; c) amplitude decrements midway in the task.

3: Moderate: Any of the following: a) more than 5 interruptions during the movement or at least one longer arrest (freeze) in ongoing movement; b) moderate slowing in speed; c) amplitude decrements after the first tap.

4: Severe: Cannot or can only barely perform the task because of slowing, interruptions or decrements

RUE	LUE

**3.9 Arising from chair** (patient attempts to arise from chair with arms folded across chest)

0: Normal: No problems. Able to arise quickly without hesitation.

1: Slight: Arising is slower than normal; or may need more than one attempt; or may need to move forward in the chair to arise.

No need to use the arms of the chair.

2: Mild: Pushes self up from arms of chair without difficulty.

3: Moderate: Needs to push off, but tends to fall back; or may have to try more than one time using arms of chair, but can get up without help.

4: Severe: Unable to arise without help.

Arise from Chair

**3.13 Posture**

0: Normal: No problems.

1: Slight: Not quite erect, but posture could be normal for older person.

2: Mild: Definite flexion, scoliosis or leaning to one side, but patient can correct posture to normal posture when asked to do so.

3: Moderate: Stooped posture, scoliosis or leaning to one side that cannot be corrected voluntarily to a normal posture by the patient.

4: Severe: Flexion, scoliosis or leaning with extreme abnormality of posture.

<b>Posture</b>

**3.10 Gait**

0: Normal: No problems.

1: Slight: Independent walking with minor gait impairment.

2: Mild: Independent walking but with substantial gait impairment.

3: Moderate: Requires an assistance device for safe walking (walking stick, walker) but not a person.

4: Severe: Cannot walk at all or only with another person's assistance.

<b>Gait</b>

**3.12 Postural Stability** (Response to sudden, strong posterior displacement produced by pull on shoulders while patient is standing with feet shoulder width apart)

0: Normal: No problems: Recovers with one or two steps.

1: Slight: 3-5 steps, but subject recovers unaided.

2: Mild: More than 5 steps, but subject recovers unaided.

3: Moderate: Stands safely, but with absence of postural response; falls if not caught by examiner.

4: Severe: Very unstable, tends to lose balance spontaneously or with just a gentle pull on the shoulders.

<b>Postural stability</b>

**3.14 Body bradykinesia and hypokinesia** (combining slowness, hesitancy, decreased arm swing, small amplitude and poverty of movements in general)

0: Normal: No problems.

1: Slight: Slight global slowness and poverty of spontaneous movements.

2: Mild: Mild global slowness and poverty of spontaneous movements.

3: Moderate: Moderate global slowness and poverty of spontaneous movements.

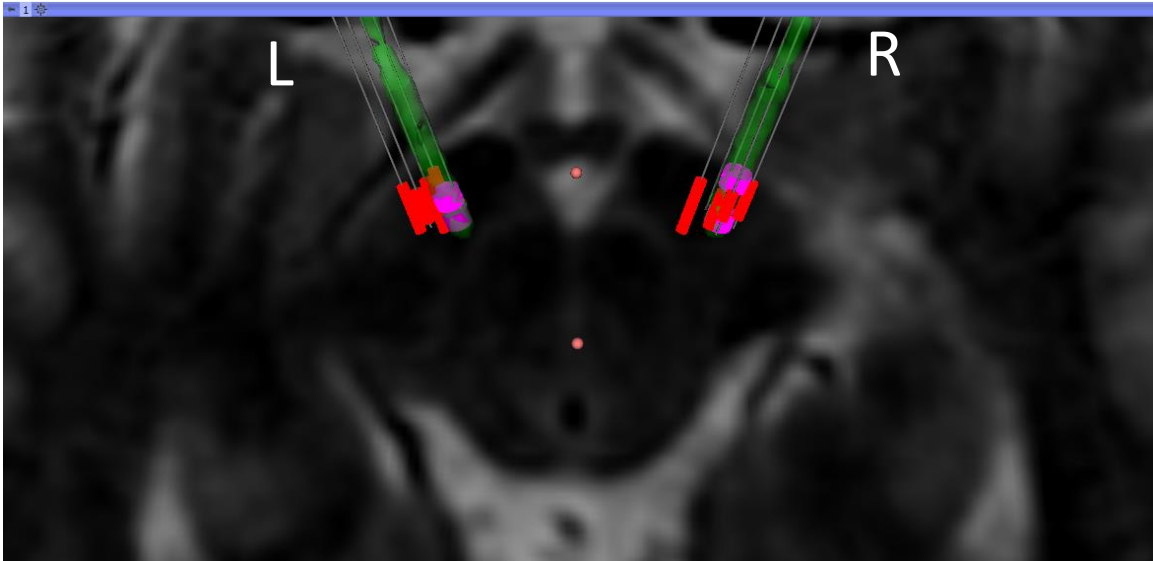
4: Severe: Severe global slowness and poverty of spontaneous movements.

<b>Body Bradykinesia</b>

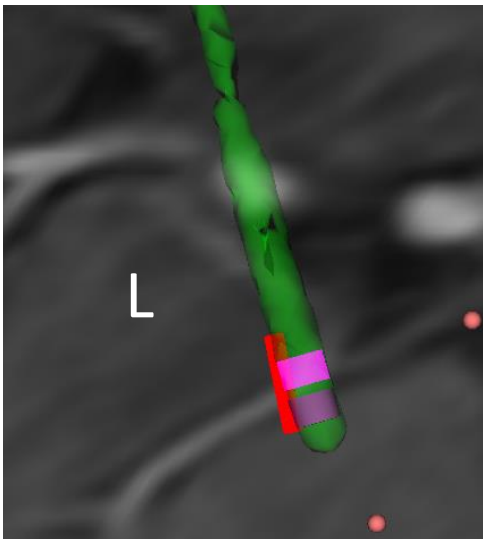
**Total UPDRS score:** \_\_ \_\_

## Appendix 4: Electrode Localization

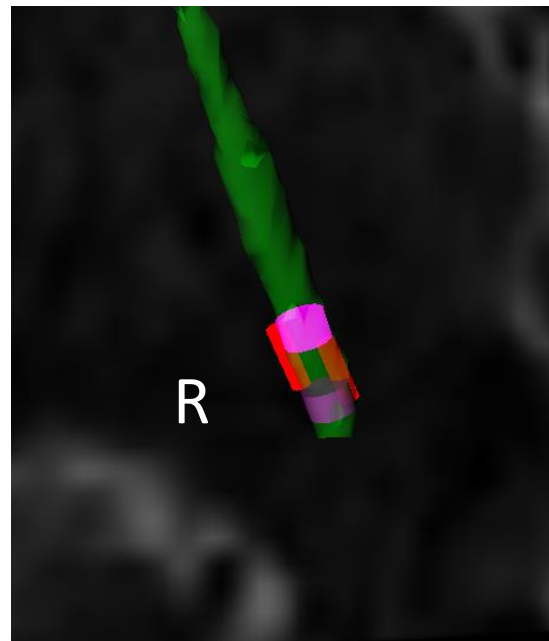
### BSC 02



Superior/posterior view of electrode localization. Green mass represents implanted macroelectrode (lead), pink rings represent active contacts chosen for stimulation, microelectrode recordings represented as tracks surrounding each lead with red cylinders representing subthalamic nucleus (STN) location. L: left STN; R: right STN



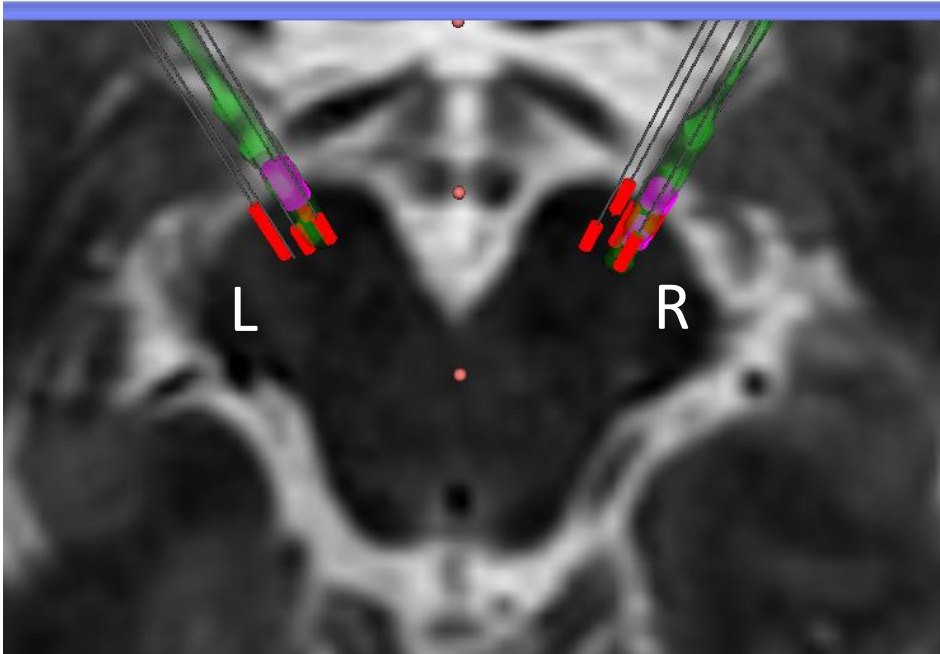
Closer look showing both contacts are within the left STN (red cylinder).



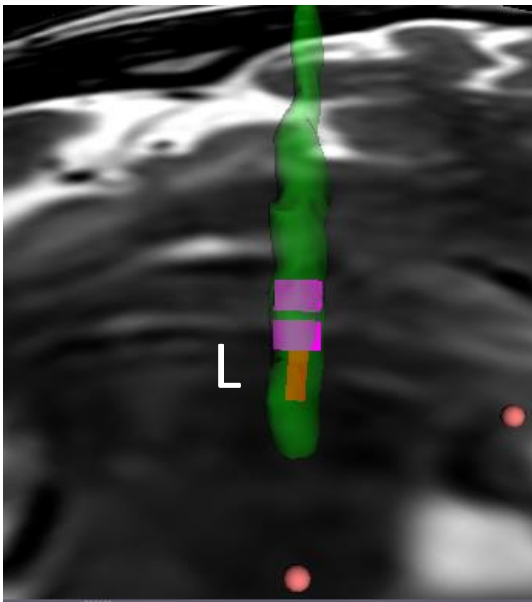
Closer look showing both contacts are within the right STN (red cylinders).



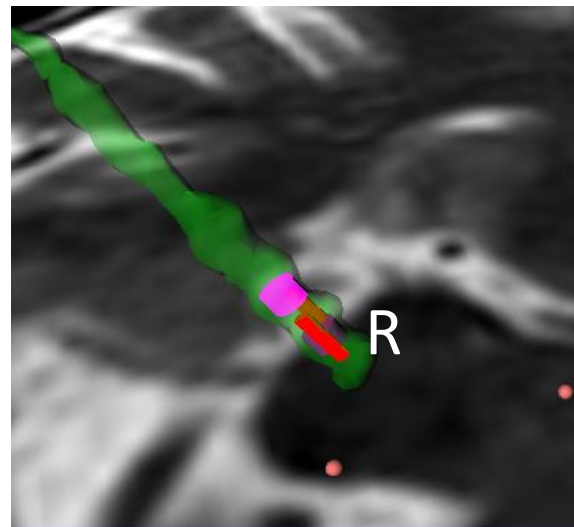
## BSC 03



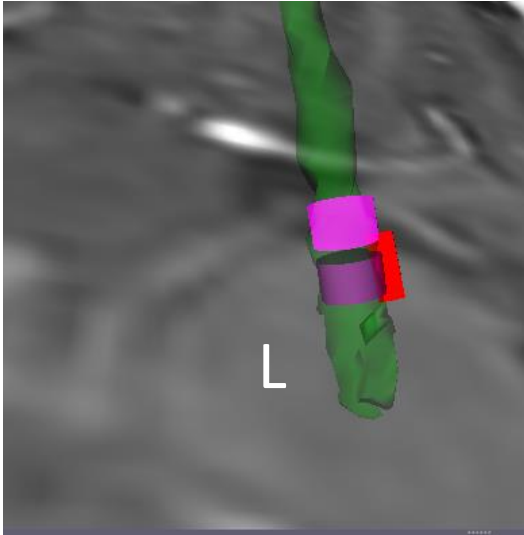
Superior/posterior view of electrode localization. Green mass represents implanted macroelectrode (lead), pink rings represent active contacts chosen for stimulation, microelectrode recordings represented as tracks surrounding each lead with red cylinders representing subthalamic nucleus (STN) location. L: left STN; R: right STN



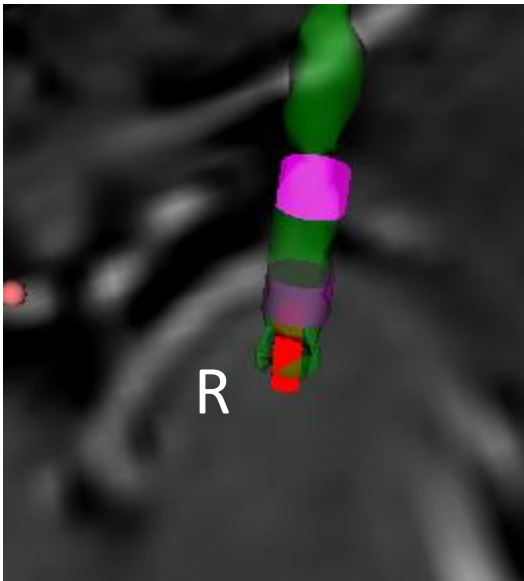
Closer look shows only the more ventral contact is within the left STN (red cylinder).



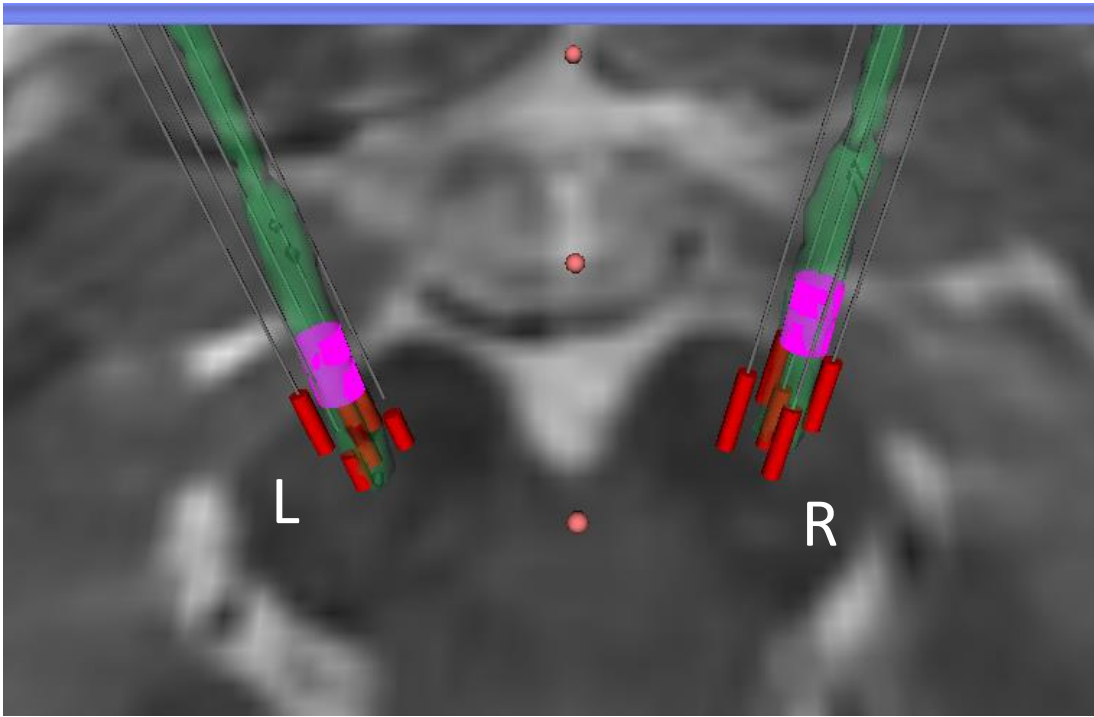
Closer look showing both contacts are within the right STN (red cylinders).

BSC 05

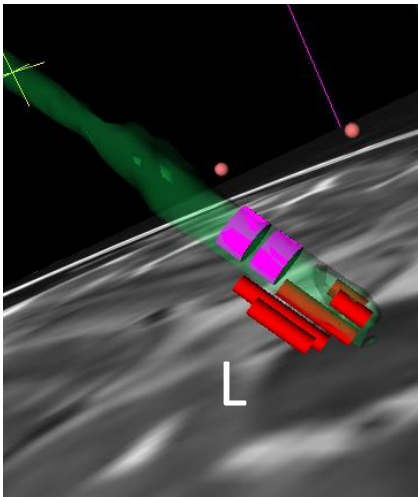
Left lead (green) showing active contacts (purple) are within the left STN (red cylinder). More dorsal contact is mostly outside the STN.



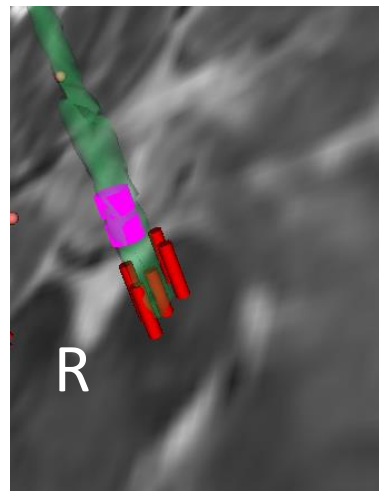
Only the more ventral active contact is within the right STN (red cylinder). More dorsal contact is outside the STN.

BSC 06

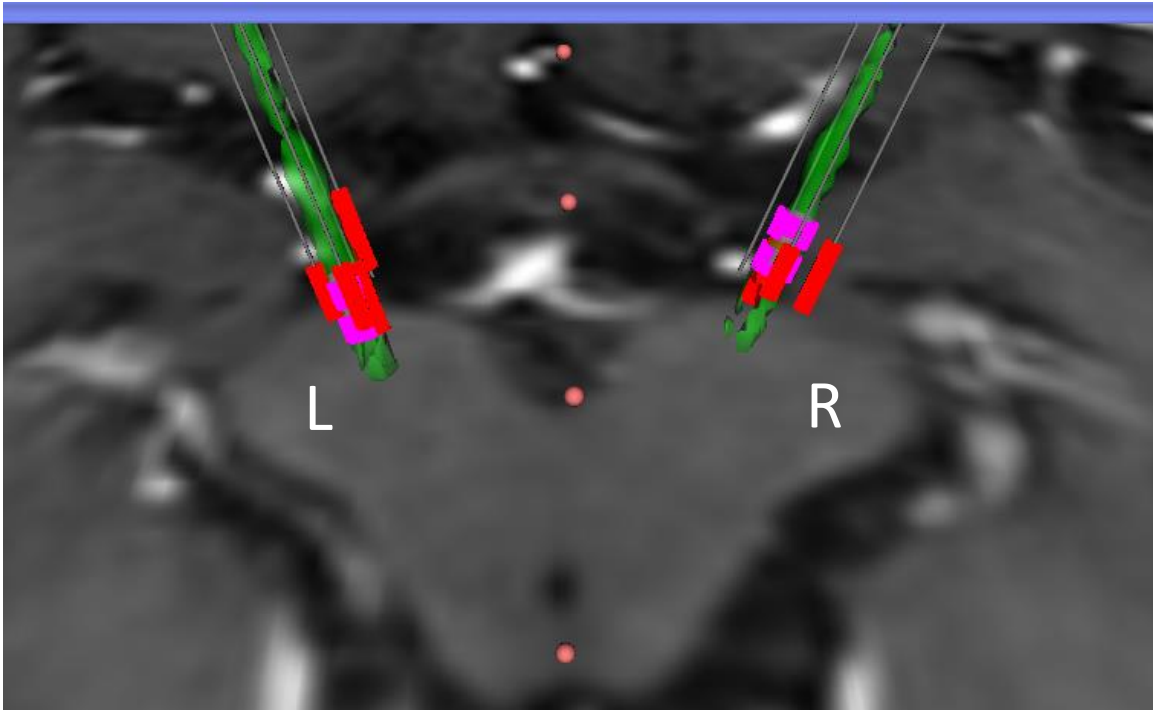
Superior/posterior view of electrode localization. Green mass represents implanted macroelectrode (lead), pink rings represent active contacts chosen for stimulation, microelectrode recordings represented as tracks surrounding each lead with red cylinders representing subthalamic nucleus (STN) location. L: left STN; R: right STN



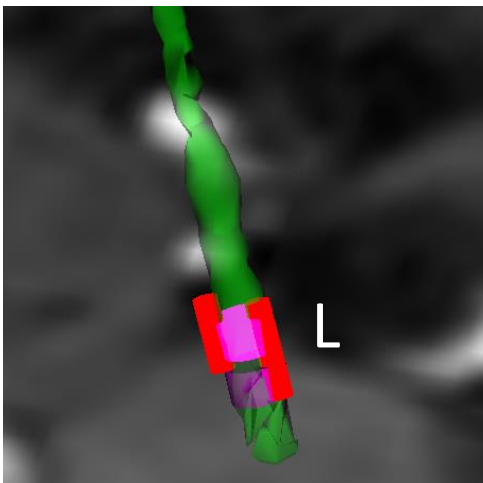
Closer look showing both contacts are outside the left STN (red cylinders).



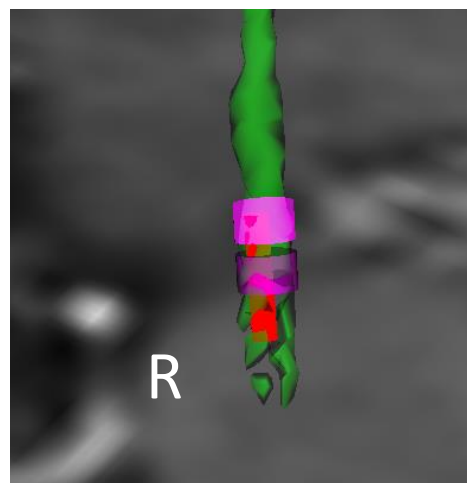
Closer look showing both contacts are outside the right STN (red cylinders).

BSC 07

Superior/posterior view of electrode localization. Green mass represents implanted macroelectrode (lead), pink rings represent active contacts chosen for stimulation, microelectrode recordings represented as tracks surrounding each lead with red cylinders representing subthalamic nucleus (STN) location. L: left STN; R: right STN



Closer look showing both contacts are within the left STN (red cylinders).



Closer look showing both contacts are within the right STN (red cylinder).

## Appendix 5: Copyright

### Frontiers Copyright Statement

All content included on Frontiers websites (including Loop), such as text, graphics, logos, button icons, images, video/audio clips, downloads, data compilations and software, is the property of Frontiers if created by Frontiers, or of the person or entity who or which owned it prior to submission to Frontiers. If not owned by Frontiers, it is licensed to Frontiers Media SA (Frontiers) or its licensees and/or subcontractors.

The copyright in the text of individual articles (including research articles, opinion articles, book reviews, conference proceedings and abstracts) is not the property of Frontiers, and its ownership is not affected by its submission to or publication by Frontiers. Frontiers benefits from a general licence over all content submitted to it, and both Frontiers and its users benefit from a [Creative Commons CC-BY licence](#) over all content, as specified below.

Images and graphics not forming part of user-contributed materials are the property of or are licensed to Frontiers may not be downloaded or copied without Frontiers' explicit and specific permission or in accordance with any specific copyright notice attached to that material.

The combination of all content on Frontiers websites, as well as the design and the look and feel of the Frontiers websites, and the copyright and all other rights in such content and combination, are the sole property of Frontiers.

As an author or contributor you grant permission to others to reproduce your articles, **including any graphics and third-party materials supplied by you**, in accordance with the [Frontiers Terms and Conditions](#). The licence granted to third parties over all contents of each article, **including third-party elements**, is a Creative Commons Attribution ("CC BY") licence. The current version is [CC-BY, version 4.0](#), and the licence will automatically be updated as and when updated by the Creative Commons organisation.

You may include a requirement to reproduce copyright notices in materials contributed by you, but you may not restrict the right to reproduce the entire article, including third-party graphics. This means that you must obtain any necessary third-party consents and permissions to reproduce third-party materials in your articles submitted to Frontiers.

E-books are subject to the same licensing conditions as the articles within them.

**Articles published prior to the effective date of this notice:** Please note that reproduction of third-party graphics and other third-party materials contained in articles published prior to the effective date of this notice may be subject to third-party notices prohibiting their reproduction without permission. You must comply with those notices.

**Articles published prior to July 2012:** The licence granted for these articles may be different and you should check the pdf version of any article to establish what licence was granted. If an article, dating from before July 2012, carries only a non-commercial licence and you wish to obtain a commercial licence, please contact Frontiers at [editorial.office@frontiersin.org](mailto:editorial.office@frontiersin.org).

All software used on this website, and the copyright in the code constituting such software, is the property of or is licensed to Frontiers and its use is restricted in accordance with the [Frontiers Terms and Conditions](#). All copyright, and all rights therein, are protected by national and international copyright laws.

This Copyright Statement comes into effect on **25th May, 2018**.

## 19. Licences (Permissions) You Grant as an Author

When you submit an article to Frontiers, you grant to Frontiers and to the world at large a permanent, non-cancellable, free-of-charge, worldwide licence (permission) to publish, display, store, copy and re-use that article – **including any third-party materials** – and to create derivative works from it. You can not terminate that licence. You must **ensure that you have all necessary permissions from third parties**. Ownership by the third party of the copyright can still be notified on the relevant materials, and attribution must be made in accordance with usual scholarly practices.

The licence (permission) you grant over your article (including any third-party materials included in your article) is a **Creative Commons attribution licence** (known as a **'CC-BY'** licence). You can not terminate that licence.

In summary, the CC-BY licence means that anyone may copy, re-publish and/or re-use your content, and create derivative works from it, for commercial or non-commercial purposes, without charge, but must clearly attribute the work to you and any co-authors, and they must cite Frontiers as the original publisher of that content. Complete information can be found [here](#).

You agree that as the Creative Commons organisation updates the CC-BY licence, the licence terms granted by you are automatically updated to the new version.

Reproduction of all or part of an article is also subject to compliance with usual academic attribution practices, which must be scrupulously complied with in addition to the CC-BY requirements.

You may **not** reproduce or publish any content in any forum (online or not) which advocates any political, religious, anti-religious, racist, extremist, violent or disrespectful viewpoints. If you post any Frontiers content in such a forum, you must remove it immediately on request by Frontiers.

You may also not reproduce any content from our websites in order to denigrate Frontiers.

The same CC-BY licence also applies to any other content, such as reviews, opinions, conference abstracts and blog posts, which you may submit to Frontiers.

You irrevocably grant us permission to use any non-patented ideas set out in your content or in any message sent or submitted to Frontiers, without any charge and without restriction, for any purpose in any part of the world.

Any content of yours appearing on a non-Frontiers website remains subject to the terms and conditions of that website.



## Attribution 4.0 International (CC BY 4.0)

This is a human-readable summary of (and not a substitute for) the [license](#). [Disclaimer](#).

### You are free to:

**Share** — copy and redistribute the material in any medium or format

**Adapt** — remix, transform, and build upon the material for any purpose, even commercially.

The licensor cannot revoke these freedoms as long as you follow the license terms.



### Under the following terms:



**Attribution** — You must give [appropriate credit](#), provide a link to the license, and [indicate if changes were made](#). You may do so in any reasonable manner, but not in any way that suggests the licensor endorses you or your use.

**No additional restrictions** — You may not apply legal terms or [technological measures](#) that legally restrict others from doing anything the license permits.

### Notices:

You do not have to comply with the license for elements of the material in the public domain or where your use is permitted by an applicable [exception or limitation](#).

No warranties are given. The license may not give you all of the permissions necessary for your intended use. For example, other rights such as [publicity, privacy, or moral rights](#) may limit how you use the material.



## How to attach a user license

Elsevier requires authors posting their accepted manuscript to attach a non-commercial Creative Commons user license (CC-BY-NC-ND). This is easy to do. On your accepted manuscript add the following to the title page, copyright information page, or header/footer: © YEAR. Licensed under the Creative Commons [insert license details and URL].

### Order Details

Journal of the neurological sciences

Billing Status:  
N/A

**Order detail ID:** 71624325  
**ISSN:** 1878-5883  
**Publication Type:** e-Journal  
**Volume:**  
**Issue:**  
**Start page:**  
**Publisher:** Elsevier Science  
**Author/Editor:** World Federation of Neurology

**Permission Status:** **Granted**  
**Permission type:** Republish or display content  
**Type of use:** Thesis/Dissertation  
**Order License Id:** 4455441479882

[Hide details](#)


<b>Requestor type</b>	Academic institution
<b>Format</b>	Electronic
<b>Portion</b>	chart/graph/table/figure
<b>Number of charts/graphs/tables/figures</b>	1
<b>The requesting person/organization</b>	Fathima Shabna Iftikar Mohideen
<b>Title or numeric reference of the portion(s)</b>	Figure 1.b
<b>Title of the article or chapter the portion is from</b>	Characterization of multi-joint upper limb movements in a single task to assess bradykinesia
<b>Editor of portion(s)</b>	N/A
<b>Author of portion(s)</b>	Delrobaei M., Tran S., Gilmore G., McIsaac K., Jog M.
<b>Volume of serial or monograph</b>	368
<b>Issue, if republishing an article from a serial</b>	September
<b>Page range of portion</b>	337-342
<b>Publication date of portion</b>	26 July 2016
<b>Rights for</b>	Main product
<b>Duration of use</b>	Life of current edition
<b>Creation of copies for the disabled</b>	no
<b>With minor editing privileges</b>	yes
<b>For distribution to</b>	Worldwide
<b>In the following language(s)</b>	Original language of publication
<b>With incidental promotional use</b>	no




☆ This is an open access article under the CC BY license (<http://creativecommons.org/licenses/by/3.0/>).

1353-8020/\$ – see front matter

<http://dx.doi.org/10.1016/j.parkreldis.2013.07.021>

 creative commons

[Share your work](#) | [Use & remix](#) | [What we do](#) | [Blog](#)



## Attribution 3.0 Unported (CC BY 3.0)


This is a human-readable summary of (and not a substitute for) the license. [Disclaimer.](#)

You are free to:

**Share** — copy and redistribute the material in any medium or format


**Adapt** — remix, transform, and build upon the material for any purpose, even commercially.

The licensor cannot revoke these freedoms as long as you follow the license terms.



---

Under the following terms:



**Attribution** — You must give [appropriate credit](#), provide a link to the license, and [indicate if changes were made](#). You may do so in any reasonable manner, but not in any way that suggests the licensor endorses you or your use.

**No additional restrictions** — You may not apply legal terms or [technological measures](#) that legally restrict others from doing anything the license permits.

---

Notices:

You do not have to comply with the license for elements of the material in the public domain or where your use is permitted by an applicable [exception or limitation](#).

No warranties are given. The license may not give you all of the permissions necessary for your intended use. For example, other rights such as [publicity, privacy, or moral rights](#) may limit how you use the material.

### Oxford Open - Open Access

Articles published under our *Oxford Open - Open Access* model are clearly labeled, and made freely available online immediately upon publication, without subscription barriers to access. In addition, the majority of articles that are made available under Oxford Open, will also allow readers to reuse, republish, and distribute the article in a variety of ways, depending upon the license used. For further detail on Oxford Open and the activities permitted under our Open Access licenses, please click [here](#).

---

Received October 10, 2011. Revised November 28, 2011. Accepted December 14, 2011. Advance Access publication March 1, 2012

© The Author (2012). Published by Oxford University Press on behalf of the Guarantors of Brain.

This is an Open Access article distributed under the terms of the Creative Commons Attribution Non-Commercial License (<http://creativecommons.org/licenses/by-nc/3.0>), which permits unrestricted non-commercial use, distribution, and reproduction in any medium, provided the original work is properly cited.



## Attribution-NonCommercial 3.0 Unported (CC BY-NC 3.0)

This is a human-readable summary of (and not a substitute for) the [license](#). [Disclaimer](#).

### You are free to:

**Share** — copy and redistribute the material in any medium or format

**Adapt** — remix, transform, and build upon the material

The licensor cannot revoke these freedoms as long as you follow the license terms.

### Under the following terms:



**Attribution** — You must give [appropriate credit](#), provide a link to the license, and [indicate if changes were made](#). You may do so in any reasonable manner, but not in any way that suggests the licensor endorses you or your use.



**NonCommercial** — You may not use the material for [commercial purposes](#).

**No additional restrictions** — You may not apply legal terms or [technological measures](#) that legally restrict others from doing anything the license permits.

### Notices:

You do not have to comply with the license for elements of the material in the public domain or where your use is permitted by an applicable [exception or limitation](#).

No warranties are given. The license may not give you all of the permissions necessary for your intended use. For example, other rights such as [publicity, privacy, or moral rights](#) may limit how you use the material.

9/12/2018

RightsLink Printable License

**ELSEVIER LICENSE  
TERMS AND CONDITIONS**

Sep 12, 2018

---

This Agreement between Ms. Shabna Iftikar Mohideen ("You") and Elsevier ("Elsevier") consists of your license details and the terms and conditions provided by Elsevier and Copyright Clearance Center.

License Number	4426841013190
License date	Sep 12, 2018
Licensed Content Publisher	Elsevier
Licensed Content Publication	Trends in Neurosciences
Licensed Content Title	Pathophysiology of the basal ganglia in Parkinson's disease
Licensed Content Author	José A. Obeso, Maria C. Rodriguez-Oroz, Manuel Rodriguez, José L. Lanciego, Julio Artieda, Nancy Gonzalo, C. Warren Olanow
Licensed Content Date	Oct 1, 2000
Licensed Content Volume	23
Licensed Content Issue	n/a
Licensed Content Pages	12
Start Page	S8
End Page	S19
Type of Use	reuse in a thesis/dissertation
Portion	figures/tables/illustrations
Number of figures/tables/illustrations	1
Format	electronic
Are you the author of this Elsevier article?	No
Will you be translating?	No
Original figure numbers	Figure 1
Title of your thesis/dissertation	The use of current steering during subthalamic deep brain stimulation to alleviate upper limb symptoms of Parkinson's disease
Expected completion date	Dec 2018

<https://s100.copyright.com/AppDispatchServlet>

## Curriculum Vitae

**Name:** Fathima Shabna Iftikar Mohideen

**Post-secondary Education and Degrees:** University of Waterloo  
Waterloo, Ontario, Canada  
2011-2016 B.Sc.

The University of Western Ontario  
London, Ontario, Canada  
2016-Present M.Sc.

**Honours and Awards:** University of Waterloo Merit Scholarship  
2011

Graduation Dean's Honours List  
2016

Western Graduate Research Scholarship  
2016-2018

Mitacs Accelerate Industry Grant  
2017-2018

**Related Work Experience** Teaching Assistant  
The University of Western Ontario  
2016-2018